A STUDY OF COUPLED INTERFACIAL REACTIONS AND DIFFUSION IN MULTI-COMPONENT METALLIC/IONIC SYSTEMS

by

DUNCAN DONGKE MA, M.Sc., B.Sc.

A Thesis

Submitted to the School of Graduate Studies

in Partial Fulfilment of the Requirements

for the Degree

Doctor of Philosophy

McMaster University

August 1992

A STUDY OF COUPLED INTERFACIAL REACTIONS AND DIFFUSION IN MULTI-COMPONENT METALLIC/IONIC SYSTEMS

DOCTOR OF PHILOSOPHY (1992) McMASTER UNIVERSITY

(Materials Engineering) Hamilton Ontario

TITLE: A Study of Coupled Interfacial Reactions and Diffusion in Multi-component Metallic/Ionic Systems

AUTHOR: Duncan Dongke Ma, M.Sc., B.Sc. (Northeast University of Technology, Shenyang P.R. China)

SUPERVISOR: Professor W-K Lu

NUMBER OF PAGES: xv, 171

ABSTRACT

A study consisting of theoretical and experimental work on kinetics of simultaneous interfacial reactions in multi-component metallic/ionic systems has been carried out in the present work. General rate expressions for simultaneous interfacial reactions are proposed based on the application of mass action law to the electrodic half-cell reactions and the constraint of no net electric current. The nature of coupling among interfacial reactions is discussed by defining the coupling factor which is a collective property of the system, contributed by and common to all interfacial reactions. Kinetic behavior of each element can be individually and simultaneously described.

Experimental work is conducted in slag/metal system for the study of coupled interfacial reactions and diffusion. Considering interfacial reactions as the boundary conditions for diffusion in both phases, a mathematical model is developed. Computed results, based on thermochemical parameters mostly reported in the literature, are compared with diffusion profiles measured by electron probe microanalysis (EPMA) in silicate slag and Fe-Mn-Si alloy at 1763 ^{o}K. Values of reaction rate constants for transfer of iron, manganese and silicon are recommended through curve fitting with the experimental data.

The conventional pseudo-binary approach in the formulation of rate equations for interfacial reactions in multi-component slag/metal systems may be deduced from the present theory with simplifying assumptions and as a limiting case.

ACKNOWLEDGEMENT

The author wishes to express his sincere gratitude to his supervisor, Professor W-K. Lu for his advice and guidance throughout the course of this work and for his countless efforts to provide broad training in both educational and professional aspects. Without his continuous encouragement and criticism, the completion of this work would not have been possible. Similarly, the author extends his gratitude to other members of his Supervisory Committee, Professors G.R Purdy and J.E. Greedan for their help and guidance.

Special thanks are also extended to Professor J.S. Kirkaldy for the discussions of diffusion applied in the present work, to Dr. J.D. Ray for encouragement in carrying out this project and to Dr. Y-P Lin for help in selecting the analytical method for measurements of diffusion profiles.

The author also wishes to express his appreciation to Dr. R.H. Packwood and Ms. V. Moore in the Metal Technology Laboratory, CANMET, OTTAWA for the electron probe microanalysis, to Mr. M. van Oosten for the chemical analysis of the alloy and to Ms. Linda Palmer for the assistance in correcting grammar.

Financial assistance from Chinese Government in the form of a scholarship and the Department of Materials Science and Engineering, McMaster University for a teaching assistantship and a scholarship and the operating grant of NSERC to Professor W-K. Lu are greatly appreciated. Without their support, the present study could not have been carried out.

TABLE OF CONTENTS

LIST OF TABLES

LIST OF FIGURES

All illustrations are located at the end of the thesis.

CHAPTER ONE

INTRODUCTION

Studies of reaction kinetics in metallic/ionic systems are of primary importance for applications in slag/metal reactions, metal/inclusion reactions, metal/glass joints, composite materials, refractory coated metals, etc. They may be characterized in the following three essential steps:

(1) Diffusion of reactants from bulk metallic (or ionic) phase to interface;

(2) Interfacial chemical reactions;

(3) Diffusion of products from interface to bulk ionic (or metallic) phase.

Metallic phase is made of neutral atoms and ionic phase is made of charged ions. Thus, interfacial reactions involve transfer of charges. The systems of any practical importance are generally multi-component in nature. Therefore, all interfacial reactions would take place simultaneously but at various reaction rates.

Diffusion in multi-component metallic or ionic phase has been extensively studied (Kirkaldy and Young, 1987, Okongwu, 1973, Cooper and Varshneya, 1972, 1968). However, the study of multi-component and simultaneous interfacial reactions in this type of system is still in a preliminary stage. The usual approach, which has been shown in textbooks, involves simplifications based on rate controlling steps. For example, when mass transport of a component to or

from the interface is controlling the overall reaction rate, the interfacial reactions may be assumed to be at an equilibrium state. The advantage is that the interfacial compositions may be calculated.

On the other hand, in the well stirred systems, interfacial reactions may be assumed to be the rate limiting step, therefore, it implies that there is no concentration gradients in the bulk phase. The simplification is that interfacial and bulk concentrations are equal and readily available by sampling and chemical analysis.

Another common simplifying assumption is to ignore certain chemical elements to idealize the stoichiometry of chemical reactions. For example, in a metal/metal oxide system, the overall reaction is idealized to either the formation of a metal oxide or its decomposition. This assumption will lead to the simple relation between fluxes of these two chosen chemical elements. The transfer of all other elements across the interface would have to be ignored. In order to force the data to fit certain curves, it is common that rate constant for the reaction under investigation may have to be expressed as functions of concentrations of the ignored elements to include their effect in this artificial manner (Chang and Goldman, 1948, Goldman, Derge and Philbrook, 1954).

The most important advances in this field, experimentally and theoretically, were made in the mid 1950's. King & Ramachandran (1956) observed the reversal in directions of the transfer of elements across interface in the slag/metal reaction. This phenomenon was explained by Wagner (1956) that interfacial reactions are electrochemical in nature and coupled. It was suggested that all interfacial reactions may be described by simultaneous electrodic half-cell reactions, viz,

$$M_i = M_i^{z_i} + z_i\, e\,, \qquad (i=1,2,...,p)$$

The common electric field which exists at interface, e.g. through the formation of electric double layer (Bockris and Reddy, 1970) or unbalanced transfer of charged ions, would be felt by all ions. All electrodic half-cell reactions which contribute to and are influenced by the field, are thus coupled. The formulation of kinetic expressions has been attempted by several authors (Wagner, 1956, Hemptinne, Eyring and Yee, 1961, Lu, 1971 and Tokuda, 1971). Efforts were made to connect this non-measurable electric field to measurable thermodynamic quantities and reaction rate constants. The lack of progress in this field in recent years is mainly due to the fact that (i) the theoretical formulations contain too many kinetic parameters to be evaluated; and (ii) the experimental data are too scare and incomplete to validate any theory.

At McMaster University, efforts have been made. Okongwu (Ph.D., 1973) studied diffusion in ionic/ionic systems experimentally and formulation of interfacial reaction kinetics in metallic/ionic systems with a simplifying assumption that the reaction driving force may be linearized (details are given in chapter two). Ray (Ph.D., 1981) conducted experiments to measure reaction rate constants for transfer of iron and oxygen in $Fe/CaF_2/FeO$ system at 1723 ^{o}K. The lack of complete thermodynamic data in practical systems which are usually multi-component, hinders the application of this type of complex theory of kinetics in interfacial reactions. The advances in mathematical modeling of thermodynamic behavior of multi-component silicate melts (Gaye, et al. 1986) and in microprobe chemical analysis led us to make another attempt in the study of this challenging system. The present study includes both experimental and theoretical work.

Theoretical studies in the present work includes the development of a general rate expression for multi-component simultaneous interfacial reactions and the avoidance of the simplifying assumption used by previous authors (Chapter Three). The model of coupled interfacial reactions and diffusion with interfacial reactions as part of boundary conditions (Chapter Four) are general and comprehensive. Experimental measurements in the present work were carried out for the coupled interfacial reactions and diffusion in the system containing silicate melts and solid Fe-Mn-Si alloy under well controlled conditions at 1763 ^{o}K. Concentration profiles in both phases in the reacted specimens were measured by using electron probe microanalysis (Chapter Five). The comparison between experimental results and theoretical computations are shown in Chapter Six.

CHAPTER TWO

LITERATURE REVIEW

Of all metallic/ionic systems, silicate slags and iron alloys have been extensively studied in the past years and better documented (e.g. Gaskell, 1967, Okongwu, 1973, Richardson, 1974, Kirkaldy and Young, 1987, Gaye, 1986). Therefore, slag/metal systems have been chosen for the present studies of interfacial reaction kinetics and the literature survey is limited to this field.

2-1 Interfacial Concentrations

In textbooks (e.g. Habashi, 1969), the forward (or backward) irreversible rate of a heterogeneous reaction j are expressed with reacting species j1 to jp through the following empirical relation, viz,

$$\text{Rate} = k_j \; \Omega \; C_{j1}^{n1} \ldots C_{jp}^{np} \qquad (2\text{-}1)$$

where k_j is the specific reaction rate constant which is a function of temperature, Ω is the interfacial area, n1 to np represent the order of reaction which may be determined by experimental measurements, and C_{j1} to C_{jp} are the concentration of reactants (or products) in the reaction zone. In order to determine the reaction rates as well as the order of reactions, it is necessary that interfacial concentrations in the reaction zone are known during the course of reaction.

In principle, interfacial area in the geometric sense has no thickness. To obtain interfacial concentrations, the physical interface, in which all atoms

or ions may be readily in touch with the interfacial area, has to be defined. Thus, its thickness would be within a few diameters of atoms, i.e. no more than tens of angstroms. This has certainly ruled out the possibility of quantitative analysis using conventional chemical methods because of its inability of sampling. By using physical methods, e.g. electron probe microanalyzer, measurements of the interfacial concentrations are limited by two major factors. One is the resolution for quantitative analysis. This does not only depend on the size of the electron beam, but also the travelling distance of electrons inside the specimen as well as the projection of X-ray produced by the bombardment of electrons. The second problem is even if the resolution for quantitative analysis can be improved to a few angstroms, it is then very difficult to monitor the interfacial concentrations without the influence from bulk phases.

As reactions proceed, interfacial concentrations will change as the accumulation terms between rates of supply and rates of consumption, with interfacial reaction on one side and mass transfer to and from bulk phase on the other. Interfacial concentrations may thus be theoretically connected to measurement of concentration gradients in the bulk phase to the vicinity of interfacial area under certain restrictions such as steady state conditions. In this chapter, relevant theoretical basis and experimental work on interfacial reactions and diffusion in single phases are separately reviewed. Observed results including the coupling of diffusion and interfacial reactions are also reviewed. For simplicity in the analysis of data, one approach has been attempted to eliminate concentration gradients as unknowns by the design of experiments, i.e. by keeping both liquid phases well stirred mechanically. Interfacial concentrations were then assumed to be the same as those in the bulk phase which

could be sampled and analyzed. The effectiveness of this method in liquid-liquid system depends mainly on the intensity of stirring on one hand and the assumption of a well defined interface of constant area on the other.

2-2 Kinetic Expressions of Interfacial Reactions

2-2-1 Rate Equations of Reactions Involving Neutral Species

Chemical reactions between slag and metal have long been studied. Even though the ionic nature of slag had been well established (Doelter, 1907, Martin and Derge, 1943, Bockris, et al. 1948), chemical reactions were expressed in neutral species, i.e. atoms and compounds, so that slag/metal distribution could be calculated (e.g. Taylor and Chipman, 1943). In the late 1940's and early 1950's, rates based on reactions of neutral species were first quantitatively measured and kinetically analyzed in slag/metal systems (Chang and Goldman, 1948, Philbrook et al., 1950, 1954).

Chang and Goldman (1948) conducted experiments of desulphurization with blast furnace type slag ($CaO\text{-}SiO_2\text{-}Al_2O_3$) and carbon saturated iron (Fe-S-C). A graphite crucible which could be rotated during experiments was used. Slag and metal were melted in the crucible by induction heating. To study the kinetic effect, sampling of both slag and metal in bulk phases were taken at regular time intervals for chemical analysis. Typical results are shown in Fig. 2-1.

In theoretical analysis, they assumed that transfer of sulphur from metal to slag is proportional to the concentration of sulphur in the metal phase and from slag to metal is proportional to the concentration of sulphur in the slag phase. The net rate of sulphur from metal to slag was written as:

$$\frac{dW}{dt} = \Omega \, (K_m C_m - K_s C_s) \qquad (2\text{-}2)$$

where $\frac{dW}{dt}$ is the net transfer rate of sulphur from metal to slag (gram/min.), Ω is the interfacial area (cm^2), C_s and C_m are the concentrations of sulphur in slag and in metal respectively (wt%), and K_s and K_m are the rate constants of transfer of sulphur from slag to metal and from metal to slag, respectively (gram/cm^2/min/conc.). By fitting with experimental data, K_s and K_m were obtained and found to be not only functions of temperature, but also of slag compositions (see Fig. 2-2 and Fig. 2-3). Thus, they concluded that the reaction rate should be expressed through activities instead of concentrations, viz,

$$\frac{dW}{dt} = A\,(k_m\gamma_m C_m - k_s\gamma_s C_s) \qquad (2\text{-}3)$$

where γ_m and γ_s are activity coefficients of sulphur in metal and slag, respectively, and k_m and k_s are specific forward and backward reaction rate constants, respectively, (gram/cm^2/min/activity).

From equations (2) and (3), it follows,

$$K_m = k_m\gamma_m \qquad (2\text{-}4a)$$

$$K_s = k_s\gamma_s \qquad (2\text{-}4b)$$

In equation (4a), K_m is seen to be the product of two terms, k_m which should be a function of temperature and γ_m which is a function of both temperature and compositions in metallic phase. With this modified equation, however, it could still not be explained why K_m which is a property of metallic phase varied with slag basicity (see Fig. 2-3).

Derge, Philbrook and Goldman (1950), proposed the reaction mechanism that the overall rate of desulphurization consists of three stages. Sulphur is transferred across the interface into the slag in combination with iron and then stabilized in the slag by combining with calcium. The iron oxide, resulting from

the reaction, is then reduced to iron by carbon. This three-stage theory can be written by the following three consecutive reactions (5a), (5b) and (5c). Reactions (5a) and (5c) are heterogeneous reactions and (5b) is a homogeneous reaction which is much faster than the other two.

$$FeS_{(Fe)} = FeS_{(slag)} \tag{2-5a}$$

$$FeS_{(slag)} + CaO_{(slag)} = CaS_{(slag)} + FeO_{(slag)} \tag{2-5b}$$

$$FeO_{(slag)} + C_{(Fe,crucible)} = Fe_{(Fe)} + CO_{(gas)} \tag{2-5c}$$

Goldman, Derge and Philbrook (1954) also discussed the effect of other elements in metal alloy (such as Mn, Si, C, Al) on the rate constant K_m with acid slag (CaO/SiO_2=0.55) and basic slag (CaO/SiO_2=1.12) (see Figs. 2-4 and 2-5). Among these elements, the increase of manganese in liquid iron would reduce the activity coefficient of sulphur (Sherman and Chipman, 1952, also Elliott, et al. 1963). Results in Figs. 2-4 and 2-5 show that an increase of Mn in iron still helps to remove sulphur from metal, i.e. opposite to the effect due to solution thermodynamics. This was explained by a proposal of reaction mechanism similar to equations (5).

$$MS_{(Fe)} = MS_{(slag)} \tag{2-6a}$$

$$MS_{(slag)} + CaO_{(slag)} = CaS_{(slag)} + MO_{(slag)} \tag{2-6b}$$

$$MO_{(slag)} + R_{(Fe)} = M_{(Fe)} + RO_{(slag\ or\ gas)} \tag{2-6c}$$

where R = C, Si, Al, Mn and M = Fe, Mn, Si.

For the different element M or R under investigation, there could be a number of consecutive reactions to describe the reaction mechanism of sulphur removal. On the basis of the observed reactions between sulphur, iron and manganese, manganese as an alloying element not only replaces iron as indicated in reaction (6a), but causes the overall process to proceed more rapidly.

The above theory has been consistent with many experimental observations and applied to other slag/metal systems (e.g. Fruehan, 1978, Min and Fruehan, 1992). Further development in this direction, both theoretical and experimental, has so far not gone beyond the scope of the above work

It is interesting to note that, in their experiments between CaO-SiO_2-Al_2O_3 slag and Fe-C-S alloy, Derge, Philbrook and Goldman (1950) observed that sulphur and iron concentrations in slag increase in the early stage of reaction to a peak value and then decrease (see Fig. 2-6). Their explanation of this phenomenon was quoted by the following. "First, sulphur enters the slag from metal as iron-sulphur compound. The maximum in the iron curve indicates that this compound disappears through reaction with other constituents in the slag."

However, due to the fact that both concentrations of iron and sulphur in slag increase in the early stage of reaction and decrease later, the disappearance of iron-sulphur compound, according to the three-stage mechanism, is a result of production of calcium-sulphur compound which should not lead to the decrease of sulphur in slag.

In the middle of the 1950's, King and Ramachandran (1956) conducted nearly identical experiments for the reaction between CaO-SiO_2-Al_2O_3 slag and Fe-C-S-Si alloy. To intensify stirring of liquid slag and metal, a stationary paddle against a rotating crucible was installed. A typical result containing initial 0.1% Si in metal is shown in Fig. 2-7. One may see that all four elements of C, S, Si and Fe reacted simultaneously. Si and Fe were removed from metal to the slag in the early stage of reaction but reversed later. At the final state of reaction, nearly all Fe was removed from the slag and Si in the metal increased up to 0.5%. To understand the simultaneous interfacial reactions, electrochemical

theory was proposed by Wagner (1956) and is reviewed in the next section.

2-2-2 Rate Equations of Electrodic Half-Cell Reactions

Wagner (1956) explained that interfacial reactions in slag/metal systems are electrochemical in nature and can be described in electrodic half-cell reactions, viz,

$$M_i = M_i^{z_i} + z_i\, e \qquad (i=1,2,...,p) \qquad (2\text{-}7)$$

where z_i is the valence of element M_i and e is electron. All these electrodic half-cell reactions occur simultaneously. As a whole, reactions obey the rule of neutrality. For instance, it may be expressed through equation (8) for the experiment conducted by King and Ramachandran (1956).

$$2\,\omega_S = 2\,\omega_{CO} + 2\,\omega_{Fe} + 4\,\omega_{Si} + 3\,\omega_{Al} \qquad (2\text{-}8)$$

where ω_S, ω_{CO}, etc. are net rates of reacted species. Charge transfer associated with the rate of sulphur transfer equals to the summation of charge transferred associated with rates of all other four elements. Or, in other words, all simultaneous reactions are coupled through equation (8) due to the requirement of maintaining neutrality in ionic phase. To go one step further, it is necessary to quantify these rate equations when they are used to interpret experimental work. In the following, several approaches are reviewed.

Wagner expressed rate equations in the Butler-Volmer type in terms of electrodic potential difference across a slag/metal interface, viz,

$$\omega_i = k_i C_i^{\bullet} \exp\left[(1-\alpha) z_i E \mathcal{F}/RT\right] - k_i' C_i'^{\bullet} \exp\left[-\alpha z_i E \mathcal{F}/RT\right] \qquad (2\text{-}9)$$

$$(i=1,2,...,p)$$

where ω_i is the reaction rate given as the difference of two terms for anodic dissolution of ith component and its cathodic deposition as individual electrochemical reactions, $\mathcal{F}$ is Faraday constant, E is the electrode potential difference across the interface, k_i and k_i' are the specific rate constants for anodic and cathodic processes of ith component respectively which are function of temperature only, C_i^* and $C_i'^*$ are the interfacial concentrations of ith component in metal and slag respectively and α is the charge transfer coefficient ranging from zero to one.

Another description of rate equations was given by Lu (1971) with the application of mass action law to the interfacial electrodic half-cell reactions. Attempting to apply the formulation by Lu in glass/metal system, Okongwu (1973) made the following assumptions:

(i) The glass phase is truly ionic with no electronic conduction and the metal or alloy phase is completely metallic [all free electrons exist only in metallic phase].

(ii) Mass action law is applicable to electrodic half-cell reactions in the form of electrochemical activities.

(iii) Electrochemical potential may be split into the chemical portion and the electrical portion, viz,

$$\bar{\mu}_i = \mu_i + z_i \mathcal{F} \phi \qquad (i=1,2,...,p) \qquad (2\text{-}10)$$

where $\bar{\mu}_i$ is the electrochemical potential of ith component, μ_i is the chemical potential of ith component, z_i is the valence of ith component, $\mathcal{F}$ is Faraday constant and ϕ is the electrical potential of the system. Therefore, the net reaction rates were described as:

$$\omega_i = k_i a_i - k_i' \bar{a}_i' \bar{a}_e^{z_i} \qquad (i=1,2,...,p) \qquad (2\text{-}11)$$

where k_i and k_i' are the specific forward and backward reaction rate constants of half-cell reactions (cm/sec.), a_i is the activity of ith component in metallic phase, $\bar{a}_i'$ is the electrochemical activity of ith component in ionic phase, $\bar{a}_e$ is the electrochemical activity of electrons.

Lu (1971) had shown that both approaches of Butler-Volmer type and mass action law application are mathematically equivalent. Further studies may be carried out from either one of the equations. Okongwu (1973) manipulated equation (11) as follows,

$$\omega_i = k_i a_i \left[1 - \frac{k_i' \bar{a}_i' \bar{a}_e^{-z_i}}{k_i a_i} \right] \qquad (i=1,2,...,p) \qquad (2\text{-}12)$$

and defined the electrochemical affinities $\bar{A}_i$ of the reactions following Prigogine's suggestion (1967), viz,

$$\frac{k_i' \bar{a}_i' \bar{a}_e^{-z_i}}{k_i a_i} = \exp\left[- \frac{\bar{A}_i}{RT} \right] = \exp\left[- \frac{\bar{\mu}_i^{(s)} - \bar{\mu}_i^{(m)} - z_i \bar{\mu}_e}{R\ T} \right] \qquad (2\text{-}13)$$

$$(i=1,2,...,p)$$

where superscript (s) and (m) represent the electrochemical potential in glass and metal respectively, $\bar{\mu}_e$ is the electrochemical potential of electrons in metal. Reaction rate ω_i in equation (12) can then be re-written to be the same as Prigogine's equation:

$$\omega_i = k_i a_i \left[1 - \exp\left[- \frac{\bar{A}_i}{RT} \right] \right] \qquad (i=1,2,...,p) \qquad (2\text{-}14)$$

In these equations, the electrochemical affinities of reactions contain two portions, chemical and electrical. The electrical portion, which is common to all reacting elements, can not be directly measured (Bockris and Reddy, 1970). Thus,

there are p equations but p+1 unknowns (p reaction rates plus one electric term) to be determined.

In one special case, Hemptine, Eyring and Yee (1959) attempted to develop a quantitative relationship by using rate equations similar to equation (9). The theory was based on the measurable rate of evolved CO which was assumed to be part of interfacial reactions. Thus, one unknown was removed from the above equations. The simplification of systems and debatable assumptions made by Hemptine et al., were discussed by Lu (1971) and will not be repeated here. The question is, if there is no gas phase involved in the system, apparently, further studies of interfacial reactions could not be continued by using this approach. The same problem also exists in another theory of electrochemistry by introducing the concept of mixed electrode potential (Tokuda and Ohtani, 1971) since the reference state is also chosen from the measurable rate of evolved CO.

In another special case considered, Okongwu (1973) assumed that the exponential term containing electrochemical affinities $\bar{A}_i$ could be linearized, viz,

$$\exp\left[-\frac{\bar{A}_i}{RT}\right] \cong 1 - \frac{\bar{A}_i}{RT} \qquad (i=1,2,...,p) \qquad (2\text{-}15)$$

providing that $\frac{\bar{A}_i}{RT} << 1$. Then equation (14) is approximated as:

$$\omega_i \cong k_i a_i \frac{\bar{A}_i}{RT} \qquad (i=1,2,...,p) \qquad (2\text{-}16)$$

By applying the constraint of no-net electric current, viz,

$$\sum_{i=1}^{p} z_i \omega_i \equiv 0 \qquad (2\text{-}17)$$

electrical portion of electrochemical affinities can be calculated by knowing thermodynamic data and rate constants of all reactions in the system. Through these equations, Yamada (1977) discussed the coupling effect between electric field and charged reacting species by computed results in the idealized systems. Due to the lack of thermodynamic data in multi-component metallic/ionic systems, this theory has not yet been applied to a practical system.

The assumption that $\frac{\bar{A}_i}{RT} << 1$ implies that the electrochemical potential difference of every reaction between two phases is smaller than RT. In most cases, this assumption may not be valid at the beginning of reaction. The removal of this restrictive assumption becomes very important in the application of the theory to a practical system. It is one of the goals in the present work.

Another theoretical problem is the definition of ion activities in ionic solutions. From equation (10), the electrochemical activity of ions defined by the electrochemical potential of ions can be given as the product of chemical activity with one additional term containing the electrical portion of the electrochemical potential (Yamada, 1977), viz,

$$\bar{a}_i^{\prime} = a_i^{\prime} \exp\left[\frac{z_i \mathcal{F} \phi}{RT}\right] \qquad (i=1,2,...,p) \qquad (2\text{-}18)$$

where $a_i^{\prime}$ is the chemical activity of ions. However, chemical activity of ions in ionic solutions has not been properly defined (Forland, Forland and Ratkje, 1988) and the validity of the concept of ion activities in a general system was questioned by several authors (Blander, 1977, Forland and Grjotheim, 1978). Therefore, it is theoretically important to understand the meaning of ion activities in the above kinetic expressions. Studies of this subject is beyond the scope of the present thesis and discussions will be presented in Appendix A.

2-2-3 Determination of Interfacial Area in Experimental Studies

In earlier studies (Chang and Goldman, 1948, Goldman, Derge and Philbrook, 1954, and King and Ramachandran, 1956), interfacial area was assumed to be the same as that of the cross section of the crucible used. When both phases are liquid, this assumption could introduce very large errors in strongly mechanically stirred systems by using a rotating crucible and with CO gas evolution, or system with externally imposed electric field. It is very difficult to determine the interfacial area in these type of experiments.

To avoid the disturbance of interfacial area, Ray (1981) carried out experiments between rotating iron crucible and ionic melts contained in the crucible. By using metallographic analysis of inclusions in metallic phase, Ray reported that specific rate constant of Fe was of the order of magnitude of 10^{-4} cm/sec and that of oxygen 10^{-3} cm/sec at 1723 ^{o}K. With one solid phase, the assumption, that the interfacial area can be determined by the area of iron crucible in contact with the ionic liquid, should not be far from the true situation.

2-3 Diffusion in Multi-Component Systems

2-3-1 Phenomenological Theory of Diffusion

The phenomenological basis for multi-component diffusion was defined by Onsager (1945), de Groot and Mazur (1962) and reviewed by Kirkaldy and Young (1987). For a near equilibrium situation, there is a linear dependence between the forces and fluxes for one dimensional diffusion, viz,

$$J_i = \sum_{j=1}^{p} L_{ij} X_j \qquad (i=1,2,...,p) \qquad (2\text{-}19)$$

where J_i and X_i are any of the Cartesian components of independent fluxes and thermodynamic driving forces. The quantities L_{ij} are called the phenomenological coefficients. The internal entropy production per unit time and per unit volume, given by σ in equation (20) can be described by the sum of product of fluxes and forces (de Groot and Mazur, 1962, Prigogine, 1967), viz,

$$T\,\sigma = \sum_{i=1}^{p} J_i X_i \geq 0 \tag{2-20}$$

When fluxes and forces of components are independent of each other, reciprocal relations hold between the phenomenological coefficients, viz,

$$L_{ij} = L_{ji} \tag{2-21}$$

and it follows that the matrix L_{ij} must be positive definite, i.e.

$$L_{ii} > 0 \tag{2-22}$$

and

$$L_{ii}L_{jj} - L_{ij}L_{ji} > 0 \tag{2-23}$$

The validity of the Onsager reciprocal relations has been experimentally studied by Gosting and co-workers in liquid electrolytes (1952, 1953, 1956). Kirkaldy and co-workers (1957, 1958, 1962-1966) have amplified the physical basis in multi-component liquid electrolytes and metallic crystalline systems.

For the interpretation of chemical diffusion experiments, the fluxes must be defined with respect to a suitable frame of reference. There are four most common frames of reference: (1) solvent-fixed, (2) volume-fixed, (3) lattice-fixed and (4) laboratory-fixed. The solvent-fixed frame is that the solvent flux is zero, i.e.

$$J_{solvent} = 0 \tag{2-24}$$

The volume-fixed frame is that the flux moves locally so that no net flow of

volume occurs, i.e.,

$$\sum_{i=1}^{p} J_i \bar{V}_i = 0 \qquad (2\text{-}25)$$

where $\bar{V}_i$ is the partial molar volumes.

$$\bar{V}_i = \left(\frac{\partial V}{\partial N_i}\right)_{T,P,n_j(j\neq i)} \qquad (i=1,2,...,p) \qquad (2\text{-}26)$$

The lattice-fixed and laboratory-fixed frames of reference can be similarly defined. Any convenient reference frame can be chosen and a transformation exists from one to another (Kirkwood et al., 1960).

2-3-2 Diffusion in Non-Ionic Solutions

For chemical diffusion in a non-ionic system with p components, the chemical driving forces X_i are chemical potential gradients. Therefore, equation (20) for entropy production rate can be given by the following equation (de Groot and Mazur, 1962):

$$T\sigma = -\sum_{i=1}^{p} J_i \frac{\partial \mu_i}{\partial x} \qquad (2\text{-}27)$$

when $X_i = -\frac{\partial \mu_i}{\partial x}$, (i=1,2,...,p).

Since chemical potentials are not independent and can be related by Gibbs-Duhem equation, viz,

$$\sum_{i=1}^{p} N_i d\mu_i = 0 \qquad (2\text{-}28)$$

the reciprocal relation (21) is not applicable. If the volume-fixed frame of reference is chosen, this can be re-written from equation (25) as:

$$T\sigma = - \sum_{i=1}^{p-1} J_i \frac{\partial(\mu_i - \frac{\bar{V}_i}{\bar{V}_p}\mu_p)}{\partial x} \qquad (2\text{-}29)$$

which has a bilinear form in terms of independent fluxes J_i and forces:

$$X_i = - \frac{\partial(\mu_i - \frac{\bar{V}_i}{\bar{V}_p}\mu_p)}{\partial x} \qquad (2\text{-}30)$$

The relation between the fluxes and forces will have the form:

$$J_i = - \sum_{j=1}^{p-1} L_{ij} \frac{\partial(\mu_j - \frac{\bar{V}_j}{\bar{V}_p}\mu_p)}{\partial x} \qquad (i=1,2,...,p\text{-}1) \qquad (2\text{-}31)$$

In equation (31), Onsager reciprocal relation (21) is valid.

The phenomenological description of diffusion implied by equation (31) fully takes account of the cross effect of all other constituents of the system through chemical potential on the flux of any one species. Thus, the diffusion process in any multi-component system, no matter how complex, can be completely characterized once the phenomenological coefficients are known as functions of temperature, compositions and pressure.

For instance, in solid iron alloys (Kirkaldy and Young, 1987), iron may be chosen as the element p. The volume-fixed frame of reference may be approximated as laboratory-fixed frame of reference when impurity elements are dilute. On the other hand, a change of partial molar volume $\bar{V}_i$ and chemical potential of iron, μ_{Fe} along with diffusion pat . is assumed to be very small and negligible. Thus, equation (31) may be simplified by the following equation:

$$J_i^m = - \sum_{j=1}^{p-1} L_{ij} \frac{\partial \mu_j}{\partial x} \qquad (i=1,2,...,p-1) \qquad (2\text{-}32)$$

where J_i^m represents flux in metallic phase. In solution thermodynamics, chemical potentials of dilute elements are defined as:

$$\mu_i = \mu_i^o + RT \ln (f_i N_i) \qquad (2\text{-}33)$$

where μ_i^o is the reference chemical potential using Henrian scale, N_i is the mole fraction in metallic phase and f_i is Henrian activity coefficient which can be described by Wagner interaction parameters ε_i^j:

$$\ln f_i = \sum_{j=1}^{p-1} \varepsilon_i^j N_j \qquad (2\text{-}34)$$

By assuming the interaction parameters ε_i^j are independent of compositions, chemical potential gradients in equation (32) can thus be re-written as:

$$\frac{\partial \mu_i}{\partial x} = \frac{RT}{N_i} [1 + N_i \varepsilon_i^i] \frac{\partial N_i}{\partial x} \qquad (2\text{-}35)$$

Following Kirkaldy and Young (1987), the mobility matrix in equation (32) can be related to that in Kirkendall reference frame in the following way, viz,

$$L_{ii} = (1 - 2N_i) (L_{ii})_\kappa + (N_i)^2 \sum_{k=1}^{p-1} (L_{kk})_\kappa \qquad (\text{for } i=j) \qquad (2\text{-}36)$$

and

$$L_{ij} = - N_i (L_{jj})_\kappa - N_j (L_{ii})_\kappa + N_i N_j \sum_{k=1}^{p-1} (L_{kk})_\kappa \qquad (\text{for } i \neq j) \qquad (2\text{-}37)$$

where $(L_{ii})_\kappa$, $(L_{jj})_\kappa$ and $(L_{kk})_\kappa$ are the elements of mobility matrix in the Kirkendall reference frame where all cross terms are zero.

$$(L_{ii})_\kappa = \frac{\rho_m D_i^m N_i}{RT} \qquad (2\text{-}38)$$

where ρ_m is the molar density of the metallic phase (mole/cm^3).

Substituting equations (35), (36) and (37) into the flux equation (32), a flux equation described by mutual diffusion coefficients D^m_{ij} in metallic phase is obtained, viz,

$$J^m_i = - \sum_{j=1}^{p-1} D^m_{ij} \frac{\partial N_j}{\partial x} \qquad (i=1,2,...,p-1) \qquad (2\text{-}39)$$

where

$$D^m_{ij} = \frac{RT}{N_j} (1 + \varepsilon^j_i N_j) L_{ij} \qquad (2\text{-}40)$$

2-3-3 Diffusion in Ionic Solutions

The understanding of diffusion in ionic systems is complicated by the fact that the diffusion species are charged and there exist associations between ionic species. Thus, the forces in equation (19) should be described by the electrochemical potential gradients, (see also section 2-2), viz,

$$X_i = - \frac{\partial \bar{\mu}_i}{\partial x} \qquad (i=1,2,...,p) \qquad (2\text{-}41)$$

and therefore, the flux equation becomes:

$$J^s_i = - \sum_{j=1}^{p} L_{ij} \frac{\partial \bar{\mu}_j}{\partial x} \qquad (i=1,2,...,p) \qquad (2\text{-}42)$$

where superscript "s" represents the flux in ionic solutions. The application of the phenomenological theory to this type of system has been made by several authors (Okongwu, 1973, Nagata and Goto, 1976) and will be reviewed as follows.

Nagata and Goto (1976) attempted to evaluate all L_{ij}'s under following assumptions:

(1) the electrochemical potential can be separated into chemical potential of ions and another term containing electrical potential [equation (10)];

(2) diffusion generally proceeds under the condition of zero net current:

$$\sum_{i=1}^{p} z_i J_i^s \equiv 0 \tag{2-43}$$

and (3) the chemical potential of ions may be expressed by the chemical potential of neutral species in the case of inter diffusion experiments (e.g. oxides).

From the first assumption, mass flux equation (42) can be re-written as:

$$J_i^s = -\sum_{j=1}^{p} L_{ij} \left(\frac{\partial \mu_j}{\partial x} + z_j \mathcal{F} \frac{\partial \phi}{\partial x} \right) \qquad (i=1,2,...,p) \tag{2-44}$$

Then, by substituting equation (44) into (43), condition of no net electric current becomes the following alternative equation:

$$\sum_{i=1}^{p} \sum_{j=1}^{p} z_i L_{ij} \left(\frac{\partial \mu_j}{\partial x} + z_j \mathcal{F} \frac{\partial \phi}{\partial x} \right) \equiv 0 \tag{2-45}$$

Thus, electrical potential gradient is solved and mass flux may be expressed in such a way, viz,

$$J_i^s = -\sum_{j=1}^{p} T_{ij} \frac{\partial \mu_j}{\partial x} \tag{2-46}$$

where

$$T_{ij} = L_{ij} - \left(\sum_{k=1}^{p} z_k L_{ik} \sum_{l=1}^{p} z_l L_{lj} \right) / \sum_{k=1}^{p} \sum_{l=1}^{p} z_k z_l L_{kl} \tag{2-47}$$

From the third assumption, a general equation to connect with chemical potential of ions and neutral species was obtained, viz,

$$\mu_\alpha/z_\alpha + \mu_\beta/|z_\beta| = \mu_{\alpha\beta}/z_\alpha$$
$$= \mu_{\alpha B}/z_\alpha + \mu_{A\beta}/z_A - \mu_{AB}/z_A \qquad (2\text{-}48)$$

where α and β represent cation and anion respectively, $\alpha\beta$, AB, $A\beta$ are neutral combinations, A and B are the cation and anion which are selected expediently as the reference. Furthermore, the mass flux equation (46) can be rewritten as:

$$J_i = -\sum_\alpha T_{i\alpha}\frac{\partial \mu_{\alpha B}}{\partial x} + \sum_\alpha (z_\alpha/z_A)T_{i\alpha}\frac{\partial \mu_{AB}}{\partial x} - \sum_\alpha (|z_\beta|/z_A)T_{i\beta}\frac{\partial \mu_{A\beta}}{\partial x} \qquad (2\text{-}49)$$

In this approach, it is required that all L_{ij}'s (including both diagonal and off-diagonal items) in Onsager's matrix should be known. This has made the theory and mathematical operations very complicated. It has only been applied so far to diffusion couples of ternary slags (Goto et al. 1976, 1977).

To simplify the theory and formulations, it is necessary to avoid the evaluation of Onsager cross terms. In condensed phases, there exists a frame of reference for diffusion fluxes J_i in which all cross terms in the L_{ij} matrix are approximately zero. For the substitutional solution of metals, this has been recognized as the Kirkendall frame and for ionic liquid solutions, the frame depends on relative ionic radii (Lane and Kirkaldy, 1964).

In another approach, Okongwu (1973) derived diffusion equations for studies in glass phase. In addition to the first two assumptions shown in the above approach, Okongwu proposed that (1) the anion sublattice is fixed, i.e. a solvent-fixed frame of reference; and (2) the Onsager cross terms L_{ij} are small relative to the diagonal terms L_{ii}. The flux in the laboratory frame has the following relations:

$$J_i^s = -L_{ii}[\,\mathrm{grad}(\mu_i) - z_i\mathcal{F}E\,] \qquad (2\text{-}50)$$

or

$$J_i^s = - L_{ii} \frac{RT}{C_i'} \left[\frac{\partial C_i'}{\partial x} + C_i' \frac{\partial \ln \gamma_i}{\partial x} + z_i C_i' \frac{\mathcal{F}}{RT} \frac{\partial \phi}{\partial x} \right] \qquad (2\text{-}51)$$

$$(i=1,2,...,p)$$

where C_i' and γ_i are the ion concentration and activity coefficient of ith ionic species, respectively and E is the electric field given by electrostatic gradient, viz:

$$E = - \frac{\partial \phi}{\partial x} \qquad (2\text{-}52)$$

Following Darken (1951), the mobilities L_{ii} can be related to the tracer diffusion coefficients, D_i^s:

$$L_{ii} = \frac{D_i^s C_i'}{RT} \left[1 + C_i' \frac{\partial \ln \gamma_i}{\partial C_i'} \right]_{E=0} \qquad (2\text{-}53)$$

or in Einstein's approximation:

$$L_{ii} = \frac{D_i^s C_i'}{RT} \qquad (2\text{-}54)$$

The approximation from equation (53) to (54) implies that the activity coefficients γ_i vary slightly with C_i'.

With Einstein's approximation (54), the Nernst-Planck equation is thus derived:

$$J_i^s = - D_i^s \left[\frac{\partial C_i'}{\partial x} + \frac{z_i \mathcal{F} C_i'}{RT} \frac{\partial \phi}{\partial x} \right] \qquad (i=1,2,...,p) \quad (2\text{-}55)$$

In equation (55), electrostatic gradient is not directly measurable. Similarly, zero net current condition may be applied, viz,

$$\sum_{i=1}^{p} z_i D_i^s \left[\frac{\partial C_i'}{\partial x} + \frac{z_i \mathcal{F} C_i'}{RT} \frac{\partial \phi}{\partial x} \right] = 0 \qquad (2\text{-}56)$$

and electrostatic gradient can be calculated through equation (57).

$$-\frac{\partial \phi}{\partial x} = \frac{RT}{\mathcal{F}} \frac{\sum_{j=1}^{p} D_j^s z_j \frac{\partial C_j'}{\partial x}}{\sum_{j=1}^{p} D_j^s z_j^2 C_j'} \qquad (2\text{-}57)$$

By substituting equation (57) to equation (55) and using ion fractions as the concentration unit, the coupled diffusional flux can then be described by the following equation:

$$J_i^s = -\sum_{j=1}^{p} D_{ij}^s \frac{\partial (N_j' \rho_s)}{\partial x} \qquad (i=1,2,...,p) \qquad (2\text{-}58)$$

where

$$D_{ii}^s = D_i^s \left[1 - \frac{D_i^s z_i^2 N_i'}{\sum_{k=1}^{p} D_k^s z_k^2 N_k'} \right] \qquad (\text{for } i=j) \qquad (2\text{-}59)$$

and

$$D_{ij}^s = -\frac{D_i^s D_j^s z_i z_j N_i'}{\sum_{k=1}^{p} D_k^s z_k^2 N_k'} \qquad (\text{for } i \neq j) \qquad (2\text{-}60)$$

where N_i' represents the ion fraction in ionic solutions and ρ_s is the molar density of the ionic solution (mole/cm^3).

2-4 Coupled Interfacial Reactions and Diffusion

Measurements of concentration profiles for diffusion couples in single solid or glass phase have been well studied in many metallic or ionic systems (Kirkaldy and Young, 1987). Borom and Pask (1967) conducted experiments of diffusion measurements between Na_2O-SiO_2 glass and metal Fe at 950 ^oC. So far, to the best knowledge of the writer, this is the only experimental work reported in

the literature for the coupled interfacial reactions and diffusion in metallic/ionic systems. However, the results were given with measured concentration profiles of single element Fe in glass phase by using an electron probe microanalyzer with the probe beam size of 5 μm (see Fig. 2-8). Change in concentrations of all other elements in glass as well as those in metal was not reported. This is a case of measuring and studying a single element which may have the most pronounced changes in a multi-component system. However, it has been shown that interfacial concentration of iron in the glass phase, which could be extrapolated from the curves of concentration profiles in Fig. 2-8, changes with reaction time. It implies that, the reaction rate of Fe transfer at interface and its diffusion flux in the glass phase are related and of comparable magnitude.

These type of measurements could be further improved by using modern equipment of electron probe microanalyzer with an electron beam size of 50 nm or below and a resolution of 1 μm for quantitative analyses.

In slag/metal systems, slag is presumably in the liquid state. Mass transport in a liquid phase may take place by the diffusional process and convective flow due to local density difference. To include convective flow in the present work would make the theoretical formulations much more complicated. In order to focus our attention on studies of interfacial reactions, the elimination of convective flow is assured in the design of experiments in the present work by keeping metallic phase in the solid state.

Goto and co-workers (1976, 1977) studied the diffusion couples in slag/slag system. In one case, silicate slags (containing CaO, SiO_2 and Al_2O_3) were held in a capillary tube (ϕ4 mm) at uniform temperature of 1823 $\pm$ 2 ^{o}K to

minimize the convective flow. By comparing the measured concentration gradients with computed diffusion profiles, it was concluded that mass transport in slags with this experimental system took place by the diffusional process only.

CHAPTER THREE

KINETIC EXPRESSIONS OF INTERFACIAL REACTIONS IN MULTI-COMPONENT METALLIC/IONIC SYSTEMS

Based on the generally accepted conclusion that interfacial reactions in metallic/ionic systems are electrochemical in nature, a study of chemical kinetics leading to a quantitative expression for multi-component systems is outlined in this chapter. These rate equations will be a part of the model to be compared with experimental data in the present work.

3-1 General Rate Equations of Interfacial Reactions

3-1-1 Rate Equations of Electrodic Half-Cell Reactions

It has been shown in Chapter Two that the rate equations proposed by Wagner (1965), Prigogine (1967) and Lu (1971) are all mathematically equivalent. In this section, Prigogine's equation is used as the starting point for further developments.

$$\omega_i = k_i a_i \left[1 - \exp\left(- \frac{\bar{A}_i}{RT} \right) \right] \qquad (i=1,2,...,p) \quad (2\text{-}14)$$

where ω_i is the specific reaction rate in moles per unit area of interface, and $\bar{A}_i$ is the electrochemical affinity of ith reaction, a transfer of the element from metallic to ionic phase, which may be separated into a chemical portion and an electrical portion (Prigogine, 1967), viz,

$$
\begin{aligned}
-\bar{A}_i &= \bar{\mu}_i^{(s)} + z_i\bar{\mu}_e - \mu_i^{(m)} \\
&= (\mu_i^{(s)} - \mu_i^{(m)}) + z_i\left[\bar{\mu}_e + \mathcal{F}(\Delta\phi - \Delta\phi_{eq})\right] \\
&= \Delta\mu_i + z_i\left[\bar{\mu}_e + \mathcal{F}(\Delta\phi - \Delta\phi_{eq})\right] \qquad (i=1,2,...,p) \qquad (3\text{-}1c)
\end{aligned}
$$

where $\bar{\mu}_i^{(s)}$ is the electrochemical potential of ith ion, $\mu_i^{(s)}$ and $\mu_i^{(m)}$ are the chemical potential of the ion in ionic phase and the element in metallic phase, $\Delta\mu_i$ is, $\mu_i^{(s)} - \mu_i^{(m)}$, the chemical potential difference of the reaction across the interface, $\mathcal{F}$ is Faraday constant, $\bar{\mu}_e$ is the electrochemical potential of electrons in metallic phase, $\Delta\phi$ is the difference of electrical potential between ionic phase and metallic phase, i.e. $\Delta\phi = \phi_{ionic} - \phi_{metallic}$, and $\Delta\phi_{eq}$ is the value of $\Delta\phi$ at the equilibrium state, i.e. net flux of every element in the system is zero.

Chemical potential difference of the reaction $\Delta\mu_i$ can be evaluated by chemical activities of species in both phases, viz,

$$\Delta\mu_i = \Delta\mu_i^o + RT \ln \frac{a_i'}{a_i} = RT \ln \frac{a_i'/a_i}{(a_i'/a_i)_{eq}} \qquad (3\text{-}2)$$

where $\Delta\mu_i^o$ is the difference of chemical potentials at their standard states for half-cell reaction (2-7), a_i' is the chemical activity of ith ion in ionic solutions (definition of ion activity and its standard state are discussed in Appendix A), a_i is the chemical activity of ith element in metallic solution and 'eq' indicates the two-phase equilibrium state, i.e. $\Delta\mu_i=0$ (i=1,2,...,p).

$\bar{\mu}_e$ may be related to the electrochemical activity of electrons in the metallic phase.

$$\bar{\mu}_e = \bar{\mu}_e^o + RT \ln \bar{a}_e = RT \ln\left[\bar{a}_e/(\bar{a}_e)_{eq}\right] \qquad (3\text{-}3)$$

By substituting equation (1) into Prigogine's equation (2-14), reaction rates of

individual reactions can be expressed as follows:

$$\omega_i = k_i a_i \left[1 - \exp\left(\frac{\Delta\mu_i}{RT} \right) \exp\left(\frac{z_i \left[\bar{\mu}_e + \mathcal{F}(\Delta\phi - \Delta\phi_{eq}) \right]}{RT} \right) \right] \qquad (i=1,2,...,p) \qquad (3\text{-}4)$$

where $\Delta\phi = \phi_{ionic} - \phi_{metallic}$. In this way, the exponential term containing the electrochemical affinity of ith reaction in equation (2-14) is expressed as a product of two terms in equation (4). One is a function of chemical potential difference of the heterogeneous reaction, which may be evaluated through thermochemical data, and the other contains the electrical potential difference across interface. By using two different symbols, the general reaction rate equations are given in equations (5) to (7), viz,

$$\omega_i = k_i a_i \left[1 - L_i U^{z_i} \right] \qquad (i=1,2,...,p) \qquad (3\text{-}5)$$

where:

$$U = \exp\left(\frac{\bar{\mu}_e + \mathcal{F}(\Delta\phi - \Delta\phi_{eq})}{RT} \right) \qquad (3\text{-}6)$$

and

$$L_i = \exp\left(\frac{\Delta\mu_i}{RT} \right) = \frac{a_i'/a_i}{(a_i'/a_i)_{eq}} \qquad (3\text{-}7)$$

The parameter U is shown as a function of $(\Delta\phi - \Delta\phi_{eq})$ and electrochemical potential of electrons in equation (6). L_i depends exponentially on the chemical potential difference of the reaction. Both U and L_i are positive quantities. When chemical potential difference of a reaction is zero, it leads to $L_i = 1$. During the course of reaction, L_i may approach the final value, unity, from either side. In equation (5), L_i, a_i and k_i may be evaluated experimentally if the value of U is known. The collective property of the system, U, is not determinable

because $\Delta\phi$ at interface is not directly measurable (Bockris and Reddy, 1970). The system parameter, U, has to be determined simultaneously with all other unknowns in the system. Equation (5) stands for p equations for a system of p reacting elements but there are p+1 unknowns (U, ω_i, i=1,....,p) to be determined. One more equation is required to define the system (see the following section).

3-1-2. The Constraint of No Net Electric Current

Considering static charges, Guggenheim (1967) showed that for electrochemical considerations, electroneutrality may be assured in ionic solutions. Any departure from neutrality which exists would be far too small to be detected chemically. In one computed example, Guggenheim demonstrated that if the system contains an excess of 10^{-10} moles of an ionic species with charge number +1 in a system of spherical shape of a diameter of 10 mm, the electrical potential will increase up to 0.86×10^{7} volts. This huge electric field could be encountered only in specialized high tension laboratories. Thus, the constraint of no net electric current that leads to no further change from initial electric state (also stated as an electroneutrality condition) may be applied to reactions at interface of metallic/ionic systems, viz,

$$\sum_{i=1}^{p} z_i\omega_i = 0 \qquad (3\text{-}8)$$

In equation (8), reaction rates of transfer of all elements in the system are coupled. Thus, it may be called the coupling equation in the present work. Combining equations (5) and (8), p+1 unknowns in the form of ω_i's, L_i's, k_i's and U can be uniquely determined and numerically solved once other parameters and initial conditions are defined. The detailed mathematical methods are presented

in Appendix B where the system parameter U is solve by the coupling equation (8). So that it is named as the "coupling factor" through which coupling effect among interfacial reactions can be illustrated in the following sections.

3-2 Electrical Over Potential Difference Across Interface

In equation (6), the coupling factor, U, is a function of two quantities, i.e., $(\Delta\phi-\Delta\phi_{eq})$, a measure of the deviation of electric field from the final state at interface and $\bar{\mu}_e$, electrochemical potential of electrons. It may be further assumed that there is little change of the electrochemical potential of electrons during the course of reaction, when there is no drastic change in chemical compositions. Then we arbitrarily define $\bar{\mu}_e \equiv 0$. This means that $(\Delta\phi-\Delta\phi_{eq})$ can be related to U through the simplified equation (9).

$$\Delta\phi - \Delta\phi_{eq} = \frac{RT}{\mathcal{F}} \ln U \qquad (3\text{-}9)$$

When $\Delta\phi - \Delta\phi_{eq}$ approaches zero, the coupling factor U approaches unity. This is a state of zero interaction through an electric field and all reactions may proceed independently under their own chemical driving forces. At this stage, $\Delta\phi = \Delta\phi_{eq}$.

When the coupling factor U is not unity, it implies that the electrical over potential difference across interface deviates from its equilibrium state. Since $\Delta\phi = \phi_{ionic} - \phi_{metallic}$, when $\Delta\phi>0$, it indicates that electrical potential in ionic phase is larger, i.e. $\phi_{ionic}>\phi_{metallic}$ and vice versa. Direction of the electric field is thus defined. For instance, when $\Delta\phi-\Delta\phi_{eq}$ is greater than zero, the electric field will assist anions and hinder cations into the ionic phase from the metallic phase (see Table 3-1).

TABLE 3-1: RELATIONSHIP BETWEEN CALCULATED ELECTRIC OVER POTENTIAL DIFFERENCE ACROSS INTERFACE AND THE INFLUENCE ON TRANSFER OF IONS INTO IONIC PHASE

$\Delta\phi - \Delta\phi_{eq} > 0$ $U > 1$	$\Delta\phi - \Delta\phi_{eq} = 0$ $U = 1$	$\Delta\phi - \Delta\phi_{eq} < 0$ $U < 1$
Attracting Anions & Repelling Cations	Zero Interaction	Attracting Cations & Repelling Anions

3-3 Discussion of Coupling Among Interfacial Reactions

3-3-1 The Coupling Factor and the Coupling Effect Term

The thermodynamic driving force of every spontaneous electrodic half-cell reaction at interface may be the lowering of electrochemical potential difference associated with this reaction. The consequence of accepting that an electrochemical potential may be split into a chemical portion and an electrical portion, is that even a spontaneous reaction will result in lowering the electrochemical potential difference of the reaction, but not necessarily both chemical and electrical potential differences. The decrease in the sum is not necessarily due to lower values in both parts.

From the formulations in Section 3-1-1, it is clear that interactions among co-existing species or simultaneous reactions take place through two parameters, i.e. thermodynamic activities a_i and electric field across the interface which is characterized by the coupling factor U.

The variation of a_i as a function of compositions of the solution is included in the formulation and numerical computations (see Section 6-1-2). Our discussion here is focused on the dependence of ω_i on L_i and z_i which are properties of individual reactions under consideration and the coupling factor U

which is a collective property of the system.

To facilitate the discussion on the role of the electric field in interfacial reactions, a separation of L_i and U in the general rate expression is needed. It may be done as follows:

$$\omega_i = k_i a_i \left[1 - L_i U^{z_i}\right] - k_i a_i L_i + k_i a_i L_i$$

$$= k_i a_i \left[1 - L_i\right] + k_i a_i L_i \left[1 - U^{z_i}\right] \qquad (3\text{-}10)$$

When U = 1, it is the case that effective interference of electric field on the movement of ions is absent. The mass flux across interface will be determined by the chemical portion of driving force and may be labeled by ω_i^{CH}, which is called the intrinsic chemical reaction rate, viz,

$$\omega_i^{CH} = k_i a_i \left[1 - L_i\right] \qquad (i=1,2,...,p) \qquad (3\text{-}11)$$

where $(1 - L_i)$ may be defined as the intrinsic chemical driving force of the half-cell reaction. The second term in equation (10), therefore, may be labeled as the coupling effect term.

$$\text{Coupling Effect Term} = k_i a_i L_i \left[1 - U^{z_i}\right] \qquad (3\text{-}12)$$

In this way, the magnitude of the coupling effect term depends on two terms, "$k_i a_i L_i$" which is a function of state of reacting elements under investigation and $(1 - U^{z_i})$. The sign of this term, however, depends on the value of $(1 - U^{z_i})$. For the reaction involving a cation, i.e. $z_i > 0$, the coupling effect becomes negative when U>1 or positive when U<1.

3-3-2 Directions of Mass Fluxes with Coupling

Since L_i and U are both non-negative quantities, directions of mass fluxes are determined by $(1 - L_i)$ and $(1 - U^{z_i})$ in equation (10). When $(1 - L_i) > 0$, the intrinsic chemical reaction of ith element tends to move from the metallic phase to the ionic phase, and vice versa. The term $(1 - U^{z_i})$ stands for the influence of an electric field which can either attract ions to or repel ions from the ionic phase, depending on the direction of the field and the sign of charges carried by these mobile ions (see Table 3-1).

Therefore, the direction of the mass flux can be referred to the result of interaction between the intrinsic chemical reaction and the electric field at interface. There are following cases to be considered.

3-3-2-1 Both driving forces of intrinsic chemical reactions and electric field are in the same direction

When these two driving forces are reinforcing each other, one may say that the intrinsic chemical reaction is accelerated by electrical force. From equation (10), this condition may be mathematically described as $(1 - L_i)/(1 - U^{z_i}) > 0$. To satisfy this inequality, L_i and U^{z_i} should be either both larger or smaller than unity. The physical state of these two cases are:

(1) $L_i < 1$ and $U^{z_i} < 1$

Both terms in equation (10) are positive. The intrinsic chemical reaction proceeds from metallic phase to ionic phase. It may be the case that cations are attracted to negatively charged ionic phase or anions to positively charged ionic phase.

(2) $L_i > 1$ and $U^{z_i} > 1$

Both terms in equation (10) are negative. The intrinsic chemical reaction proceeds from ionic phase to metallic phase. It may be the case that anions are repelled from a negatively charged ionic phase or cations from a positively charged ionic phase.

3-3-2-2 Driving forces of intrinsic chemical reactions and electric field are in opposite directions, i.e. the resultant direction of an individual mass flux is determined by the one of larger magnitude

In this case, the intrinsic chemical reaction rate and the coupling term in equation (10) tend to cancel each other. The sign of the resultant mass flux, i.e. observed mass flux, is determined by the larger term. This can be characterized as $(1 - L_i)/(1 - U^{z_i}) < 0$. In addition to the requirement that $(1 - L_i)$ and $(1 - U^{z_i})$ are of different signs, further refinements are needed. Discussion may be facilitated with the use of ratios of ω_i (observed) to ω_i^{CH} (intrinsic), from equations (5) and (11),

$$\frac{\omega_i}{\omega_i^{CH}} = \frac{1 - L_i U^{z_i}}{1 - L_i} \tag{3-13}$$

Various cases in which the electric field hinders the interfacial reaction will be discussed in terms of equation (13). In comparison with ω_i^{CH}, the resultant ω_i has to be smaller in magnitude which may or may not be in the same direction. Therefore, the following inequality would be true.

$$\frac{\omega_i}{\omega_i^{CH}} < 1 \tag{3-14}$$

Furthermore, equation (14) may be subdivided into the following three cases.

(1) The coupling term is smaller in magnitude, i.e. the resultant mass flux is in the direction of intrinsic chemical reaction, i.e.

$$0 < \frac{\omega_i}{\omega_i^{CH}} < 1 \tag{3-15}$$

By substituting equation (13) into equation (15), we obtain that:

$$0 < \frac{1 - L_i U^{z_i}}{1 - L_i} < 1 \tag{3-16}$$

This shows that the driving force of the intrinsic chemical reaction is larger than the electrical force and that the intrinsic chemical reaction is retarded.

(2) Zero flux state: actual mass flux is zero but intrinsic chemical flux is not, i.e.

$$\frac{\omega_i}{\omega_i^{CH}} = 0 \tag{3-17}$$

It is the case that an instantaneous chemical driving force of the reaction is exactly cancelled by an electrical force. It is interesting to note that zero flux for the reaction does not necessarily mean that the system has reached the final equilibrium state. Only when all L_i's (i=1,2,...,p) and U reach unity should the system be regarded as the final equilibrium state. When the momentary values of U and L_i that will result in zero mass flux, meet the following condition:

$$L_i U^{z_i} = 1 \tag{3-18}$$

this zero flux state can not last because the continuation of other reactions will cause U and L_i to change, so that the relationship in equation (18) can not be maintained.

(3) The driving force of the intrinsic chemical reaction is smaller than the electrical force, i.e. resultant mass flux is determined by the coupling term and proceeds in the direction determined by the electrical force.

$$\frac{\omega_i}{\omega_i^{CH}} < 0 \qquad (3\text{-}19)$$

The charged ion is then attracted or repelled by the electric field but the direction of mass flux is against the chemical driving force of the reaction. As the consequence of the resultant flux, the chemical driving force of the reaction may be increased with time. When electrical force diminishes as the result of reaction, the chemical driving force of the reaction increases. It gradually leads to a zero flux situation. In the later stage of reaction, the driving force of the electric field decreases so that the resultant flux would then be determined by the chemical driving force. The direction of mass flux of this element across the interface is reversed.

From the above, it has been seen that the coupling among simultaneous reactions at interface may be discussed in terms that an intrinsic chemical reaction may be accelerated or retarded by the electric field. As reactions proceed, both chemical driving forces of reactions [$(1 - L_i)$, i=1,2,...,p] and the coupling factor U will change with reaction time. It is of theoretical interests to understand how individual reactions under different chemical driving forces, which may be characterized by different initial conditions, proceed. In the present work, it will be demonstrated through slag/metal reactions in Chapter Seven.

3-4 Rate Expressions for Slag/Metal Reactions

In the general rate equation (5), intrinsic chemical driving force of the half-cell reactions ($1 - L_i$) is defined through ion activities and reaction rate constants, k_i (i = Fe, Mn, etc.) for the first order reaction, are defined with the unit of cm/sec since chemical activities of elements in metallic phase are defined by the molar concentrations (mole/cm^3) for each element. In the current literature, reaction thermodynamics relating to ionic solutions such as silicate melts are reported in the form of neutral species and solution thermodynamics in metallic phase are documented through Henrian activities for solutes and Raoultian activities for the solvent. In order to directly apply these thermochemical data reported, the rate equations must be modified.

In the system consisting of the silicate slag (SiO_2, FeO, MnO, Al_2O_3 and CaO) and iron alloy (Fe, Mn, Si, Ca, Al and O), the modified rate expressions for these six elements are shown below by using oxygen anion as the reference. The coupling factor U is then replaced by the parameter U_o. Rate equations are expressed as a function of specific rate constants, activities of elements in metallic phase, activities of oxides in silicate melts and equilibrium constants of chemical reactions of formation of oxides (see Apendix B for details). For transfer of iron, Raoultian activity coefficient of iron is used, i.e.

$$\omega_{Fe} = k_{Fe} C_{alloy} \gamma_{[Fe]} N_{[Fe]} \left[1 - \frac{a_{FeO}}{K_{FeO} \gamma_{[Fe]} N_{[Fe]}} U_o^2 \right] \qquad (3\text{-}20)$$

and for transfer of solutes in the alloy, Henrian activities are given, viz,

$$\omega_{Mn} = k_{Mn} \frac{C_{alloy} \gamma^o_{Mn}}{W_{Mn} \sum_i^p ([\%i]/W_i)} h_{[Mn]} \left[1 - \frac{a_{MnO}}{K_{MnO} h_{[Mn]}} U_o^2 \right] \qquad (3\text{-}21)$$

$$\omega_{Ca} = k_{Ca} \frac{C_{alloy} \gamma^{o}_{Ca}}{W_{Ca} \sum_{i}^{p} ([\%i]/W_i)} h_{[Ca]} \left[1 - \frac{a_{CaO}}{K_{CaO} h_{[Ca]}} U_o^2 \right] \quad (3\text{-}22)$$

$$\omega_{Al} = k_{Al} \frac{C_{alloy} \gamma^{o}_{Al}}{W_{Al} \sum_{i}^{p} ([\%i]/W_i)} h_{[Al]} \left[1 - \frac{a^{1/2}_{Al_2O_3}}{K^{1/2}_{Al_2O_3} h_{[Al]}} U_o^3 \right] \quad (3\text{-}23)$$

$$\omega_{Si} = k_{Si} \frac{C_{alloy} \gamma^{o}_{Si}}{W_{Si} \sum_{i}^{p} ([\%i]/W_i)} h_{[Si]} \left[1 - \frac{a_{SiO_2}}{K_{SiO_2} h_{[Si]}} U_o^4 \right] \quad (3\text{-}24)$$

$$\omega_{O} = k_{O} \frac{C_{alloy} \gamma^{o}_{O}}{W_{O} \sum_{i}^{p} ([\%i]/W_i)} h_{[O]} \left[1 - \frac{1}{h_{[O]}} U_o^{-2} \right] \quad (3\text{-}25)$$

where $\gamma_{[Fe]}$ is Raoultian activity coefficient of iron, γ^{o}_{Mn}, etc. are Henrian constants, $h_{[Mn]}$, etc. are Henrian activities of these impurity elements using one weight percent as the standard state, W_i is the molar weight (i = Fe, Mn, etc.), C_{alloy} is the density of alloy in moles per unit volume (for the alloy used in the present study, C_{alloy} = 0.125 mole/cm^3), a_{FeO}, etc. are activities of oxides in silicate melts and K_{FeO}, etc. are equilibrium constants of the following reactions:

$$[Fe] + [O] = (FeO) \quad (3\text{-}26)$$

$$K_{FeO} = \left[\frac{a_{(FeO)}}{\gamma_{[Fe]} N_{[Fe]} h_{[O]}} \right]_{eq.}$$

$$[Mn] + [O] = (MnO) \quad (3\text{-}27)$$

$$K_{MnO} = \left[\frac{a_{(MnO)}}{h_{[Mn]} h_{[O]}} \right]_{eq.}$$

$$[Ca] + [O] = (CaO) \quad (3\text{-}28)$$

$$K_{CaO} = \left[\frac{a_{(CaO)}}{h_{[Ca]} h_{[O]}} \right]_{eq.}$$

$$2\,[Al] + 3\,[O] = (Al_2O_3) \qquad (3\text{-}29)$$

$$K_{Al_2O_3} = \left[\frac{a_{(Al_2O_3)}}{h^2_{[Al]} h^3_{[O]}} \right]_{eq.}$$

$$[Si] + 2\,[O] = (SiO_2) \qquad (3\text{-}30)$$

$$K_{SiO_2} = \left[\frac{a_{(SiO_2)}}{h_{[Si]} h^2_{[O]}} \right]_{eq.}$$

In equations (20) to (25), U_O is a common term containing the coupling factor given in equation (31):

$$U_O = U \left[\frac{(a_{O^=(Ca^{++})}/h_{[O]})_{eq}}{a_{O^=(Ca^{++})}} \right]^{1/2} \qquad (3\text{-}31)$$

where $a_{O^=(Ca^{++})}$ is the activity of oxygen anion in slag by selecting neutral species CaO as the standard state (detailed definition is shown in Appendix A). Applying the constraint of no net electric current to this system, we have:

$$2\omega_{Ca} + 2\omega_{Fe} + 2\omega_{Mn} + 3\omega_{Al} + 4\omega_{Si} - 2\omega_{O} \equiv 0 \qquad (3\text{-}32)$$

The kinetic behavior of this slag/metal system of six elements is defined by seven equations, (20) to (25) and (32).

CHAPTER FOUR

A MATHEMATICAL MODEL OF THE COUPLING OF INTERFACIAL REACTIONS AND DIFFUSION IN SLAG/METAL SYSTEM

In this chapter, the development of a mathematical model of the coupling of interfacial reactions and diffusion in slag/metal systems will be presented. Interfacial reactions will serve as part of the boundary conditions for the diffusion equations in both ionic and metallic phases. Comparison between computed results and experimental data will be shown in Chapter Six.

4-1 The Law of Conservation of Mass

During the course of reaction, mass fluxes across the interface will cause changes of interfacial concentrations in both phases. Concentration gradients are induced near the interface due to the consumption of reactants and the creation of products. The consequence of the presence of concentration gradients, of course, are diffusion between interfacial region and bulk phases. Based on the law of conservation of mass for the one dimensional system, the gradient of diffusional flux of ith element in a bulk phase can be related to change of concentrations with time.

$$\frac{\partial C_i}{\partial t} = - \frac{\partial J_i}{\partial x} \qquad (i=1,2,...,p) \qquad (4\text{-}1)$$

where C_i is the concentration (mole/cm^3) and J_i is the diffusional flux (mole/cm^{2}sec.) of ith element. To solve this equation, the expression of J_i as a

function of concentrations, and initial and boundary conditions are required. In slag/metal system, flux equations are used in the present work. For metallic phase, the approach of Kirkaldy and Young (1987) will be followed and for slag phase, Okongwu's (1973) formulism is adopted. It is also assumed that the interfacial surface is flat so that diffusion equations are one dimensional in the direction perpendicular to the interface. Thus, two sets of partial differential equations, one for slag and the other for metallic phase, which are related by sharing interfacial reactions at the phase boundary are to be solved numerically. In the following equations, the single spatial variable x is defined by locating the slag/metal interface at x=0, slag in the region of x<0 and metal phase x>0.

(1) Diffusion in Slag

By substituting equation (2-58) which satisfies the neutrality condition in ionic phase into equation (1) and taking ion fraction as the concentration unit, we obtain that,

$$\frac{\partial N_i'}{\partial t} = \sum_{j=1}^{p} \frac{\partial}{\partial x}\left(D_{ij}^{s} \frac{\partial N_j'}{\partial x} \right) = \sum_{j=1}^{p} \left(\frac{\partial D_{ij}^{s}}{\partial x} \frac{\partial N_j'}{\partial x} + D_{ij}^{s} \frac{\partial N_j'^{2}}{\partial x^{2}} \right) \qquad (4\text{-}2)$$

$$(i=1,2,\ldots,p)$$

with the initial condition (I.C.):

$$N_i' \ (t = 0,\ x < 0) = N_i'^{o} \qquad (4\text{-}3)$$

and the boundary conditions (B.C.):

$$N_i' \ (t = t,\ x = -\infty) = N_i'^{o} \qquad (4\text{-}4)$$

and

$$\rho_s \frac{\partial N_i'}{\partial t} (t = t,\ x = 0^{-}) = \frac{\omega_i}{\delta x_s} \qquad (4\text{-}5)$$

where D_{ij}^{s} is the diffusion coefficient for ith flux due to the jth concentration

gradient in the ionic phase defined in equations (2-59) and (2-60), N_i' is ion fraction in slag (see Appendix A for definition), ρ_s is molar density of slag and δx_s is thickness of physical interface on slag side.

(2) Diffusion in Metal

Similarly, equation (2-39) may be substituted into equation (1), viz,

$$\rho_m \frac{\partial N_i}{\partial t} = \sum_{j=1}^{p} \frac{\partial}{\partial x} \left[D_{ij}^m \frac{\partial N_j}{\partial x} \right] = \sum_{j=1}^{p} \left[\frac{\partial D_{ij}^m}{\partial x} \frac{\partial N_j}{\partial x} + D_{ij}^m \frac{\partial N_j^2}{\partial x^2} \right] \quad (4\text{-}6)$$

$(i=1,2,...p)$

with the initial condition (I.C.):

$$N_i\ (t = 0,\ x > 0) = N_i^o \quad (4\text{-}7)$$

and the boundary conditions (B.C.):

$$N_i\ (t = t,\ x = \infty) = N_i^o \quad (4\text{-}8)$$

and

$$\rho_m \frac{\partial N_i}{\partial t}(t = t,\ x = 0^+) = -\frac{\omega_i}{\delta x_m} \quad (4\text{-}9)$$

where D_{ij}^m is the diffusion coefficient for ith flux due to the jth concentration gradient in the metallic phase defined in equation (2-40), N_i is the mole fraction of ith element, ρ_m is molar density of alloy and δx_m is thickness of physical interface on the metal side.

In equations (5) and (9), ω_i is the rate for transfer of ith element. δx_m and δx_s are the thickness of metallic and ionic portions of the interfacial reaction zone and will be discussed in Chapter Six.

Therefore, there are two sets of partial differential equations of the second order with semi-infinite boundary conditions to be solved. Since values of ω_i and interfacial concentrations are computed by using numerical methods (see

Appendix B), the observation of boundary conditions described in equations (5) and (9) may be presented numerically in the following section. These partial differential equations are to be solved by using finite difference method (Appendix C).

4-2 The Strategy of Computations

In computations, the simultaneous process of chemical reactions and diffusion in a physical system may be replaced by sequential steps, alternating between chemical reactions and diffusion. As an example shown in Fig. 4-1, the computation starting at t=0 is presented. In the computation of chemical reactions, calculation of diffusion is pending. Two sets of important parameters are chosen, i.e. δx_m and δx_s for the size of reaction zone, and the time interval Δt_R and n for calculation of concentration changes and number of iterations.

When $t = n\ \Delta t_R$, the calculation of changes due to chemical reactions is off, and then the computation of diffusion is switched on. With concentrations obtained in the reaction zone at $t = n\ \Delta t_R$ as boundary conditions, calculation of semi-infinite diffusion involves the exchange of chemical elements between the reaction zone and bulk phases. In numerical solutions, the spacing Δx in both phases and the time interval Δt_D are chosen. The calculation is then repeated m times.

When $t = m\ \Delta t_D$, the calculation of diffusion is turned off and that of chemical reactions starts again. By this alternating method, the computation of kinetics can be continued until a pre-determined time or equilibrium state is approached. The time intervals, Δt_R and Δt_D, are separately determined to seek a compromise between the convergence of numerical solutions and the effort of

computations. By adjusting the number of iterations, i.e. m and n, in the calculation of changes due to chemical reactions and diffusion, the total time period, n Δt_R and m Δt_D, must be equal to reflect the reality in the simultaneous processes. Details of choosing these time intervals are shown in Chapter Six. The computer program for slag/metal reactions is attached in Appendix F.

CHAPTER FIVE

EXPERIMENTAL PROCEDURES AND RESULTS

In the selection of a metallic/ionic system for experimentation, it is essential that the documentation of solution thermodynamics in both phases are adequate to carry out theoretical analysis for comparison. For this reason, slag and iron alloy which are free of carbon were chosen. The following considerations should also be taken into account: (1) diffusion is the primary process of mass transport from bulk phase to interface and vice versa; (2) kinetic parameters for diffusion in both phases are available because the primary subject of study in the present work is the coupling of interfacial reactions. The experimental procedures and results are presented in this chapter.

5-1 Materials Preparation

Slags and alloy were made from chemicals of known purity in our laboratory. Chemical reagents, SiO_2 powders (99.995+%), Al_2O_3 powders (99.99%), CaO powders (99.95%), iron lumps (99.9+%), manganese flakes (99.98%) and silicon lumps (99.9+%) were used. SiO_2, iron lumps and manganese flakes were supplied by Aldrich Chemical Company, Inc. and others from Alfa Products. Most individual impurity elements were below 100 ppm in each of the chemical reagents. Some of the lot analyses reported on the labels are given in Appendix D.

5-1-1 Slag preparation

Two slags were used in the experiments. The target compositions of slags

are listed in Table 5-1, i.e. one is slightly acid (50 wt% SiO_2 and 30 wt% CaO) and the other is essentially neutral (40 wt% SiO_2 and 40 wt% CaO). The preparation procedures of slags are outlined as follows. Powders of CaO, Al_2O_3 and SiO_2 of reagent grade chemicals were heated at 673 ^oK for more than 2 hours to assure that all chemicals were water-free. Then, these powders were weighed and mixed in a ceramic bowl to give the required compositions. The mixed powders were held in a platinum container (ϕ50 mm) and heated to 1873 ^oK in a furnace, which will be described in Section 5-2-3 under atmosphere of high purity Ar (99.999%). Melting of the mixtures could be observed through the window at the top of the furnace when the furnace was heated above 1573 ^oK. To assure that the mixtures were completely melted and the melt was homogeneous, the slag was superheated to 1873 ^oK and kept for one hour. When the furnace was cooled down, the acid slag was found to be transparent and the neutral slag was found to be translucent. These slags were crushed into small pieces (less than 2 mm in size) and ready for use.

No additional chemical analysis was made on these slag pieces which will be used in experiments. The determination of slag compositions will be made by microprobe analysis which will be shown in Section 5-4.

5-1-2 Preparation of Fe-Mn-Si Alloy

In order to control the loss of manganese due to vaporization, a Fe-Mn alloy was prepared first from starting materials. The mixture of measured amounts of iron lumps and manganese flakes was put on a water-cooled brass container in a vacuum chamber and heated by an electric arc gun from above. In this process, the electric arc gun was movable in different directions on metal surface. Thus, it served for both melting of the alloy and stirring of the bath. A Fe-Mn alloy of

homogeneous composition (containing 22.33% of manganese, see Appendix D) was obtained.

The Fe-Mn alloy, Si and Fe lumps were then packed together in an alumina crucible of high purity (McDanel 998) and heated in a RF induction furnace with flowing argon of ultra high purity (99.9999%). The loss of manganese due to vaporization was minimized. Complete chemical analysis, by sampling at four randomly different locations in the crucible, is listed in Table 5-2 in which all elements except oxygen were analyzed by AtomComp direct reading spectrometers from Allied Analytical System (AAS). Oxygen was analyzed by inert gas fusion technique (Leco). It shows that concentrations of Mn and Si in the alloy were close to target values (see Table 5-1) within the difference of 0.1wt%. Aluminum and oxygen in the alloy, which were part of the reacting elements, were about 251 ppm and 77 ppm in average, respectively. Total amounts of all other major impurity elements (such as P, S, Cu, etc.) were about 220 ppm. The alloy was then cast into the rod shape (ϕ5 mm) and ready for use.

TABLE 5-1: TARGET COMPOSITIONS OF SLAGS AND ALLOY

Cases	Slag Composition			Alloy Composition	
	(%CaO)	(%SiO_2)	(%Al_2O_3)	[%Mn]	[%Si]
Slag #1	30.0	50.0	20.0	1.40	1.50
Slag #2	40.0	40.0	20.0		

TABLE 5-2: CHEMICAL ANALYSIS OF THE Fe-Si-Mn ALLOY

Element	Sample #1	Sample #2	Sample #3	Sample #4	Average
Mn (wt%)	1.35	1.38	1.35	1.43	1.38
Si (wt%)	1.45	1.49	1.45	1.54	1.48

Average concentration of trace elements (ppm):

Al	P	S	Cu	Co	Pb	As	Sn	Nb	B	O
251	38	62	58	4	9	2	33	12	1	77

5-2 Experimental Design

5-2-1 Determination of Temperature and Time

Fujisawa, Imaoka and Sakao (1978) reported solid-liquid equilibrium temperatures as a function of concentrations in Fe-Mn-Si alloy. The equation was given as:

$$t_e(^{o}K) = 1811 - 4.73\ [\%Mn] - 11.4\ [\%Si] \qquad (5\text{-}1)$$

According to this equation, melting temperature for the alloy Fe-1.5%Si-1.4%Mn is about 1783 ^{o}K . To assure that the alloy phase was in a solid state, experimental temperature was decided to be 1763 ^{o}K, 20 ^{o}K below the calculated melting temperature. At this temperature, the slags should be molten.

In slag/metal system, at the above chosen temperature, chemical reactions would proceed quickly. To study kinetics, short reaction time of experiments would be more desirable. On the other hand, there exist uncertainties in defining time zero due to time required for heating of the assembly, melting of slag and temperature control at initial stage of experiments. These uncertainties in defining the reaction time might take one or two minutes. In view of these

difficulties, the starting time of experiments for all specimens was the time when the assembly of slag and metal was lowered into the hot zone from the colder area (see Section 5-3). For experiments of shorter reaction time, 10 minutes were set. In order to see the pronounced difference in measured data, time for longer experiments was set for 80 minutes. Beyond this time, it was anticipated that interfacial reactions would be too slow.

5-2-2 Assembly for Slag/Metal System

A high purity alumina tube (closed at one end) from McDanel, Inc. (I.D.ϕ5 mm and O.D. ϕ7 mm) was used to hold the alloy bar (ϕ5 × 5 mm) and slag particles (0.5 grams and less than 2.0 mm in size) which were stacked on top of the metal rod. The open end of the alumina tube was tightened to a mullite rod (ϕ8.5 mm) which could be moved up and down to let the assembly reach the hot zone of the furnace (see Fig. 5-1).

When CaO is less than 40 % and Al_2O_3 is 20%, viscosity of the melts is reported to be greater than 8 poise (dyne-sec./cm) at 1773 ^{o}K (The Making, Shaping and Treating of Steel, 8th Ed. 1964). In the present system, the temperature is 10 ^{o}K lower, and the viscosity might be slightly higher. Goto and co-workers (1976, 1977) reported that convective flow in the slag of $CaO\text{-}Al_2O_3\text{-}SiO_2$ (viscosity is estimated to be 4 poise and higher) may be negligible in a capillary tube (ϕ4 mm) at a uniform temperature of 1873 ± 2 ^{o}K. Since slag used in the present work may be more viscous than theirs, convective flow in the slag is assumed to be negligible in the analysis of experimental results.

Following Kirkaldy and Young (1987), diffusion distance ($\sqrt{2Dt}$) may be estimated based on the self diffusion coefficient and time. Based on the values

of diffusion coefficients listed in Tables 6-6 and 6-7. the longest diffusion distance in 80 minutes, which were the longest reacting time in the experiments, is estimated to be less than 3 mm in slag and 0.3 mm in metal alloy. In the present work, the liquid slag column was estimated to be 10 mm high based on the magnitude of slag density at 1773 ^{o}K (The Making, Shaping and Treating of Steel, 1964) and the metal rod was about 5 mm long. Thus, consideration of semi-infinite diffusion in both phases can be justified.

Four specimens were prepared with two different slag compositions, i.e. acid and neutral slags. To separate these specimens, they were labeled as specimens 1a and 1b with the acid slag and 2a and 2b with the neutral slag. The specimens 1a and 2a will be used for shorter reaction time (i.e. 10 minutes) and the other two for longer reaction time (i.e. 80 minutes) of experiment.

5-2-3 Furnace Used For the Experiments

A vertical tubular furnace with the trade name "Rapid Temperature Furnace" was specially designed and made by C-M Inc., Bloomfield, N.J., USA, was used. It is heated by six pairs of U-shape lanthana resistors (about 500 mm in length) with a maximum temperature capacity of about 2023 ^{o}K (see Fig. 5-1). The furnace tube is made of high purity alumina (I.D. ϕ60 $\times$ 900 mm, McDanel 998), fitted and sealed at each end with water-cooled brass caps. Both brass caps were designed to allow gas to pass through and centrally located openings equipped with a swagelock. A thermocouple in the protection sheath was inserted into the working area of the furnace from the bottom of the furnace and sealed by using an O-ring. Through the opening on the top cap, a ceramic rod, connected with the assembly of slag and metal, described in Section 5-2-2, could move up and down. It could also be

fixed at any required position by using the swagelock. The length of hot zone at 1773 ± 5 ^{o}K in the furnace tube is about 200 mm with the flow rate 2.0 ml/min of Ar. During experiments, Ar of ultra high purity (99.9999%), dried by silica gel and P_2O_5 and deoxidized by Cu wires at 873 ^{o}K, was passing through from the bottom of furnace. The oxygen partial pressure was controlled at 10^{-13} atm.

Furnace temperature was controlled by the controller/programmer provided by the manufacturer (Eurotherm, type 822) and calibrated by Pt-6%Rh/Pt-13%Rh thermocouples inserted into the working area from the bottom of the furnace.

5-3 Experimental Procedures

Before experiments started, the assembly of slag and metal was initially located in the colder zone in the upper part of the furnace. The furnace was heated under purified Ar at a flow rate of 2.0 ml/min. When the temperature in the hot zone reached 1763 ^{o}K, measured by Pt-6% Rh/Pt-13% Rh thermocouples in the furnace and stabilized within the variation of ± 2 ^{o}K, the assembly was then lowered into the hot zone. A drop of temperature of about 10 ^{o}K was observed. In about one minute, the temperature would recover and stabilize at 1763 ± 2 ^{o}K. The moment the assembly was placed in the hot zone, was then taken as time zero of the experiment.

When the pre-determined time (10 minutes or 80 minutes) was reached, the whole assembly was taken out by opening the upper brass cap and quenched in blowing air. The slag and metal, which were contained in the alumina tubes, would be further prepared for microprobe analysis.

5-4 Electron Probe Microanalysis (EPMA)

By using a low speed diamond cutter, slag and metal together with the alumina tubes were cut along the direction of diffusion. The cross section of slag and metal was roughly ground on SiC papers of different grits, ranging from 240, 320, 400, to 600. Buehler AB Alpha polishing alumina type C (1.0 micron) and type A (0.3 micron) were used for fine polishing. The surface was then washed profusely with alcohol and dried under blowing air. The polished surface of specimens was coated with carbon for conduction purposes for microprobe analysis.

The electron probe microanalyzer (CAMECA, in Metals Technology Laboratories, CANMET, Ottawa) with three spectrometers, controlled electron beam current (±0.5%/24 hours) and 40^{o} X-ray take off angle was used. Elements in each phase were analyzed by stationary counting for 10 seconds on their characteristic X-rays with an accelerating voltage of 20 kV.

Resolutions of measurements were estimated to be about 1 - 2 μm in metallic phase and 2 - 3 μm in ionic phase (Packwood, 1991). Under the electron microscope, separation of slag and metal with a gap of 20 μm, due to different thermal expansion properties, was observed. The measurements started from the closest vicinity of the interface of slag and metal to the bulk phases, in the step of 10 μm for 100 μm and then the step of 50 μm for next 500 μm. The concentrations near the far end of the slag and alloy were also measured by EPMA. Pure elements were used as the standard to determine concentrations of each component. All X-ray data were converted by using the conventional ZAF method and listed in Appendix E.

5-5 Results and Discussion

5-5-1 Error Analysis

Errors introduced in the measurements may come from various instruments and treatment of X-ray data. The errors, due to counting and statistical treatment of X-ray intensities, depend on not only the instrument used, but also the chemical properties of the elements to be measured (e.g. atomic number) and physical properties of the slags and the alloy such as density, electrical conductivities, etc. Based on the capability of the instrument used at CANMET (Packwood, 1991), the precision of the electron probe microanalyzer from X-ray statistics is about ± 0.07 % Si and ± 0.03% Mn in the alloy. The accuracy from correction of data by the ZAF method is about 2% of the amount of silicon and 1% of the amount of manganese and iron present, respectively. In slag, precision and accuracies of Fe, Si and Mn are estimated lower than those in the metallic phase by a factor of two due to its lower density and low conductivity to electric current at ambient temperature. Errors of Al and Ca measurement in slags are of about the same magnitude as that of Si.

To examine these errors, concentrations measured by EPMA at the far end of the specimens, beyond the affected zone and the target values are compared (see Table 5-3). The results show that slag compositions in specimens 1a, 1b and 2a agree well with the target compositions within the error range. In specimen 2b, the measured value of Al_2O_3 by EPMA is about 5 wt% higher than the expected value. However, since the ratio of CaO to SiO_2 in 2a and 2b is nearly the same, an increase of Al_2O_3 by 5 wt%, would have little changes on the thermodynamic properties in the system. Especially activity coefficients of MnO in both 2a and 2b are about the same at concentrations of MnO below 8.0% (see Fig. 6-1). In the

alloy, it is shown in Table 5-3 that measured concentrations of Si and Mn by EPMA are within ±0.1 wt% of the target values, which would not have significant influence on values of thermodynamic activities of these elements.

TABLE 5-3: COMPARION BETWEEN TARGET COMPOSITIONS AND MEASURED VALUES BY EPMA AT FAR ENDS OF SPECIMENS

	Target Values	Specimens #1a	#1b	Target Values	Specimens #2a	#2b
(%CaO)	30.0	31.6±1.3	30.6±1.2	40.0	39.8±1.6	36.2±1.4
($\%Al_2O_3$)	20.0	19.8±0.8	20.3±0.8	20.0	19.8±0.8	25.5±1.0
($\%SiO_2$)	50.0	48.3±1.9	49.1±1.9	40.0	40.4±1.6	38.3±1.5
[%Mn]	1.40	1.46±0.03	1.45±0.03	1.40	1.46±0.03	1.45±0.03
[%Si]	1.50	1.65±0.07	1.62±0.07	1.50	1.41±0.07	1.43±0.07

5-5-2 Measured Concentration Profiles

In the present system, there are six elements, Mn, Fe, Ca, Al, Si and O taking part in the reactions. Since the alloy is free of carbon, no gas phase is evolved through chemical reactions, i.e. all chemical elements are conserved in condensed phases. Initially, there are three elements (Fe, Mn, Si) in the alloy and four (Al, Ca, Si, O) in the slags. When the reactions proceed, Fe and Mn move from metal to slag and Si moves in the opposite direction. Since solubilities of Al, Ca and O in the solid alloy are very low, at ppm levels, changes of concentrations or mass fluxes of Al, Ca and O in reactions may be too small to be comparable with the other three elements, particularly in maintaining the

electroneutrality condition.

By using the electron probe microanalyzer, Al, Ca and O in the alloy may be detected from beams of characteristic X-ray but can not be quantitatively analyzed for such low concentrations. Mn and Si can be quantitatively measured at their concentration levels observed in these specimens. Fe is the solvent in the alloy and its concentration may be obtained by the difference, once concentrations of all other solutes are measured. Since oxygen ion is too light for microprobe and it is the only anion in the slag, therefore, oxygen in the slag may be determined indirectly by stoichiometric relationships with the cations. The measured results are then presented in the form of concentration profiles of oxides (MnO, FeO, SiO_2, Al_2O_3, CaO) in the slag and those of Mn and Si in the alloy.

The measured concentrations in the unreacted zones are listed in Table 5-3 and the complete analysis is given in Appendix E. In Figs. 5-2 to 5-5, these data are plotted against diffusion distance and time. The error bars shown in these figures reflect the values discussed in the preceeding section. Due to large scales for the concentrations of SiO_2, CaO and Al_2O_3 in these figures, error ranges may be referred to the size of data points in these figures.

5-5-3 Discussion

In the current experimental work, we wish to use the measured results to validate our theory of kinetics of interfacial reactions in the slag/metal system. Measured concentration profiles of these elements must be of a quality that is adequate for this purpose. In the slag/metal system, iron and manganese are the heaviest elements and can be dissolved in both phases at concentrations high

enough for quantitative measurement by EPMA with good accuracies. Another element is silicon which can also be found in both phases at high concentrations but the accuracies in measurement by EPMA are lower, because Si is a lighter element.

From the above considerations, we designed our experimental system in such a way that initially iron and manganese all exist in metallic phase, i.e. there are no iron and manganese in slags. The alloy compositions were determined by a compromise between the applicable range of thermodynamic data in solutions reported in the literature and the effort of measurements by EPMA. In slags, two compositions with different concentrations of SiO_2 and CaO were used. In this system, reactions of manganese and iron at interface would initially have the largest chemical driving forces to enter the slag phase, and all other elements would behave likely through coupling. For example, through coupling, silicon should be driven across the interface to the metallic phase, that may or may not be against its own chemical driving force. During the course of reaction, the dominant role of Fe and Mn diminishes with time.

From Figs. 5-2 to 5-5, it can be seen that in the alloy, concentration of Mn decreases and that of Si increases. Thus, concentration gradients are induced by interfacial reactions. For the acid slag (in specimens 1a and 1b), the amount of silicon transferred to the alloy is noticeably larger by comparing concentrations of silicon near the reaction zone in the alloy between Figs. 5-2 and 5-4 or between Figs. 5-3 and 5-5. In the slag, initially there was no manganese and iron except as minor impurities carried from chemical reagents (at ppm levels). The increase of manganese and iron in the slag was observed by EPMA. Changes of concentrations of SiO_2, CaO and Al_2O_3 can be seen within the error range of X-ray analysis.

Among the measured results, concentration gradients of FeO and MnO in slag and manganese and silicon in alloy are more reliable. But changes of concentrations of FeO in slag and Si in alloy are relatively small, close to errors of measurements. Changes of concentrations of MnO in slag and manganese in alloy are the most pronounced. By plotting concentration profiles of MnO in slag and Mn in alloy from different specimens into a single figure (Fig. 5-6), the difference of Mn concentrations along the diffusion paths and at different times is clearly demonstrated. By extrapolating the concentration gradients of MnO and Mn to the interface, concentrations of Mn in the reaction zone of the alloy side and MnO in the slag side are shown to be functions of time.

In the next chapter, all above measured data will be compared with computed results, with particular emphasis on that of manganese.

CHAPTER SIX

COMPARISON BETWEEN EXPERIMENTAL AND COMPUTED RESULTS

In order to carry out the computations in this system, the values of equilibrium constants, chemical reaction rate constants, diffusion coefficients, activity coefficients, thickness of the reaction zone at interface and time intervals for the numerical solutions have to be determined. In this chapter, the evaluation of these parameters will be discussed. Thermochemical data reported in the literature will be examined. Parameters which have not been reported, will be determined by curve fitting, i.e. by comparing computed and measured results.

6-1 Thermochemical Data Reported in the Literature

6-1-1 Equilibrium Constants

It has been shown in the preceeding chapter that there are six reacting elements (Al, Ca, Fe, Mn, Si, O) distributed in two phases, slag and metal. These six elements may form five different oxides by five independent chemical reactions, as shown in Table 6-1, where standard Gibbs Free Energies of formation of these oxides are given. Both slag and metal are solutions. The standard states for the evaluation of activities of these chemical species in slag and alloy are in general chosen for the convenience of study.

In the present work, pure oxides are chosen as the standard states for neutral species in slag. In the metallic phase, iron is the solvent which may be assumed to obey Raoult's law. The other elements are solutes. Henrian scale by

using hypothetical one weight percent as the standard state is chosen for activities of solutes.

In the current literature, thermodynamic data for dissolution of elements in liquid iron have been extensively documented (e.g. Elliott, et al., 1963, 1974, 1985), but those for solid solutions at elevated temperatures are far from complete. Thermodynamic data for dissolution of Mn, Si and O in solid iron alloys but near the melting temperature were measured by Fujisawa, Imaoka and Sakao (1978), and Swisher and Turkdogan (1967). For the other two elements, Al and Ca, their solubilities are very low in liquid iron and would be even lower in the solid alloy. To the best of our knowledge, there is no report of thermochemical data for dissolution of aluminum and calcium in solid iron alloys. For computations in the present work, data for dissolution of Ca and Al in liquid iron are used without any changes. It is shown in Section 6-3 that reaction rates of Al and Ca moving across the interface are too low, in view of errors in our measurements, to be of any important consequence for the present study. Thus, the evaluation of parameters concerning these two elements would not have noticeable influence on major kinetic events of the present study. Changes of standard Gibbs Free Energy for dissolutions of the elements are listed in Table 6-2.

From the data in Tables 6-1 and 6-2, equilibrium constants at 1763 ^{o}K, which are included in the kinetic formulations are calculated and listed in Table 6-3.

TABLE 6-1: LIST OF RELEVANT CHEMICAL REACTIONS IN THE PRESENT WORK AND VALUES OF STANDARD GIBBS FREE ENERGIES OF FORMATION

Reactions	Free energies of formation (Joules)	Temperature (^{o}K)
$2Al\ (l) + \frac{3}{2}O_2 = Al_2O_3\ (s)$	$\Delta G_f^o = -1,679,470 + 321.70\ T$ *	1500 - 2000
$Ca\ (g) + \frac{1}{2}O_2 = CaO\ (s)$	$\Delta G_f^o = -785,990 + 191.20\ T$ *	1765 - 2000
$Fe\ (s) + \frac{1}{2}O_2 = FeO\ (l)$	$\Delta G_f^o = -229,440 + 43.80\ T$ *	1665 - 1809
$Mn\ (s) + \frac{1}{2}O_2 = MnO\ (s)$	$\Delta G_f^o = -384,600 + 72.78\ T$ **	298 - 1500
$Si\ (s) + O_2 = SiO_2\ (s)$	$\Delta G_f^o = -902,000 + 173.60\ T$ **	700 - 1700

* - data from Elliott, Gleiser and Ramakrishna (1963);

** - data from Kubaschewski and Alcock (1979).

TABLE 6-2: CHANGE OF STANDARD GIBBS FREE ENERGIES FOR DISSOLUTION REACTIONS AND HENRIAN CONSTANTS IN IRON ALLOY

Reactions	γ_i^o	ΔG^o (Joules/mole)	Temperature (^{o}K)
$\frac{1}{2}O_2(1\ atm) = [O]_{(s,1wt\%)}$	$\frac{9.5}{(1773\ ^{o}K)}$	- 41,860 + 14.46 T *	1673 - 1823
$Mn\ (s) = [Mn]_{(s,1wt\%)}$	1.55	-35.20 T **	1773
$Si\ (s) = [Si]_{(s,1wt\%)}$	0.001	-89.10 T **	1773
$Al\ (l) = [Al]_{(l,1wt\%)}$	200	- 63,160 - 27.9 T ***	1873
$Ca\ (g) = [Ca]_{(l,1wt\%)}$	2240	- 39,445 + 49.4 T ***	1873

* - data from Swisher and Turkdogan (1967);

** - data from Fujisawa et al. (1978);

*** - Sigworth and Elliott (1974).

TABLE 6-3: CHEMICAL REACTIONS AND EQUILIBRIUM CONSTANTS BETWEEN SILICATE SLAG AND IRON ALLOY OBTAINED FROM DATA IN TABLES 6-1 AND 6-2

Reactions	ΔG^{o} (Joules)	Equilibrium Const. at 1763 ^{o}K
[Fe] + [O] = (FeO)	- 54,350 - 16.70 T	300
[Mn] + [O] = (MnO)	- 218,360 + 53.90 T	4000
[Ca] + [O] = (CaO)	- 704,680 + 127.30 T	5.9×10^{15}
2[Al] + 3[O] = (Al_2O_3)	- 1,427,570 + 334.10 T	7.0×10^{24}
[Si] + 2[O] = (SiO_2)	- 551,785 + 141.70 T	8.8×10^{8}

TABLE 6-4 LIST OF INTERACTION PARAMETERS e_i^j, IN LIQUID IRON (data from Sigworth and Elliott, 1974)

i \ j	Al	Ca	O	Mn	Si
Al	0.045	-0.047	-6.6	0.0 *	0.0056
Ca	-0.072	-0.002	0.0 *	0.0 *	-0.097
O	-3.9	-0.45	-0.20	-0.021	-0.131
Mn	0.0 *	-0.07	-0.083	0.0	0.0
Si	0.058	0.18	-0.23	0.002	0.11

* - due to lack of data, the value zero is used in computations.

TABLE 6-5 LIST OF INTERACTION PARAMETERS IN THE ALLOY Fe-Mn-Si AT SOLID-LIQUID EQUILIBRIUM TEMPERATURE (Fujisawa, 1978)

e_{Mn}^{Mn} = - 0.004; Mn (s) < 1.9%	e_{Mn}^{Si} = - 0.123; Si (s) < 0.6%
e_{Si}^{Mn} = - 0.057; Mn (s) < 0.5%	e_{Si}^{Si} = 0.086; Si (s) < 1.4%

6-1-2 Activities in Alloy and Slag

In the metallic phase, Henrian activities and activity coefficients of dilute elements may be defined through following equations:

$$\log f_i = \sum_{j=1}^{p} e_i^j [\%j] \tag{6-1}$$

$$h_i = f_i [\%i] \tag{6-2}$$

where e_i^j is the first order interaction parameter of element j on element i, h_i and f_i are Henrian activity and activity coefficient of ith element using one weight percent as the standard state, respectively.

In the literature, considerable information is available on thermodynamic interactions among solutes in liquid iron (e.g. Sigworth and Elliott, 1974) and the relevant data are listed in Table 6-4. Fujisawa, Imaoka and Sakao (1978) reported interaction parameters between manganese and silicon in solid Fe-Mn-Si alloys near solid-liquid equilibrium temperature (Table 6-5). In the present study, the iron alloy was in the solid state, about 20 ^{o}K below melting temperature. Thus, data from Fujisawa et al. are the most relevant to our system.

Therefore, interaction parameters between Mn and Si from Fujisawa et al. will be used in the following computations. For the other elements, i.e. aluminum, calcium and oxygen, since there is no report of interaction parameters in solid iron to our best knowledge, values reported for liquid iron will be used. Since concentrations of aluminum, calcium and oxygen in the alloy are much lower (at ppm levels) than those of manganese and silicon, the use of values for liquid iron would not have significant influence on the study of kinetic behavior in our system.

In slag, the IRSID model (Gaye, Riboud and Welfringer, 1986) is used to

calculate activities of SiO_2, Al_2O_3, CaO and FeO, and have been shown by these authors to be in good agreement with measured data reported by other authors (e.g. Elliott, et al., 1963). For activity of MnO, Abraham, Davis and Richardson (1960), as well as Filer and Darken (1952) reported that when MnO is below 8 wt%, activity coefficient of MnO is constant at a constant ratio of $CaO:Al_2O_3:SiO_2$. When the ratio changes, e.g. by increasing SiO_2 from 40 wt% to 50 wt% with 20% of Al_2O_3 present, activity coefficient of MnO is reduced to nearly half from about 1.0 to 0.5 at 1873 ^oK (see Fig. 6-1). These values are much smaller than those calculated from the IRSID model.

In the present system, it is seen from the measured concentration profiles of oxides in slags (see Figs. 5-2 to 5-5) that changes of concentrations of CaO, Al_2O_3 and SiO_2 are within the error range. Activity coefficient of MnO may then be assumed to be constant during the course of reaction. To test the sensitivity of computed results to different values of activity coefficient of MnO, the computed results are compared with measured data in Fig. 6-2. It shows that computed MnO concentrations in the reaction zone by using values calculated from IRSID model are much smaller than measured values. This suggests that the activity coefficient of MnO computed from the IRSID model may be over estimated. Then, the relationship reported from Richardson et al. (1960) is used in the following computations.

6-1-3 Self Diffusion Coefficients

The measurements of self diffusion coefficients of iron, manganese, aluminum and silicon in iron alloys and cations of iron, silicon, calcium and aluminum and oxygen anion in silicate slag have been reported in the literature

and are listed in Table 6-6 and Table 6-7. Among these data reported, there were two values of diffusion coefficients of manganese in iron alloy at the same temperature which are different by two orders of magnitude. The diffusion coefficient of oxygen was documented only at a temperature of 1473 ^{o}K and below. On the other hand, diffusion coefficients of manganese ion in slag and calcium in the alloy have not been documented (to our best knowledge). Following the rules recommended by Kirkaldy and Young (1987), self diffusion coefficients of manganese ion in silicate melts and calcium in solid metal may be estimated to be of the order of magnitude of 10^{-5} cm^2/sec. and 10^{-7} cm^2/sec., respectively.

From the reacted specimens in our experiments, concentration gradients of manganese in alloy and MnO in slag are measured with confidence. The concentration gradients of other species, i.e. FeO, SiO_2, CaO, Al_2O_3 in slag and Al, Ca, O, Si in the alloy are less reliable than those of MnO and Mn, considering errors introduced by EPMA and the precision of the instrument. Therefore, the values reported or estimated which are reviewed above will be evaluated in Section 6-3.

TABLE 6-6: LIST OF SELF DIFFUSION COEFFICIENTS IN IRON ALLOY

System	Diffusing Elements	Temperature (^{o}K)	D ($cm^2/sec.$)	Reference
	Fe	1630	6.5×10^{-10}	Seith (1955)
	Mn (3wt%)	1673	1.0×10^{-7}	
	Al	1323	2.0×10^{-8}	
	Si (5wt%)	1708	1.1×10^{-7}	
Fe(1.15 wt%Mn)	Fe	1623	1.4×10^{-9}	Elliott (1963)
Fe(0.20 at%Mn)	Mn	1673	1.7×10^{-9}	
γ-Fe	Al	1373	3.7×10^{-8}	
γ-Fe	O	1473	1.0×10^{-9}	
Fe(0-4%Si)	Si	1708	$1.1(\pm0.2)\times10^{-7}$	
Fe (δ)	Fe	1773	2.0×10^{-7}	Askill (1970)

TABLE 6-7: LIST OF SELF DIFFUSION COEFFICIENTS IN SILICATE MELTS

Diffusing Ions	Compositions	Temperature (^{o}K)	D ($cm^2/sec.$)	Reference
Al^{26}	43%CaO-10%Al_2O_3-47%SiO_2	1760	1.2×10^{-8}-2.0×10^{-4}	Elliott (1963)
Si^{26}	39%CaO-20%Al_2O_3-41%SiO_2	1760	1.1×10^{-8}-3.3×10^{-6}	
Ca	40%CaO-21%Al_2O_3-39%SiO_2	1773	3.8×10^{-6}	
Si	39%CaO-21%Al_2O_3-40%SiO_2	1703	1.1×10^{-7}	
O^{18}	40%CaO-20%Al_2O_3-40%SiO_2	1773	1.6×10^{-5}	
Fe	43%CaO-22%Al_2O_3-35%SiO_2	1773	5.0×10^{-6}	Yang and Derge (1961)

6-1-4 Chemical Reaction Rate Constants

In the literature, there are numerous publications on the study of chemical kinetics in slag/metal systems. However, most of the experimental measurements were carried out for liquid slag and liquid metal which had been stirred with various intensities. In the extraction of reaction rate constants from the changes of concentrations in bulk phases as a function of time, there are two difficulties in heterogeneous systems, which are not usually recognized by authors, that: (1) the contribution of transport step, i.e. the existence of concentration gradients, is not corrected for and (2) the actual interfacial area is not known.

Among these experimental studies, the work which is relevant to our system has been reported by Derge and Birchenall (1953) and Ray (1981). Derge, et al. studied the transfer of radioactive isotope of iron from liquid iron to iron-silicate slag. In their measurements, a rotating crucible containing both slag and metal was used. Reaction rate constant of iron transfer was thus reported at 1873 ^{o}K to be that $k_{Fe} = 0.006$ sec^{-1}, by using the simple model of kinetics for pseudo-homogeneous systems, viz,

$$Fe^{*}(\text{iron}) \rightarrow Fe^{*}(\text{slag}) \tag{6-3}$$

$$-\frac{dC^{*}_{Fe}}{dt} = k_{Fe}C^{*}_{Fe} \tag{6-4}$$

With the assumption that convection and stirring were adequate to maintain a uniform composition in the slag and constant interfacial area, the above reaction rate constant may be converted to the value of a proper set of units for heterogeneous systems, i.e. $k_{Fe} = 1.4\times10^{-5}$ cm/sec.

To avoid the uncertainty of interfacial area in data analysis, Ray (1981) studied kinetics of interfacial reactions in Fe-CaF_2 and Fe-FeO systems at 1723 ^oK by using solid iron in the experiments. To obtain the reaction rate constants for iron and oxygen transfer, both electrochemical and chemical approaches were used and interfacial reactions in this system were described through the following simultaneous reactions:

$$Fe \rightarrow Fe^{2+} + 2\ e^- \tag{6-5}$$

$$O + 2\ e^- \rightarrow O^{2-} \tag{6-6}$$

In the electrochemical experiments, an external electrical current was imposed on the Fe/CaF_2 system where transfer of iron across the interface may be considered as the dominant reaction in the system. The net Faradiac current from the transfer of iron across the interface was expressed as:

$$i_F = i_o \left[\exp(-\frac{\alpha z \mathcal{F}}{RT}\eta_t) - \exp(-\frac{(1-\alpha) z \mathcal{F}}{RT}\eta_t)\right] \tag{6-7}$$

where i_o denotes the exchange current density and may be related to the reaction rate constant k_{Fe}, concentration C_{Fe}, activation energy ${}_oE_a$ and the potential difference at equilibrium $\Delta\phi_{eq}$, viz,

$$i_o = z\mathcal{F}k_{Fe}C_{Fe} \exp\{-({}_oE_a - (1-\alpha)z\mathcal{F}\Delta\phi_{eq})/RT\} \tag{6-8}$$

and η_t is a charge transfer overpotential, $\eta_t = \Delta\phi - \Delta\phi_{eq}$. In this approach, kinetic data, i.e. changes in values of electrical overpotential η_t with time were recorded through "Double Pulse Measurements". Then values of i_o and the order of magnitude of reaction rate constant of iron were obtained. The value, $k_{Fe} = 0.6\times10^{-3}$ cm/sec, was then suggested.

In the chemical experiments, thin iron foils were welded on the side wall of a rotating iron crucible to cover the holes on the iron crucible which were

drilled on purpose. The iron foils had contacts with FeO on one side (inside of iron crucible) and CaF_2 on the other surface. Oxygen in the iron foils was reported to be saturated. Therefore, there would be a very large chemical potential difference for oxygen transfer across the interface to molten CaF_2. For reaction of oxygen, mass flux was written as:

$$\omega_O = k_O \bar{a}_O \bar{a}_e^{-2} - k'_O \bar{a}'_O \qquad (6\text{-}9)$$

which is of identical form as those shown in Chapter Three. By monitoring change of the amount of oxide markers, which had been created in the iron foils before experiments, with reaction time through metallographic analysis, the mass flux for transfer of oxygen across the iron foils was observed. Considering the continuity of flux in the system and assuming that oxygen transfer from metal to CaF_2 was irreversible, the measured mass flux, i.e. 1.3×10^{-7} moles of oxygen/cm^2sec was observed. Thus, the value of the reaction rate constant of oxygen transfer was extracted, i.e. $k_O = 1.3\times10^{-7}/6\times10^{-5} = 2.2\times10^{-3}$ cm/sec, where 6×10^{-5} is the concentration of oxygen (mole O/cm^3).

So far, these are the most relevant data of chemical reaction rate constants in the literature for the application in our system. These values at 1723 ^{o}K, that $k_{Fe} = 0.6\times10^{-3}$ and $k_O = 2.2\times10^{-3}$ cm/sec which also serve as the guideline to estimate reaction rate constants of other elements, will be used to start the model computations. In Section 6-3, reaction rate constants for transfer of Fe, Mn and Si will be further evaluated through our experimental measurements.

6-2 Determination of the Thickness of Reaction Zone, δx_m, δx_s and Time Intervals for Computations

In the mathematical model, the reaction zone is divided by interface into two portions, one in the metallic phase and the other in the ionic phase. In the absence of any better criterion, we assume that the sum of atoms and ions taking part in reactions in the reaction zone are the same on each side of the interface, i.e.

$$\Omega\, C_s\, \delta x_s \equiv \Omega\, C_m\, \delta x_m \tag{6-10}$$

Relationship between δx_m and δx_s may be described as follows, viz,

$$\frac{\delta x_m}{\delta x_s} \equiv \frac{C_s}{C_m} \tag{6-11}$$

where C_m and C_s are the molar densities of alloy and slag, respectively and Ω is the interfacial area.

For the iron alloy and the silicate slags used in the present work, the molar densities at 1773 ^{o}K are calculated to be $C_m = 0.125$ mole/cm^3 for the alloy and $C_s = 0.05$ mole/cm^3 for the slag (The Making, Shaping and Treating of Steel, 1964). From equation (11), the ratio, $\delta x_m/\delta x_s = 0.4$, is calculated. In our computations, sensitivity on the ratio of $\delta x_m/\delta x_s$ has been tested. Varying $\delta x_m/\delta x_s$ by a factor of two, i.e. $\delta x_m/\delta x_s = 0.2$ or 0.8, and keeping all other parameters constant, in the case of manganese transfer, equation (11) gives the best fitting of curves as shown in Fig. 6-3.

The time intervals, for the computation of changes of concentrations due to chemical reactions (Δt_R) and for diffusion (Δt_D) (see Chapter Four), are determined to be 1.0 ms and 0.5 ms respectively in order for the numerical results to be convergent. Any further reductions of the size of time intervals only

result in a difference at the fourth digit of computed concentrations. The influence of the selection of total time period for the computation of chemical reactions (n Δt_R) before switching to diffusion calculation for the period of m Δt_D, and vice versa, are tested between 5 ms (n = 5 and m = 10) and 50 ms (n = 50 and m = 100). The difference of computed concentrations between 5 ms and 50 ms is in the third digit or smaller, which is within the error ranges of experimental results. Thus, the total time period of n $\Delta t_R \equiv$ m Δt_D = 50 ms is used for further computations.

During 1.0 ms of reactions, the mean diffusion distance of an atom in the alloy or an ion in the slag which may be either reactants or products of interfacial reactions, may be calculated ($\sqrt{2Dt}$) to be about 0.1 μm in iron alloy and 1.0 μm in slag. With these two values in mind, the thickness of reaction zone at interface for following computations is chosen to be that δx_m=0.4 μm and δx_s=1.0 μm.

6-3 Computed Results and Comparison with Experimental Data

In experimental measurements by EPMA, concentration profiles of elements in alloy and oxides in slag were obtained. Therefore, computed results should also be presented in the form of concentration profiles in order to be compared with experimental results. In the previous sections, it had been shown that most physical parameters have been documented in the literature. However, there are several parameters which are either estimated, based on the recommended rules in the literature (e.g. diffusion coefficients of manganese ion in slag and calcium in iron alloy) or assumed (i.e. chemical reaction rate constants of Al, Ca, Mn and Si).

In this section, the effort will be made to evaluate these physical parameters by using our experimental measurements in view of accepted errors. Through the method of curve-fitting between computed results and experimental data, chemical reaction rate constants for transfer of iron, manganese and silicon and diffusion coefficient of manganese ion in slag at 1763 ^{O}K will be extracted from our data.

TABLE 6-8: INITIAL VALUES OF THERMOCHEMICAL PARAMETERS FOR COMPUTATIONS

	Fe	Mn	Si	Al	Ca	O
Rate Constant (cm/sec)	6.0×10^{-4}	2.2×10^{-3}#	2.2×10^{-3}#	2.2×10^{-3}#	2.2×10^{-3}#	2.2×10^{-3}
Equilibrium constant for formation of oxides	300	4000	8.8×10^{8}	7.0×10^{24}	5.9×10^{15}	-
D_i^m (cm^2/sec.)	2.0×10^{-7}	1.0×10^{-7}	1.1×10^{-7}	2.0×10^{-8}	1.0×10^{-7}*	1.0×10^{-9}
D_i^s (cm^2/sec.)	5.0×10^{-6}	5.0×10^{-5}*	1.1×10^{-7}	1.0×10^{-7}	3.8×10^{-6}	1.6×10^{-5}

* - values estimated based on the recommended rules (Kirkaldy and Young, 1987);

- values assumed to be the same as reaction rate constant of oxygen transfer (Ray, 1981).

6-3-1 Computed Results of Kinetics of Interfacial Reactions Based on the Initial Values of Thermochemical Parameters

For the start of computations, reaction rate constants for transfer of elements, other than iron and oxygen are assumed to be the same as the value of reaction rate constant of oxygen transfer ($k_o = 2.2\times10^{-3}$ cm/sec) reported by Ray (1981). Values of all thermochemical parameters are listed in Table 6-8.

Based on these values in Table 6-8, the computed results are demonstrated for reactions with the acid slag (i.e. specimens 1a and 1b). From results of computed interfacial reaction rates at various times, reaction rates of aluminum, calcium and oxygen are found to be several orders of magnitude smaller than those of iron, manganese and silicon.

In view of the coupling through the constraint of no net electric current, chemical reactions of aluminum, calcium and oxygen are less influential in the system than those of the other three elements. It implies that the computed changes of interfacial concentrations for iron, manganese and silicon are insensitive to the variation of values of chemical reaction rate constants for transfer of aluminum, calcium and oxygen. On the other hand, because of the lack of reliable data for aluminum, calcium and oxygen in our experiments, the evaluation of associated parameters for chemical reactions and diffusion of these three elements can not be as critical as with other elements. Thus, more attention will be paid to iron, manganese and silicon. Especially, concentration profiles of manganese in alloy and manganese oxide in slag are the most reliable data in the present work and will be used most often in the following discussions.

6-3-2 Recommended Values of Chemical Reaction Rate Constants for Transfer of Iron, Manganese and Silicon

The comparison between computed and experimental results in terms of concentration profiles of manganese and manganese oxide, based on values of thermochemical parameters listed in Table 6-8 for acid slag, are demonstrated in Fig. 6-4a. By extrapolating measured concentration profiles of manganese and manganese oxide to the interface, it can be seen that interfacial concentrations of manganese in alloy was about 0.39% at 10 minutes and went down to 0.32 at 80 minutes of reactions. For manganese oxide in slag, the interfacial concentrations at 10 minutes was about 1.4% and increased to 1.7% at 80 minutes. The corresponding computed values are: for manganese in alloy 0.3846 at 10 minutes and 0.3851 at 80 minutes; for manganese oxide 1.851 at 10 minutes and 1.855 at 80 minutes.

The interfacial concentration of a particular element is determined by the relative rate of its supply and removal. One of the steps for the reactant is mass transfer from the bulk phase and the other is interfacial chemical reaction, and vice versa for the product of interfacial reaction. For the case that the chemical reaction is extremely fast in relation to the rate of mass transfer, the two portions of interfacial reaction zone will reach equilibrium and overall reaction rates will be limited by the supply of reactants and removal of the products. The interfacial concentrations will be rapidly adjusted to values which are very close to its final, i.e. equilibrium values. On the other hand, if the diffusion process is extremely fast, there should be no concentration gradients at all

For data shown in Fig. 6-4a, neither extreme case could be used to

describe our experimental observations concerning the transfer of manganese. However, the computed results indicate that the parameters listed in Table 6-8 lead to a case that the chemical reaction for manganese transfer was assumed relatively too fast. A similar situation for the transfer of iron and silicon across the interface lead to the same argument that the chemical reaction rate constant of iron transfer listed in Table 6-8 was large and that of silicon transfer was in relatively good agreement with our experimental data. Our approach in the curve fitting is to vary values of these chemical reaction rate constants in computations. Through a sequence of computed results, it is found that the best fitting between computed and experimental concentration profiles of manganese and manganese oxide are shown in Fig. 6-4b. These curves are obtained with the following values of chemical reaction rate constants, i.e. k_{Fe} = 1.0×10^{-8}, k_{Mn} = 8.0×10^{-7} and k_{Si} = 1.2×10^{-3} cm/sec, without changes of any other parameters in Table 6-8.

6-3-3 Self Diffusion Coefficients of Manganese in Alloy and Manganese Ion in Slag

In the present work, the measured concentration gradients of iron, iron oxide, silicon and silicon oxide are relatively small and less accurate. Thus, the present experimental data could not lead to a critical evaluation or confirmation of these diffusion coefficients. The values reported in the literature are then accepted.

For diffusion of manganese in iron alloy, there are two values of self diffusion coefficient of manganese reported in the literature, 1.0×10^{-7} and 1.7×10^{-9} cm^2/sec (see Table 6-6). The computed concentration profiles of

manganese for the cases with three chosen values of self diffusion coefficient of manganese, i.e. D^m_{Mn} = 5.0×10^{-8}, 1.0×10^{-7} and 5.0×10^{-7} cm^2/sec are shown in Fig. 6-6. The value that D^m_{Mn} = 1.0×10^{-7} cm^2/sec reported by Seith (1955) gives the best fitting (see right side of Fig. 6-6b) to our experimental data and is thus accepted.

In slag, the value of diffusion coefficient of manganese ion is estimated following the rules recommended by Kirkaldy and Young (1987). In computations, three values, i.e. D^S_{Mn} = 1.0×10^{-5}, 5.0×10^{-5} and 1.0×10^{-4} cm^2/sec for the acid slag (specimens 1a and 1b), are tested and computed results are shown on the right side of Fig. 6-7. It appears that computed results with either value of 5.0×10^{-5} or 1.0×10^{-4} cm^2/sec will fit equally well with the experimental data. For slag of different compositions, due to the existence of silicate network, the diffusion coefficient may be a function of compositions, i.e. degree of polymerization. In specimens 2a and 2b where the slag is less acid, the diffusion coefficient of manganese ion may be larger. A good fitting is obtained when the diffusion coefficient of manganese ion is chosen to be 2.0×10^{-4} cm^2/sec. (shown in Figs 6-10 and 6-11).

Therefore, values of self diffusion coefficient of manganese ion may be recommended: 5.0×10^{-5} cm^2/sec in 50%SiO_2-30%CaO-20%Al_2O_3 slag and 2.0×10^{-4} cm^2/sec. in 40%SiO_2-40%CaO-20%Al_2O_3 slag at 1763 ^oK.

6-3-4 Computed Results Based on Recommended Thermochemical Parameters

In summary, a complete list of recommended thermochemical parameters has been obtained and is listed in Table 6-9. By using these parameters, computed results of interfacial reaction rates are calculated and listed in Table 6-10. It

can be seen that, even though values of chemical reaction rate constants for iron and manganese are smaller, the reaction rates of aluminum, calcium and oxygen are still several orders of magnitude lower than those of iron, manganese and silicon. For a longer period of reactions (e.g. 10 minutes), the computed changes in concentrations for Fe, Mn and Si are still insensitive to the variations of thermochemical parameters for aluminum, calcium and oxygen.

The computed concentration profiles for all oxides in slag, silicon and manganese in iron alloy as well as these experimental data are presented in Figs. 6-8 and 6-9 for the acid slag, i.e specimens 1a and 1b and in Figs. 6-10 and 6-11 for the neutral slag, i.e. specimens 2a and 2b. Good agreement between computed and experimental results are obtained considering the experimental errors shown in these figures.

TABLE 6-9: RECOMMENDED VALUES OF THERMOCHEMICAL PARAMETERS FOR COMPUTATIONS

	Fe	Mn	Si	Al	Ca	O
Rate constant (cm/sec)	1.0×10^{-8}*	8.0×10^{-7}*	1.2×10^{-3}*	2.2×10^{-3}	2.2×10^{-3}	2.2×10^{-3}
Equilibrium constant for Formation of oxides	300	4000	8.8×10^{8}	7.0×10^{24}	5.9×10^{15}	-
D^{m} (cm^2/sec.)	2.0×10^{-7}	1.0×10^{-7}	1.1×10^{-7}	2.0×10^{-8}	1.0×10^{-7}	1.0×10^{-9}
D_i^{s} (cm^2/sec.)	5.0×10^{-6}	5.0×10^{-5}** 2.0×10^{-4}***	1.1×10^{-7}	1.0×10^{-7}	3.8×10^{-6}	1.6×10^{-5}

* - values recommended through curve-fitting method in the present work.

** - value recommended for 50%SiO_2-30%CaO-20%Al_2O_3 slag.

*** - value recommended for 40%SiO_2-40%CaO-20%Al_2O_3 slag.

TABLE. 6-10: COMPUTED INTERFACIAL CHEMICAL REACTION RATES OF EACH ELEMENT FOR THE SPECIMENS 1a AND 1b AT VARIOUS TIMES (mole/cm^{2}sec) BASED ON THERMOCHEMICAL PARAMETERS IN TABLE 6-9

Time (min)	Fe	Mn	Si	Al	Ca	O
0	1.0×10^{-9}	5.3×10^{-9}	-9.4×10^{-10}	-9.6×10^{-12}	-2.5×10^{-13}	4.0×10^{-9}
1	5.4×10^{-10}	2.7×10^{-9}	-1.6×10^{-9}	-2.1×10^{-14}	-9.5×10^{-17}	2.4×10^{-14}
10	1.1×10^{-10}	7.3×10^{-10}	-4.2×10^{-10}	-6.7×10^{-15}	-3.0×10^{-17}	6.3×10^{-15}
80	3.4×10^{-13}	2.6×10^{-11}	-1.3×10^{-11}	-3.4×10^{-16}	-1.0×10^{-18}	2.6×10^{-16}

6-3-5 Test of Sensitivity of Computed Results on Chemical Reaction Rate Constants and Equilibrium Constants

In Table 6-9, a set of thermochemical parameters have been recommended for use of the model computations. In this section, the changes in computed results due to variations of values of chemical reaction rate constants and equilibrium constants, one at one time, will be demonstrated and sensitivity of computed concentration profiles tested, by comparing with experimental data.

6-3-5-1 Chemical Reaction Rate Constants

(1) Chemical reaction rate constant of manganese transfer

Through comparison of concentration profiles of manganese between computed and experimental results, the impact of variation in chemical reaction rate constant of manganese transfer is shown for three cases, i.e. $k_{Mn} = 1.6\times10^{-7}$, 8.0×10^{-7} and 1.6×10^{-6} cm/sec in Fig. 6-12. The computed concentration profiles

are plotted in Figs. 6-12a, 6-12b and 6-12c. It can be seen that, in the case with $k_{Mn} = 8.0\times10^{-7}$ cm/sec, the agreement is satisfactory, in view of the experimental errors. It is the value listed in Table 6-9.

(2) Chemical reaction rate constant of silicon transfer

In the present experimental data, because changes of concentrations of both silicon oxide in slags and silicon in iron alloy are relatively small in relation to experimental errors (see Figs. 5-2 to 5-5), i.e. their measured concentrations are less reliable than those of manganese. Thus, a direct comparison between measured and computed data of silicon and silicon oxide has been inconclusive and could not lead to a meaningful examination of the value of k_{Si}.

However, an indirect approach by comparing its effect on the transfer of manganese is used. The influence of values of k_{Si} on concentration profiles of MnO and Mn is shown in Fig. 6-13, in which the best fitting is with $k_{Si} = 1.2\times10^{-3}$ cm/sec. When this value is reduced to half, i.e. 6.0×10^{-4}, the reaction rate of Si decreases. Furthermore, it must be pointed out that the reaction of Mn is also slowed down clearly in the first 10 minutes due to coupling among reactions of Fe, Mn and Si. Since silicon ion in slag is driven to metal by the transfer of iron and manganese to slag. A decrease of k_{Si} implies that resistance to the proceeding of Mn and Fe reactions is increased. Thus, reaction rates of Mn and Fe become smaller. When the value of k_{Si} is increased, the opposite is also true as shown in Fig. 6-13a. Thus, the chemical reaction rate constant of silicon transfer recommended to be 1.2×10^{-3} cm/sec in Table 6-9 is further substantiated.

(3) Chemical reaction rate constant of iron transfer

Similarly, the evaluation of the chemical reaction rate constant of iron transfer has to be examined indirectly because of the relatively poor quality of the measured data. The influence of the value of the chemical reaction rate constant of iron transfer on the reaction rate of manganese is shown in Fig. 6-14. The computed concentration profiles for manganese and manganese oxide are less sensitive to the variation of rate constant of iron in the range from 1.0×10^{-7} to 1.0×10^{-8} cm/sec. This indicates that, coupling effect between reactions of manganese and silicon transfer is stronger than that between manganese and iron for a reaction time longer than 10 minutes. It is shown in Table 6-11, however, that if k_{Fe} is 1.0×10^{-7} cm/sec., the mass flux of iron to slag becomes initially large and subsequently is reversed in direction in less than one minute. The reaction time in the present work is relatively long (10 and 80 minutes) and the reversal of iron transfer could not be discerned in our measurements. Thus, rate constant of iron transfer chosen to be 1.0×10^{-8} cm/sec in Table 6-9 is acceptable.

TABLE 6-11: DEMONSTRATION OF REVERSED MASS FLUX OF IRON WITH k_{Fe} EQUAL TO 1.0×10^{-7} cm/sec FOR SPECIMENS 1a AND 1b

Time (min)	Fe	Mn	Si	Al	Ca	O
0	1.0×10^{-8}	4.8×10^{-9}	-5.4×10^{-9}	-1.3×10^{-11}	-9.5×10^{-13}	4.0×10^{-9}
1	-5.2×10^{-11}	2.8×10^{-9}	-1.4×10^{-9}	-2.5×10^{-14}	-1.1×10^{-15}	2.8×10^{-14}
10	-2.8×10^{-11}	8.3×10^{-10}	-4.0×10^{-10}	-8.3×10^{-15}	-3.5×10^{-17}	7.6×10^{-15}
80	-1.3×10^{-12}	3.9×10^{-11}	-1.9×10^{-11}	-4.1×10^{-16}	-1.7×10^{-18}	3.5×10^{-16}

6-3-5-2 Equilibrium Constants for Chemical Reactions of Formation of FeO, MnO and SiO_2

In this section, equilibrium constants are tested in the similar way to the preceeding section. Based on the reported values given in Table 6-8, computed results on variations of K_{MnO} = 2000, 4000 and 6000, K_{FeO} = 300 and 1000 and K_{SiO_2} = 8.8×10^8 and 1.0×10^9 are plotted in Figs. 6-15, 6-16 and 6-17. The computed results, based on the reported values of equilibrium constants, i.e. K_{MnO} = 4000, K_{FeO} = 300 and K_{SiO_2} = 8.8×10^8, are shown to be fitting well with experimental data in these figures. When equilibrium constant of SiO_2 is arbitrarily increased from 8.0×10^8 to 1.0×10^9, the computed reaction rate of manganese transfer (shown in Fig. 6-16) is shown to be slowing down. An increase of equilibrium constant of FeO from 300 to 1000, on the other hand, shows no noticeable influence on concentration profiles of manganese and manganese oxide. However, with the larger equilibrium constant (at K_{FeO} = 1000), it will give computed interfacial concentration of FeO in slag over one weight percent, which is inconsistent with the present experimental data (see Fig. 5-2 to 5-5). Thus, it can be concluded that computed results shown in this section, based on the reported values of equilibrium constants for formation of MnO, FeO and SiO_2, listed in Table 6-9 have been confirmed for the validity of the thermodynamic data.

6-4 Concluding Remarks

Through the method of curve fitting between computed and experimental results, chemical reaction rate constants of transfer of manganese, iron and silicon, and self diffusion coefficient of manganese ion in slag, which have not been well established in the literature, are obtained. The complete list of

recommended and reported values of physical parameters for the model computations in slag/metal system is shown in Table 6-9. By using these values, the computed concentration profiles for all oxides in slag and silicon and manganese in metal are considered to be in good agreement with all available data in our experiments. It may be concluded that the theory of coupled interfacial reactions and diffusion in both phases presented in Chapter Three and Chapter Four is validated to the extent of accuracy of experimental measurements in the present work and in the literature concerned.

CHAPTER SEVEN

DISCUSSIONS

The objective of the present work is to study the nature of coupling in the kinetics of interfacial reactions in multi-component metallic/ionic systems. In this chapter, discussions will be focused on the coupling effect and the electrochemical nature in interfacial reactions through computed results in slag/metal system.

7-1 The Nature of Coupling Among Interfacial Reactions

The theory which defines the coupling of interfacial chemical reactions and mass transfer of ionic components through an electric field in multi-component metallic/ionic system (see Chapter Three) is electrochemical in nature. Fluxes induced by chemical reactions in the interfacial reaction zone and difffusional fluxes in slag must maintain collectively the electroneutrality of the system, viz,

$$\sum_{i=1}^{p} z_i \omega_i \equiv 0 \qquad (3\text{-}8)$$

This is the only fundamental constraint imposed on simultaneous interfacial reactions. In the following, chemical kinetics in slag/metal system will be discussed through this relationship.

7-2 Simultaneous Chemical Reactions in Slag/Metal System

In the slag/metal system concerned, there are six elements and equation

(3-8) may be rewritten as follows:

$$\omega_{Fe} + \omega_{Mn} + 2\,\omega_{Si} + \frac{3}{2}\omega_{Al} + \omega_{Ca} - \omega_{O} \equiv 0 \qquad (7\text{-}1)$$

From the computed results shown in Chapter Six, chemical reaction rates of transfer of aluminum, calcium and oxygen across the interface are several orders of magnitude smaller than those of transfer of iron, manganese and silicon. Thus, the coupling equation (1) may be approximated, viz,

$$\omega_{Fe} + \omega_{Mn} + 2\,\omega_{Si} \cong 0 \qquad (7\text{-}2)$$

Since initially there are no iron and manganese in slag, these two elements would have relatively large thermodynamic driving forces to move into slags, resulting in mass fluxes leaving metallic phase, i.e. $\omega_{Fe} > 0$ and $\omega_{Mn} > 0$. As a consequence of the condition of electrical neutrality, silicon ion in slag is driven to the alloy, i.e. $\omega_{Si} < 0$.

By using the conventional formulations that chemical reactions may be expressed through neutral species in slag and elements in metals, presented by many authors (e.g. Philbrook, et al. 1950, 1954), the reacting system may be described by using chemical reactions that silicon oxide in slag is simultaneously reduced by manganese and iron in alloy, viz,

$$(SiO_2) + 2\,[Fe] = [Si] + 2\,(FeO) \qquad (7\text{-}3a)$$

and

$$(SiO_2) + 2\,[Mn] = [Si] + 2\,(MnO) \qquad (7\text{-}3b)$$

However, in conventional formulation which is empirical in nature, there is no way to predict relative rates of these two parallel reactions. The conventional and the present formulations for kinetics of this pseudo-ternary system will be compared.

(1) The conventional formulation (Philbrook et al., 1950, 1954)

The system would be further reduced to a pseudo-binary system by ignoring weaker reactions, such as (3a), to give reaction (3b) as the only reaction in the system, ignoring the fact that stoichiometry for reduction of SiO_2 is not satisfied through the only reaction (3b). The influence of iron on kinetics of the system is included in the chemical reaction rate constant, i.e. k_{Mn}. It is well known that the chemical reaction rate constant should be a function of temperature and independent of concentrations in both phases. In the conventional formulation, the necessity to make rate constant k of a transferring element as a function of concentrations of another in either or both phases to fit the curve is a good indication that improvement in the formulation is needed.

(2) The present work

Based on equations (3-20), (3-21) and (3-24), mass fluxes of manganese, iron and silicon in the interfacial reaction zone can be calculated, for initial compositions of both phases shown in Table 7-1, and plotted in Fig. 7-1. It can be seen that manganese serves, in higher proportion, as the more important reductant than iron for the reduction of silica and that it takes a shorter time to approach the final state in basic slag.

$$\omega_{Fe} = k_{Fe} C_{alloy} \gamma_{[Fe]} N_{[Fe]} \left[1 - \frac{a_{FeO}}{K_{FeO} \gamma_{[Fe]} N_{[Fe]}} U_O^2 \right] \qquad (3\text{-}20)$$

$$\omega_{Mn} = k_{Mn} \frac{C_{alloy} \gamma^{o}_{Mn}}{W_{Mn} \sum_{i}^{p} ([\%i]/W_i)} h_{[Mn]} \left[1 - \frac{a_{MnO}}{K_{MnO} h_{[Mn]}} U_O^2 \right] \qquad (3\text{-}21)$$

TABLE 7-1: LIST OF CASES FOR COMPUTATIONS OF CHANGES IN INTERFACIAL REACTIONS OF SLAG/METAL SYSTEM

	(%CaO)	(%Al_2O_3)	(%SiO_2)	[%Mn]	[%Si]
Case One (with the acid slag)	30	20	50	1.4	1.5
Case Two (with the neutral slag)	40	20	40		
Case Three (with the basic slag)	50	20	30		

$$\omega_{Si} = k_{Si} \frac{C_{alloy} \gamma^{o}_{Si}}{W_{Si} \sum_{i}^{p} ([\%i]/W_i)} h_{[Si]} \left[1 - \frac{a_{SiO_2}}{K_{SiO_2} h_{[Si]}} U_o^4 \right] \qquad (3\text{-}24)$$

For these three types of slags, the pseudo-ternary reacting system of iron, manganese and silicon in reactions (3a) and (3b) are shown in Fig. 7-2. At the beginning of the reactions, the error by ignoring reaction (3a) is about 16% in all slags. As reactions proceed, both FeO and MnO will increase in slags and net reaction rates for transfer of iron and manganese will decrease. In equations (3-20) and (3-21), it shows that the reverse reaction term depends on equilibrium constant for formation of MnO or FeO (i.e. K_{MnO} or K_{FeO}), and activities of MnO or FeO, respectively. In Chapter Six, it is shown that data of K_{MnO} and K_{FeO} measurements have been reported in the literature to be 4000 and 300, respectively (see Table 6-3), which are common for all three slags. From equilibrium constants alone, the second term in the bracket in equation (3-20) increases faster than that in equation (3-21) for comparable amount of oxide formed. This is the main

reason why reaction (3a) diminishes faster than reaction (3b).

Considering the activity of FeO and MnO, e.g. in acid slag, values of activity coefficients of FeO and MnO are about constant during the course of reaction, i.e. about 1.6 and 0.5 respectively. This is also the case shown in Fig. 7-1a. The rate of manganese transfer is faster than that of iron transfer and the reaction (3b) becomes more dominating at the later stage of reactions (see solid lines in Fig. 7-2).

From the acid to the neutral slag, the activity of SiO_2 is lowered and the activity coefficient of MnO is nearly doubled, i.e. from 0.5 to 1.0 and that of FeO increases slightly from 1.6 to 1.9. This indicates that transfer of silicon ion to alloy and manganese and iron to slag has relatively a larger resistance. Thus, the transfer of manganese and iron to slag, in comparison with acid slag, takes place at slower rate but active for a similar duration as shown by dashed lines in Fig. 7-2.

In the basic slag, the activity of SiO_2 is further lowered and the activity coefficients of FeO and MnO further increased. Net rate of transfer of iron diminishes much faster than those of transfer of manganese and silicon. In this case, a pseudo-binary approach may be acceptable after about five minutes of reactions.

In summary, the influence of reacting elements on kinetics of interfacial reactions has been demonstrated through the coupling equations. It shows that, in multi-component metallic/ionic systems, the condition that certain reacting elements may be discarded in the kinetic formulations is that their transfer rates should be much smaller than others. Otherwise, these reacting elements must be simultaneously studied in kinetic formulations.

7-3 Computed Electrochemical Affinities of the Reactions

In our formulations shown in Chapter Three, the electrochemical affinity of ith reaction, $\bar{A}_i$, has been split into two terms, viz,

$$\exp\left[-\frac{\bar{A}_i}{RT}\right] \equiv L_i U^{z_i} \tag{7-4}$$

Thus, when L_i and U are obtained, $\bar{A}_i/RT$ can be calculated through equation (5):

$$-\frac{\bar{A}_i}{RT} = \ln L_i U^{z_i} \tag{7-5}$$

To apply this equation to the slag/metal system, expressions for $\bar{A}_i$, where i = Fe, Mn and Si, may be modified into the following equations (see Section 3-4), viz,

$$-\frac{\bar{A}_{Fe}}{RT} = \ln L_{Fe} U^2 = \ln\left[\frac{a_{FeO}}{K_{FeO}\gamma_{[Fe]}N_{[Fe]}}\,U_o^2\right] \tag{7-6}$$

$$-\frac{\bar{A}_{Mn}}{RT} = \ln L_{Mn} U^2 = \ln\left[\frac{a_{MnO}}{K_{MnO}h_{[Mn]}}\,U_o^2\right] \tag{7-7}$$

$$-\frac{\bar{A}_{Si}}{RT} = \ln L_{Si} U^4 = \ln\left[\frac{a_{SiO_2}}{K_{SiO_2}h_{[Si]}}\,U_o^4\right] \tag{7-8}$$

where U_o has been defined in equation (3-31), i.e.

$$U_o = U\left[\frac{(a_{O^{=}(Ca^{++})}/h_{[O]})_{eq}}{a_{O^{=}(Ca^{++})}}\right]^{1/2} \tag{3-31}$$

where $a_{O^{=}(Ca^{++})}$ is activity of oxygen anion in slag by selecting CaO as the standard state.

By plotting the computed values of the thermodynamic driving forces, $1 - \exp\{-\frac{\bar{A}_i}{RT}\}$, and its approximate form, $\frac{\bar{A}_i}{RT}$, against time in Fig. 7-3 for reactions with the acid slag (i.e. for specimens 1a and 1b), it can be seen that the

difference between these two functions depends on the value of $\frac{\bar{A}_i}{RT}$ as anticipated. Validity of linearization, which has been used by Okongwu (1973) and Yamada (1973), is confirmed in the case of silicon transfer for all the time and for manganese and iron at later stages of reaction.

7-4 Variations of Electrical Over Potential Difference Across Interface with Time

In Section 3-2, it has been shown that electrical over potential difference across the interface may be calculated with the value of the coupling factor U, through equation (3-9).

$$\Delta\phi - \Delta\phi_{eq} = \frac{RT}{\mathcal{F}} \ln U \qquad (3\text{-}9)$$

where $\Delta\phi = \phi_{slag} - \phi_{alloy}$. In equation (3-31), if it is further assumed that the activity of oxygen anion does not change with time, i.e. $a_{O^{=}(Ca^{++})} \equiv \{a_{O^{=}(Ca^{++})}\}_{eq}$, the coupling factor for the slag/metal system can be calculated when the parameter U_o and the value of $h_{[O]}$ at equilibrium state are obtained as results of computations in our mathematical model.

$$U = U_o \{h_{[O]}\}_{eq}^{1/2}. \qquad (7\text{-}9)$$

The computed results of the coupling factor U and electrical over potential $\Delta\phi - \Delta\phi_{eq}$ against time for both type of slags are plotted in Fig. 7-4. It can be seen that the value of electrical over potential is about -17 mV at initial state, -3 mV for about 10 minutes of reactions and approaches zero as reactions proceed further. These values are of the same order of magnitude as those reported by Ray (1981) in his electrochemical experiments.

7-5 Dissipation of Gibbs Free Energy in the System

It is stated in the second law of thermodynamics, that the entropy production rate in an isolated system must be greater than zero for irreversible process or equal to zero for reversible process. For chemical reactions in an isothermal and isobaric system, such as our systems, it may be re-stated that the rate of change of total Gibbs Free Energy, due to chemical reactions in the system, must be less than or equal to zero. In our system, the change of Gibbs Free Energy may be evaluated in two portions, one for chemical reactions in interfacial reaction zone and another for mixing due to diffusional fluxes. In this section, the discussion will be focused on the change of Gibbs Free Energy due to interfacial reactions. In our formulations, the change of Gibbs Free Energy per unit time per unit area of interface can be expressed through electrochemical affinities and rates of interfacial reactions, viz,

$$\frac{1}{\Omega}\frac{dG}{dt} = \sum_{i=1}^{p} \omega_i \bar{A}_i \le 0 \qquad (7\text{-}10)$$

From the definition of electrochemical affinities of reactions and the constraint of no net electric current, equation (10) can be re-arranged as:

$$\frac{1}{\Omega}\frac{dG}{dt} = \sum_{i=1}^{p} \omega_i \left[\Delta\mu_i + z_i[\bar{\mu}_e + (\Delta\phi - \Delta\phi_{eq})]\right] \qquad (7\text{-}11a)$$

$$= \sum_{i=1}^{p} \omega_i \Delta\mu_i + \left[\bar{\mu}_e + (\Delta\phi - \Delta\phi_{eq})\right] \sum_{i=1}^{p} z_i\omega_i \qquad (7\text{-}11b)$$

$$= \sum_{i=1}^{p} \omega_i \Delta\mu_i \le 0 \qquad (7\text{-}11c)$$

where Ω is interfacial area (cm^2), ω_i is the reaction rate of ith element

(mole/cm^{2}sec.), $\Delta\mu_i$ is the chemical potential difference of ith element between the ionic phase and the metallic phase i.e. $\Delta\mu_i = \mu_i^s - \mu_i^m$ (joule/mole) and $\bar{A}_i$ is the electrochemical affinity of the reaction for the ith element (joule/mole). Thus, change of Gibbs Free Energy per unit time, $\frac{dG}{dt}$ (joule/sec.), in the system can be calculated.

Substituting equation (1) for ω_O in equation (11c), we have:

$$\frac{1}{\Omega}\frac{dG}{dt} = \omega_{Fe}(\Delta\mu_{Fe} + \Delta\mu_O) + \omega_{Mn}(\Delta\mu_{Mn} + \Delta\mu_O) + \omega_{Ca}(\Delta\mu_{Ca} + \Delta\mu_O)$$

$$+ \frac{1}{2}\omega_{Al}(2\,\Delta\mu_{Al} + 3\,\Delta\mu_O) + \omega_{Si}(\Delta\mu_{Si} + 2\,\Delta\mu_O)$$

$$= \omega_{Fe}\Delta G_{FeO} + \omega_{Mn}\Delta G_{MnO} + \omega_{Ca}\Delta G_{CaO} + \frac{1}{2}\omega_{Al}\Delta G_{Al_2O_3} + \omega_{Si}\Delta G_{SiO_2} \qquad (7\text{-}12)$$

where ΔG_{FeO}, ΔG_{MnO}, etc. are Gibbs Free Energies of formation of oxides (joule/mole oxide). Computed results of Gibbs Free Energies of formation of these oxides are demonstrated in Fig. 7-5a and that of $\frac{dG}{dt}$ in Fig. 7-5b for reactions with the acid slag. It can be seen from Fig. 7-5a that ΔG_{SiO_2} is positive for periods of time during the course of reaction because the reduction of silicon oxide was forced by the transfer of manganese and iron through the neutrality (or no net electric current) condition. However, $\frac{dG}{dt}$, the collective property of the system, according to the second law of thermodynamics, is shown to approach zero monotonically in Fig. 7-5b. It can thus be concluded that our formulations in kinetics of simultaneous interfacial reactions in multi-component metallic/ionic systems and the nature of coupling are consistent with the second law of thermodynamics.

CHAPTER EIGHT

CONCLUSIONS

In the study of kinetics of simultaneous interfacial reactions in multi-component metallic and ionic systems, both theoretical and experimental work have been carried out and can be summarized in the following conclusions:

(1) General rate expressions for simultaneous interfacial reactions have been proposed in equations (3-5) and (3-8), based on the application of mass action law to the electrodic half-cell reactions and the constraint of no net electric current across interface. In the formulations, the coupling factor which represents the electric field at interface is defined through the coupling equation (3-8). Coupling effect among interfacial reactions has been discussed.

(2) The system of liquid silicate slags and solid Fe-Mn-Si alloy has been selected for the experimental work under well controlled conditions. Concentration profiles of Mn and Si in alloy and Al_2O_3, CaO, FeO, MnO and SiO_2 in slags, Figs. 5-2 to 5-5, are measured using an electron probe microanalysis with relatively good accuracy.

(3) A mathematical model with coupled interfacial reactions, serving as boundary conditions for diffusion, equations (4-2) and (4-6), in both phases has been developed. The computations have been carried out based on most thermochemical parameters selected from literature and reaction rate constants for transfer of iron, manganese and silicon through curve fitting with experimental data, Table 6-9. The computed results are in good agreement with experimental

measurements within accepted errors (Figs. 6-8 to 6-11). Thus, it may be concluded that the theory of kinetics of interfacial reactions developed in the present work is validated to the extent of accuracy of experimental measurements in the present work.

The above theory of kinetics for coupled interfacial reactions and diffusion in multi-component metallic/ionic systems has been complete and comprehensive for all components. However, it could be unduly complicated for certain applications. A systematic way to simplify the mathematical model is recommended:

(4) By applying the theory developed in the present work, kinetic behavior of each reacting element across the interface can be individually and simultaneously studied. Experimental results show that the reaction rates of transfer of Al, Ca and O are much smaller than those of Fe, Mn and Si. The influence of Al, Ca and O on kinetic behavior of Fe, Mn and Si is negligible. A pseudo-ternary reacting system among Fe, Mn and Si can then be approximated.

(5) The conventional pseudo-binary approach in the study of kinetics of slag/metal system [e.g. equation (2-3)] has been shown to be the limiting case of the general rate expression developed in the present work.

FUTURE WORK

(1) More experiments for different initial compositions in both metallic and ionic phases and the temperatures of reaction may be designed and carried out to further illustrate the theory and to study the dependence of reaction rate constants on temperature of the system.

(2) The methodology and theory in the present work may be applied to other metallic/ionic systems, such as ceramic/metal bonding, glass/metal joint, metal/inclusion reactions, composite materials, etc.

REFERENCES

Abraham, K.P., Davis, M.W. and Richardson, F.D. (1960), JISI, vol.196, pp.82.

Askill, J. (1970), Tracer Diffusion Data for Metal Alloys and Simple Oxides, IFI/Plenum.

Blander, M. (1977), Met. Trans., vol.B8, pp.529.

Bockris, J.O'M., Kitchener, J.A., Ignatowicz, S. and Tomlinson, J.M. (1948), Faraday. Soc. Discussion, No.4, pp.265.

Bockris, J.O'M and Reddy, A.K.N. (1970), Modern Electrochemistry, vol. II, Plenum Press, N.Y.

Borom, M.P. and Pask, J.A. (1967), Phys. Chem. Glasses, vol. 8, No. 5, pp.194.

Chang, L. and Goldman, K.M. (1948), Trans. AIME, vol.176, pp.309.

Cooper, A.R. and Varshneya, A.K. (1968), J. Amer. Ceram. Soc., vol.51, pp.103.

Darken, L.S. (1951), in Atom Movement, American Society for Metals, Cleveland.

deGroot, S.R. and Mazur, P. (1962), Non-equilibrium Thermodynamics, North-Holland, Amsterdam.

Derge, G., Philbrook, W.O. and Goldman, K.M. (1950) Trans. AIME, vol.188, pp.1111.

Derge, G. and Birchenall, C.E. (1953), Trans. AIME, vol.197, pp.1648.

Doelter, C. (1907), Monatsch, vol.28, pp.1313.

Dunlop, P.J. and Gosting, L.J. (1953), J. Amer. Chem. Soc., vol.75, pp.5073.

Dunlop, P.J. and Gosting, L.J. (1955), J. Amer. Chem. Soc., vol.77, pp.5238.

Elliott, J.F., Gleiser, M. and Ramakrishna, V. (1963), Thermochemistry for Steelmaking, vol. II, Addison-Wesley.

Elliott, J.F., Lynch, D.C. and Braun, T.B. (1975), Met. Trans. vol.B6, pp.495.

Elliott, J.F. (1985), in Electric Furnace Steelmaking, ed. by Taylor, C.R., ISS-AIME, pp.291.

Filer, E.W. and Darken, L.S. (1952), Trans. AIME, vol.194, pp.253.

Flood, H. and Grjotheim, K. (1952), JISI, vol.5, pp.64.

Flood, H., Forland, T. and Grjotheim, K. (1953), in the Physical Chemistry of Melts, Institution of Mining and Metallurgy, London, pp.46.

Forland, T. and Grjotheim, L. (1978), Met. Trans., vol.B9, pp.45.

Forland, K.S., Forland, T. and Ratkje, S.K. (1988), Irreversible Thermodynamics, John Wiley & Sons.

Fruehan, R.J. (1978), Met. Trans. vol.B9, pp.287.

Fujisawa, T., Imaoka, K. and Sakao, H. (1978), Tetsu-to-Hague, No.2, pp.196.

Fujita, H. and Gosting, L.J. (1956), J. Amer. Chem. Soc., vol.78, pp.1099.

Gaskell, D.R. (1967), The Densities of Liquid Silicates Containing Iron Oxide at 1410 ^{o}C, Ph.D. Thesis, McMaster University.

Gaye, H., Riboud, P.V. and Welfringer, J. (1986), "Slag Modelling, a Tool for Evaluating Metallurgical Treatment", Proceedings of 5th International Iron and Steel Congress, AIME, Washington, D.C.

Goldman, K.M., Derge, G. and Philbrook, W.O. (1954), Trans. AIME, vol.200, pp.534.

Gosting, L.J. and Akeley, D.F. (1952), J. Amer. Chem. Soc., vol.74, pp.2058.

Grjotheim, K. and Rosenblatt, G.M. (1966), in Selected Topics in High-Temperature Chemistry, ed. by Forland, T., et al., Universitetsforlaget, Oslo, pp.43.

Guggenheim, E.A. (1967), Thermodynamics, 5th Edition, North-Holland Publishing Company.

Habashi, F. (1969), Principle of Extractive Metallurgy, Gordon & Breach.

Hemptinne, X.De., Eyring, H. and Yee T. (1959), in Physical Chemistry of Process Metallurgy, Part I, ed. by Pierre, G.R. St., Interscience, N.Y.

King, T.B. and Ramachandran, S.: (1956), in the Physical Chemistry of Steelmaking, ed. by Elliot, J.F., MIT Press and John Wiley & Sons, pp.125.

King, T.B. and Grant, N.J. (1956), Trans. Met. Soc. AIME, vol.206, pp.1549.

Kirkaldy, J.S. (1957), Can. J. Phys., vol.35, pp.435.

Kirkaldy, J.S. (1958), Can. J. Phys., vol.36, pp.917.

Kirkaldy, J.S. and Purdy, G.R. (1962), Can. J. Phys., vol.40, pp.208.

Kirkaldy, J.S., Neichert, D. and Zia-Ul-Hag (1963), Can. J. Phys., vol.41, pp.2166.

Kirkaldy, J.S., Lane, J.E. and Masson, G.R. (1963), Can. J. Phys., vol.41, pp.2174.

Kirkaldy, J.S., Brigham, R.T. and Weichert, D.H. (1965), Acta Met, vol.13, pp.907.

Kirkaldy, J.S. and Young, D.J. (1987), Diffusion in the Condensed State, The Institute of Metals, London.

Kirkwood,J.G., Baldwin, R.L., Dunlop, P.J., Gosting, L.J. and Kegeles, G. (1960), J. Chem. Phys., vol.33, pp.1505.

Kubachemski, O., Evans, E.L. and Alcock, C.B. (1967), Metallurgical Thermochemistry, 4th ed., Pergamon Press.

Lane, J.E. and Kirkaldy, J.S. (1964), Can. J. Phys., vol.42, pp.1643.

Lane, J.E. and Kirkaldy, J.S. (1965), Can. J. Phys., vol.43, pp.1812.

Lane, J.E. and Kirkaldy, J.S. (1966), Can. J. Phys., vol.44, pp.477.

Lewis, G.N. and Randall, M. (1923), Thermodynamics, Revised by Pitzer, K.S. and Brewer, L. (1961), 2nd Edition, McGraw-Hill.

Lu, W-K. (1971), Trans. ISIJ, vol.11, pp.32.

Martin, A.E. and Derge, G. (1943), Trans. AIME, vol.154, pp.104.

Masson, C.R. (1965), Proc. Roy. Soc., vol.A287, pp201.

McGannon, H.E. (ed), (1964) The Making, Shaping and Treating of Steel, 8th Edition, USS.

Min, D.J. and Fruehan, R.J. (1992), Met. Trans., vol.B23, pp.29.

Nagata, K. and Goto, K.S. (1976), J. Electrochem. Soc., vol.123, pp.1814.

Okongwu,D.A. (1973), Coupled Ionic Diffusion in Multicomponent Silicate Glasses, Ph.D Thesis, McMaster University.

Okongwu,D.A. and Lu, W-K. (1975), J. Chem. Phys., vol.63, pp.734.

Onsager, L. (1945-1946), Ann. N.Y. Acad. Sci., vol.46, pp.241.

Packwood,R.H. (1991), Private Communication, Metals Technology Lab, CANMET.

Prigogine, I. (1967) Introduction to Thermodynamics of Irreversible Process, Third Edition, Interscience Publisher.

Ray, J.D. (1981), A Study of the Interfacial Reaction Kinetics in the Fe-CaF System at 1450 ^{o}C, Ph.D. Thesis, McMaster University.

Richardson, F.D. (1974), Physical Chemistry of Melts in Metallurgy, vol. 2, Academic Press.

Seith, W. (1955), Diffusion in Metallen, Zweite Auflage.

Sherman, C.W. and Chipman, J. (1952), Trans. AIME, vol.194, pp.597.

Sigworth, G.K. and Elliott, J.F. (1974), Metal Science, vol.8, pp.1298.

Sugawara, H., Nagata, K. and Goto, K.S. (1977), Met. Trans., volB8, pp.605.

Swisher, J.H. and Turkdogan, E.T. (1967), Trans. Met. AIME, vol.239, pp.426.

Talor, C.R. and Chipman, J. (1943), Trans. AIME, vol.154, pp.228.

Temkin, M. (1945), ACTA Physicochimica (in English), URSS, vol.XX, pp.411.

Tokuda, M. and Ontani, M. (1971), in International Symposium on Metallurgical Chemistry - Application in Ferrous Metallurgy, University of Sheffield, pp.93.

Toop, G.W. and Samis, C.S. (1962), Trans Met. Soc. AIME, vol.224, pp.878.

Varshneya, A.K. and Cooper A.R. (1972), J. Amer. Ceram. Soc., vol.55, pp.312.

Wagner, C. (1956), in the Physical Chemistry of Steelmaking, ed. by Elliot, J.F., MIT Press and John Wiley & Sons, pp.237.

Wagner, C. (1975), Met. Trans. vol.B6, pp.395.

Yamada, K. (1977), A Theoretical Study of Slag-Metal Reaction Kinetics Using a Numerical Technique, Master Thesis, McMaster University.

Yang, L. and Derge, G. (1959), in Physical Chemistry of Process Metallurgy, Part I, ed. by Pierre, G.R. St., Interscience, N.Y.

APPENDIX A

A STUDY OF ION ACTIVITIES IN IONIC SOLUTIONS

APPENDIX A

A STUDY OF ION ACTIVITIES IN IONIC SOLUTIONS

It has been shown in Chapter Three that ion activities are part of formulations in kinetics of interfacial reactions and diffusion in multi-component metallic/ionic systems. However, ion activities have not yet been properly defined in multi-component ionic solutions (Forland, Forland and Ratkje, 1988). The formulations may be subject to the inconsistencies against classical thermodynamics, especially in molten salts and slag, which had been demonstrated by several authors (Blander, 1977, and Forland and Grjotheim, 1978). In the following, effort will be made to define ion activities in ionic solutions in such a way that the inconsistencies against classical thermodynamics in ionic solutions are avoided.

A1 Literature Review

A1-1 Definition of Ion Activity in Aqueous Solutions

In aqueous solutions where strong electrolytes, e.g. NaCl, are dissolved, Lewis and Randall (1923, re-published by Pitzer and Brewer, 1961) introduced thermodynamic equation of the chemical equilibrium in the following form:

$$K_{Na\text{-}Cl} \equiv \frac{a_{Na^+} a_{Cl^-}}{a_{NaCl}} \qquad (A1)$$

where $K_{Na\text{-}Cl}$ is the dissociation constant which is a function of temperature, a_{Na^+}, a_{Cl^-} and a_{NaCl} are activities of cation Na^+, anion Cl^- and compound NaCl.

For the convenience, $K_{Na\text{-}Cl}$ may be chosen to be unity and activity of NaCl

can be expressed as the product of activities of cation Na^+ and anion Cl^-, viz,

$$a_{NaCl} = a_{Na^+} a_{Cl^-} \tag{A2}$$

This indicates that the total change of chemical potentials at the standard states for the dissociation reaction is zero, i.e.

$$NaCl\ (aq.) = Na^+ + Cl^- \tag{A3}$$

$$\Delta\mu^o \equiv 0 \tag{A3a}$$

In this definition, two type of activities in the solution, i.e. activities of neutral species and ions, are introduced. The reference state of an ion activity is defined in such a way that "the potential of a reversible hydrogen electrode with gas at one atmosphere pressure in equilibrium with a solution of hydrogen ions at unit activity shall be taken as zero at all temperatures" (Grjotheim & Rosenblatt, 1966).

In a simple case, ion activities may be calculated in a pseudo-binary solution where the electrolyte is infinitely dilute and the molalities of cation and anion are the same, thus, following relationship is obtained for ion activities, viz,

$$a_{Na^+} = a_{Cl^-} = a_{NaCl}^{1/2} \tag{A4}$$

As the amount of electrolyte increases in the solution, this relationship may be broken down at a certain concentration due to incomplete dissociation of the electrolyte (Grjotheim and Rosenblatt, 1966). When a second electrolyte, e.g. KCl, is added to the system, equation (A4) is also not valid. For concentrated and multi-component ionic solutions, Lewis and Randall (1923) proposed the geometric mean of the two ion activities, one cation and one anion, denoted by $a_{\pm}$, viz,

$$a_{\pm} = (a_{Na^+} a_{Cl^-})^{1/2} = a_{NaCl}^{1/2} \quad (A5)$$

In this way, the mean activity coefficient, $\gamma_{\pm}$ is introduced, viz,

$$\gamma_{\pm} = \frac{a_{\pm}}{m} \quad (A5a)$$

where m is molality of the electrolyte.

A1-2 Temkin's Rule

In molten salts and slag, solutions are generally multi-component in nature. Temkin (1945) treated ideal solutions of molten salts by having:

$$\Delta H^{MIX} = 0 \quad (A6)$$

Then, Gibbs Free Energy of mixing can be expressed:

$$\Delta G^{MIX} = G - G^{O} = \Delta H^{MIX} - T\Delta S^{MIX} = -T\Delta S^{MIX} \quad (A7)$$

where G is Gibbs Free Energy of the solution and G^{O} is the Gibbs Free Energy of pure components before mixing.

To calculate the entropy change of random mixing, Temkin assumed that there exist cation and anion sublattices in the solution. Entropy in cation sublattice is denoted by ΔS^{+} and in anion sublattice by ΔS^{-}, which may be calculated by equations (A8) and (A9):

$$\Delta S^{+} = k_B \ln W^{+} \quad (A8)$$

$$\Delta S^{-} = k_B \ln W^{-} \quad (A9)$$

where W^{+} and W^{-} are the densities of state of cation and anion sublattices respectively and k_B is Boltzmann constant. The total entropy of mixing is then equal to the sum of two:

$$\Delta S^{MIX} = \Delta S^{+} + \Delta S^{-} = k_B \ln (W^{+}W^{-}) \quad (A10)$$

On the other hand, Gibbs Free Energy of the solution at given temperature

and pressure can be defined by the partial molar free energies of the components:

$$G = \sum_{i=1}^{n} n_i\mu_i = \sum_{i=1}^{n} n_i(\mu_i^o + RT\ln a_i) \qquad (A11)$$

where μ_i and μ_i^o are the chemical potential and the standard chemical potential of ith component, n_i is number of moles for ith component and a_i is activity of ith component.

Following Temkin's approach, assuming that the solution is made from n_{FeO} moles of FeO, n_{MnO} moles of MnO, n_{FeS} moles of FeS and n_{MnS} moles of MnS, the densities of state of cation and anion sublattices can be computed based on number of ions in the ideal solution, viz,

$$W^+ = \frac{[\ddot{A}_V(n_{Fe^{++}} + n_{Mn^{++}})]!}{(\ddot{A}_V n_{Fe^{++}})!\ (\ddot{A}_V n_{Mn^{++}})!}$$

$$= \frac{[\ddot{A}_V(n_{FeO} + n_{MnO} + n_{FeS} + n_{MnS})]!}{[\ddot{A}_V(n_{FeO} + n_{FeS})]!\ [\ddot{A}_V(n_{MnO} + n_{MnS})]!} \qquad (A12)$$

and

$$W^- = \frac{[\ddot{A}_V(n_{O^=} + n_{S^=})]!}{(\ddot{A}_V n_{O^=})!\ (\ddot{A}_V n_{S^=})!}$$

$$= \frac{[\ddot{A}_V(n_{FeO} + n_{MnO} + n_{FeS} + n_{MnS})]!}{[\ddot{A}_V(n_{FeO} + n_{MnO})]!\ [\ddot{A}_V(n_{FeS} + n_{MnS})]!} \qquad (A13)$$

where $\ddot{A}_V$ is Avogadro's number (6.025×10^{23} /mole).

Substituting equations (A12) and (A13) into equations (A8) and (A9) and using Sterling approximation, i.e. ln n! = n ln n - n, Gibbs Free Energy of the solution is obtained in equation (A7), viz,

$$G = G^o + RT\left[n_{FeO}\ln(N_{Fe^{++}}N_{O^=}) + n_{MnO}\ln(N_{Mn^{++}}N_{O^=})\right.$$
$$\left. + n_{FeS}\ln(N_{Fe^{++}}N_{S^=}) + n_{MnS}\ln(N_{Mn^{++}}N_{S^=})\right] \qquad (A14)$$

where $N_{Fe^{++}}$, $N_{Mn^{++}}$, $N_{O^{=}}$ and $N_{S^{=}}$ are cation fractions of Fe^{++}, Mn^{++} and anion fractions of $O^{=}$ and $S^{=}$ which are defined later in equations (A23) and (A24).

Comparing equations (A14) with (A11), Temkin's rule is obtained, viz,

$$G^{o} = n_{FeO}\mu^{o}_{FeO} + n_{MnO}\mu^{o}_{MnO} + n_{FeS}\mu^{o}_{FeS} + n_{MnS}\mu^{o}_{MnS} \qquad (A15)$$

$$a^{T}_{MnO} = N_{Mn^{++}} N_{O^{=}} \qquad (A16)$$

$$a^{T}_{FeO} = N_{Fe^{++}} N_{O^{=}} \qquad (A17)$$

$$a^{T}_{MnS} = N_{Mn^{++}} N_{S^{=}} \qquad (A18)$$

$$a^{T}_{FeS} = N_{Fe^{++}} N_{S^{=}} \qquad (A19)$$

where a^{T}_{MnO}, etc. are Temkin activities of neutral species in ideal solution of ionic melts.

Following these equations, it can be seen that activities of neutral species are inter-related, i.e.

$$\frac{a^{T}_{(MnS)}\, a^{T}_{(FeO)}}{a^{T}_{(MnO)}\, a^{T}_{(FeS)}} \equiv 1 \qquad (A20)$$

where all cation and anion fractions are canceled each other. This implies that change of chemical potentials at their standard states for displacement reaction (A21) is zero, viz,

$$(MnO) + (FeS) = (MnS) + (FeO) \qquad (A21)$$

$$\Delta G^{o}_{A21} = (\mu^{o}_{FeO} + \mu^{o}_{MnS}) - (\mu^{o}_{MnO} + \mu^{o}_{FeS}) \equiv 0 \qquad (A21a)$$

This has become another condition that Temkin's ideal solutions should meet. To satisfy this condition, standard states for chemical potentials of these neutral species have to be chosen properly. In conventional thermodynamic studies, pure compounds are usually chosen to serve as the standard state for neutral species in

ionic solutions. Therefore, equilibrium constant of reaction (A21) should be a function of temperature and equation (A21a) may not be true unless either cations or anions or both have the identical thermochemical properties, e.g. isotope ions.

A1-3 Activity Coefficients of Neutral Species

To avoid the relationship given by equation (A20), Grjotheim and Rosenblatt (1966) introduced Temkin's activity coefficients, γ_{MX}, for the neutral species MX in multi-component ionic solutions and its activity may be written by the following equation, viz,

$$a_{MX} = \gamma_{MX} N_{M^+} N_{X^-} \tag{A22}$$

where N_{M^+} and N_{X^-} are cation and anion fractions defined as follows:

$$N_{M^+} = \frac{n_{M^+}}{\sum n^+} \tag{A23}$$

and

$$N_{X^-} = \frac{n_{X^-}}{\sum n^-} \tag{A24}$$

where n_{M^+} and n_{X^-} are number of cation M^+ and anion X^- and $\sum n^+$ and $\sum n^-$ are total numbers of cations and anions in the system, respectively, without consideration of the difference in charges carried by ions*. In such formulism, activities of neutral species are related to the product of cation and anion fractions.

* - For the solutions containing ions with different charges, the equivalent ion fractions, i.e. $N_{M^+} = \left(\frac{z_{M^+} n_{M^+}}{\sum z^+ n^+} \right)$ and $N_{X^-} = \left(\frac{z_{X^-} n_{X^-}}{\sum z^- n^-} \right)$ where z^+ and z^- are the valences of cation and anion respectively, are to be applied. The equivalent ion fractions are identical to the ion fractions given above when valences of ions in the system are all the same.

For the system containing four ions, i.e. Fe^{++}, Mn^{++}, $O^{=}$ and $S^{=}$, equilibrium constant of reaction (A21) can be given by the ratio of four activity coefficients, with cancellation of all cation and anion fractions, viz,

$$K_{A21} = \left[\frac{a_{(MnS)}a_{(FeO)}}{a_{(MnO)}a_{(FeS)}}\right]_{eq} = \left[\frac{\gamma_{(MnS)}\gamma_{(FeO)}}{\gamma_{(MnO)}\gamma_{(FeS)}}\right]_{eq} \qquad (A25)$$

Since the equilibrium constant is only a function of reaction temperature, this shows that there are three independent measurements of activity coefficients and the fourth one can be calculated by equation (A25).

A1-4 Typical Arguments on The Formulation of Ion Activities

Elliott, Lynch and Braun (1975) attempted to use the following alternative formulation of single ion activities to study slag/metal equilibria, viz,

$$a_{Fe^{++}} = \gamma_{Fe^{++}} N_{Fe^{++}} \qquad (A26a)$$

$$a_{O^{=}} = \gamma_{O^{=}} N_{O^{=}} \qquad (A26b)$$

In the formulations, however, the standard states for single ion activities had not been clearly defined. Blander (1977) and Forland and Grjotheim (1978) pointed out that if the relationships from equation (A2) and (A22) are accepted, cation and anion activities can be related to the activity of neutral species as follows, viz,

$$a_{(FeO)} = a_{Fe^{++}} a_{O^{=}} = \gamma_{Fe^{++}} \gamma_{O^{=}} N_{Fe^{++}} N_{O^{=}} \qquad (A27)$$

then

$$\gamma_{(FeO)} = \gamma_{Fe^{++}} \gamma_{O^{=}} \qquad (A28)$$

Similarly, the relationships in equations (A27) and (A28) were assumed to be equally valid for other neutral species in the system. Blander (1977), Forland

and Grjotheim (1978) demonstrated that activity coefficients of FeO, MnO, FeS and MnS are related through equation (A29), viz,

$$\frac{\gamma_{(FeO)}}{\gamma_{(MnO)}} \equiv \frac{\gamma_{Fe^{++}}\,\gamma_{O^{=}}}{\gamma_{Mn^{++}}\,\gamma_{O^{=}}} = \frac{\gamma_{Fe^{++}}}{\gamma_{Mn^{++}}} = \frac{\gamma_{Fe^{++}}\,\gamma_{S^{=}}}{\gamma_{Mn^{++}}\,\gamma_{S^{=}}} \equiv \frac{\gamma_{(FeS)}}{\gamma_{(MnS)}} \qquad (A29)$$

This arbitrary equality of the ratios of activity coefficients indicates that the value of equilibrium constant K_{A21} has to be unity which is not generally true. Therefore, it was concluded that use of ion activities in such formulation is against classical thermodynamics (Blander, 1977).

In this argument, however, there are implications that equation (A2) is equally applicable to activities of all four components in the solution in Raoultian scale, i.e. using pure compounds as the standard state. Since equation (A2) was originally obtained in an arbitrary manner for a pseudo-binary solution, there should be another way to relate thermodynamic quantities of ions with those of compounds in multi-component systems which will be introduced in the present study.

A2 Definition of Chemical Activities of Ions

A2-1 Formulation of Activities of Cations and Anions

Following Temkin's suggestion, an ionic solution may be conceptually split into cation and anion sublattices. However, cations and anions are next to each other and inseparable in the solution. Thermodynamic properties of ions, therefore, should be defined not only from the ions of the same set of sublattice but also through the consideration of their nearest neighbors, ions on the sublattice of opposite charges.

In a system containing cations C_i^{++} (i=1,2,...,p) and anions $A_j^{=}$

(j=1,2,...,m), chemical activity of C_i^{++} for ith cation in the solution may be defined through its chemical potential of cations in such a way:

$$\mu_{C_i^{++}} = \mu^{o}_{C_i^{++}(Y^{=})} + RT \ln a_{C_i^{++}(Y^{=})} \qquad (i=1,2,...,p) \qquad (A30)$$

where $\mu_{C_i^{++}}$ is the chemical potential of cation C_i^{++}, $\mu^{o}_{C_i^{++}(Y^{=})}$ is the chemical potential of C_i^{++} in a standard state that is in pure compound C_iY, and $a_{C_i^{++}(Y^{=})}$ is the chemical activity of cation C_i^{++} with C_iY as the standard state. The chemical activity of C_i^{++} may be further expressed by using cation fraction as concentration unit, viz,

$$a_{C_i^{++}(Y^{=})} = \gamma_{C_i^{++}(Y^{=})} \; N_{C_i^{++}} \qquad (i=1,2,...,p) \qquad (A31)$$

where $\gamma_{C_i^{++}(Y^{=})}$ is the activity coefficient of C_i^{++} with C_iY as the standard state and $N_{C_i^{++}}$ is cation fraction which is defined through number of cations [see equation (A23)].

In this definition, subscript $C_i^{++}(Y^{=})$ of the activity coefficient shown above indicates that the anions $Y^{=}$ are the nearest neighbors of cation C_i^{++}. Equation (A31) indicates that the activity coefficient is characterized by ions in both sublattices but the concentration is expressed in the property of cation sublattice only.

Similarly, for jth anion $A_j^{=}$, its activity can be defined as:

$$\mu_{A_j^{=}} = \mu^{o}_{A_j^{=}(X^{++})} + R\,T \ln a_{A_j^{=}(X^{++})} \qquad (A32)$$

and

$$a_{A_j^{=}(X^{++})} = \gamma_{A_j^{=}(X^{++})} \; N_{A_j^{=}} \qquad (A33)$$

where j=1,2,....,m. In this formulation, $A_j^{=}(X^{++})$ shows that the cation X^{++} is a

part of standard state, i.e. pure compound A_jX, in the definition of activity of anion A_j.

A2-2 The standard State of Ion Activities

In the above definition, the ion of opposite charge in ionic systems serves as a part of description of the standard state for the ion activity. To elaborate it further, the solutions containing up to four divalent ions, e.g. Mn^{++}, Fe^{++}, $O^{=}$ and $S^{=}$ are discussed in this section. For this purpose, the existence of lattice defect is ignored.

A2-2-1: Ions in A Pure Compound, e.g. MnO

In pure MnO, the nearest neighbor of a cation Mn^{++} is anions $O^{=}$ only and vice versa. The cation fraction of Mn^{++} and anion fraction of $O^{=}$ are both unity. The dissociation reaction may be written as:

$$MnO\ (pure) = Mn^{++}(O^{=}) + O^{=}(Mn^{++}) \tag{A34}$$

Chemical potentials of Mn^{++} and $O^{=}$ may be expressed in such a way:

$$\mu_{Mn^{++}} = \mu^{o}_{Mn^{++}(O^{=})} + RT \ln a_{Mn^{++}(O^{=})} \tag{A35}$$

and

$$\mu_{O^{=}} = \mu^{o}_{O^{=}(Mn^{++})} + RT \ln a_{O^{=}(Mn^{++})} \tag{A36}$$

Since there are no other ions, a standard state for both ions that $a_{Mn^{++}(O^{=})}$ and $a_{O^{=}(Mn^{++})}$ are both unity is selected. The change in reaction (A34) is in one's perception and nothing physical. Therefore, the change of chemical potentials for dissociation reaction (A34) should be zero, viz,

$$(\mu_{Mn^{++}} + \mu_{O^{=}}) - \mu_{MnO} \equiv 0 \tag{A37}$$

where

$$\mu_{MnO} = G^{o}_{MnO} + RT \ln a_{(MnO)} \qquad (A38)$$

When pure MnO is chosen to be the standard state for activity of MnO, $a_{(MnO)}$ is unity. Thus, the relationship between Gibbs Free Energy of pure MnO and chemical potentials of ions at the standard state is established, viz,

$$G^{o}_{MnO} = \mu^{o}_{Mn^{++}(O^{=})} + \mu^{o}_{O^{=}(Mn^{++})} \qquad (A39)$$

where G^{o}_{MnO} is the Gibbs Free Energy of pure MnO which can be evaluated by the convention used in classical thermodynamics.

A2-2-2: The Solution of MnO and FeO

When MnO is dissolved in FeO, cation sublattice contains two cations, Mn^{++} and Fe^{++}. To form an ionic solution, it may be considered in the following two steps:

$$MnO \text{ (pure)} = (MnO) \qquad (A40a)$$

where (MnO) stands for MnO in solution and then dissociated into cation Mn^{++} with the nearest neighbors of $O^{=}$ and anion $O^{=}$ originated from MnO to be with the nearest neighbors of both Mn^{++} and Fe^{++},

$$(MnO) = Mn^{++}(O^{=}) + O^{=}(Fe^{++},Mn^{++}) \qquad (A40b)$$

Combining equations (A40a) and (A40b), then we have the overall reaction of the dissolution of MnO in FeO,

$$MnO \text{ (pure)} = Mn^{++}(O^{=}) + O^{=}(Fe^{++},Mn^{++}) \qquad (A40c)$$

For the same reason as discussed with reaction (A34), the change of chemical potentials for reaction (A40b) should be zero and equation (A37) is applicable to reaction (A40b), i.e.

$$(\mu_{Mn^{++}} + \mu_{O^{=}}) - \mu_{MnO} \equiv 0 \qquad (A37)$$

For neutral species, pure MnO is chosen as the standard state for activity of MnO. In the selection of the standard state for ion activities, if we limit our discussion to the interaction of nearest neighbours only, cations Mn^{++} and Fe^{++} do not experience any change in environment but oxygen anion does during the formation of solution. Since the nearest neighbor of $O^{=}$ could be a combination of Mn^{++} or Fe^{++} ions, either pure MnO or pure FeO may be selected as its standard state.

Case One: Pure MnO chosen as the standard state for activity of oxygen anion

If MnO is selected, the expressions of chemical potentials of manganese cations $\mu_{Mn^{++}}$ and oxygen anions, $\mu_{O^{=}}$, are identical to equations (A35) and (A36), i.e.

$$\mu_{Mn^{++}} = \mu^{O}_{Mn^{++}(O^{=})} + RT \ln a_{Mn^{++}(O^{=})} \qquad (A35)$$

and

$$\mu_{O^{=}} = \mu^{O}_{O^{=}(Mn^{++})} + RT \ln a_{O^{=}(Mn^{++})} \qquad (A36)$$

Substituting equations (A35), (A36) and (A38) to (A37), we have:

$$[\mu^{O}_{O^{=}(Mn^{++})} + RT \ln a_{O^{=}(Mn^{++})}] + [\mu^{O}_{Mn^{++}(O^{=})} + RT \ln a_{Mn^{++}(O^{=})}]$$
$$- [G^{O}_{MnO} + RT \ln a_{(MnO)}] = 0 \qquad (A41)$$

Considering equation (A39), $[\mu^{O}_{O^{=}(Mn^{++})} + \mu^{O}_{Mn^{++}(O^{=})}]$ and G^{O}_{MnO} are cancelled. Therefore, equation (A41) results in:

$$a_{(MnO)} = a_{Mn^{++}(O^{=})}\, a_{O^{=}(Mn^{++})} \qquad (A42)$$

where $a_{(MnO)}$ is the activity of MnO with pure MnO as the standard state. This equation will be identical to Temkin's rule if the activity coefficients of ions in equation (A31) are unity, viz,

$$a_{(MnO)} = N_{Mn^{++}}\, N_{O^{=}} \qquad (A42a)$$

Case Two: Pure FeO chosen as the standard state for activity of oxygen anion

In this case, the expression of $\mu_{O^=}$ becomes:

$$\mu_{O^=} = \mu^{O}_{O^{=}_{(Fe^{++})}} + RT \ln a_{O^{=}_{(Fe^{++})}} \qquad (A43)$$

where $\mu^{O}_{O^{=}_{(Fe^{++})}}$ is the standard chemical potential of $O^{=}$ with "pure and stoichiometric FeO" as the hypothetical standard state and the change in Gibbs Free Energy for reaction (40b) can be expressed similar to equation (A41), viz,

$$\left[\mu^{O}_{O^{=}_{(Fe^{++})}} + RT \ln a_{O^{=}_{(Fe^{++})}}\right] + \left[\mu^{O}_{Mn^{++}_{(O^{=})}} + RT \ln a_{Mn^{++}_{(O^{=})}}\right]$$
$$- \left[G^{O}_{MnO} + RT \ln a_{(MnO)}\right] = 0 \qquad (A44)$$

or

$$G^{O}_{MnO} + RT \ln a_{(MnO)} = \left[\mu^{O}_{O^{=}_{(Fe^{++})}} + \mu^{O}_{Mn^{++}_{(O^{=})}}\right]$$
$$+ RT \ln \left[a_{O^{=}_{(Fe^{++})}} a_{Mn^{++}_{(O^{=})}}\right] \qquad (A45)$$

From equation (A39), G^{O}_{MnO} may be replaced by $\left[\mu^{O}_{Mn^{++}_{(O^{=})}} + \mu^{O}_{O^{=}_{(Mn^{++})}}\right]$. Then $\mu^{O}_{Mn^{++}_{(O^{=})}}$ is cancelled and equation (A45) becomes:

$$RT \ln a_{(MnO)} = \left[\mu^{O}_{O^{=}_{(Fe^{++})}} - \mu^{O}_{O^{=}_{(Mn^{++})}}\right]$$
$$+ RT \ln \left[a_{O^{=}_{(Fe^{++})}} a_{Mn^{++}_{(O^{=})}}\right] \qquad (A45a)$$

The term $\left[\mu^{O}_{O^{=}_{(Fe^{++})}} - \mu^{O}_{O^{=}_{(Mn^{++})}}\right]$ represents the difference of standard chemical potential of $O^{=}$ in different environment of cations. Its value is generally non-zero because they belong to different chemical substances. Thus, a new parameter $\theta^{(FeO)}_{MnO}$ is introduced in equation (A46):

$$\mu^{O}_{O^{=}_{(Fe^{++})}} - \mu^{O}_{O^{=}_{(Mn^{++})}} \equiv RT \ln \theta^{(FeO)}_{MnO} \qquad (A46)$$

The Raoultian activity of MnO can then be expressed as:

$$a_{(MnO)} = \theta_{MnO}^{(FeO)}\ a_{Mn^{++}(O^{=})}\ a_{O^{=}(Fe^{++})} \qquad (A47)$$

In equation (A47), pure MnO is chosen as the standard state for activity of Mn^{++} and pure FeO for activity of $O^{=}$. $\theta_{MnO}^{(FeO)}$ is the conversion factor for activity of $O^{=}$ from the standard state of pure MnO to pure FeO.

In equation (A46), $\theta_{MnO}^{(FeO)}$ is defined by two thermochemical parameters of pure compounds, i.e. $\mu^{O}_{O^{=}(Mn^{++})}$ and $\mu^{O}_{O^{=}(Fe^{++})}$ where $\mu^{O}_{O^{=}(Mn^{++})}$ is from pure MnO in equation (A39) and $\mu^{O}_{O^{=}(Fe^{++})}$ from pure FeO in equation (A48).

$$G^{O}_{FeO} = \mu^{O}_{Fe^{++}(O^{=})} + \mu^{O}_{O^{=}(Fe^{++})} \qquad (A48)$$

Thus, $\theta_{MnO}^{(FeO)}$ is only a function of temperature and pressure. Since the separations of $\mu^{O}_{O^{=}(Fe^{++})}$ and $\mu^{O}_{O^{=}(Mn^{++})}$ from G^{O}_{FeO} and G^{O}_{MnO} in equations (A39) and (A48) are perceptional, $\theta_{MnO}^{(FeO)}$ cannot be directly calculated. The alternative approach will be discussed in section A2-3.

With such a selection of standard state for activity of $O^{=}$, activity of FeO can be expressed:

$$[\mu^{O}_{O^{=}(Fe^{++})} + RT \ln a_{O^{=}(Fe^{++})}] + [\mu^{O}_{Fe^{++}(O^{=})} + RT \ln a_{Fe^{++}(O^{=})}]$$
$$- [G^{O}_{FeO} + RT \ln a_{(FeO)}] = 0 \qquad (A49)$$

i.e.

$$a_{(FeO)} = a_{Fe^{++}(O^{=})}\ a_{O^{=}(Fe^{++})} \quad \text{and} \quad \theta_{FeO}^{(FeO)} \equiv 1 \qquad (A49a)$$

A2-2-3 A Solution Containing A Second Anion, e.g. $S^{=}$

Sulphur anion $S^{=}$ may be introduced to the solution by adding either FeS or MnS. Similarly, if the standard state for activity of Fe^{++} is chosen to be FeO and $S^{=}$ to be FeS, the activity of FeS can be written by introducing the conversion factor $\theta_{FeS}^{(FeO)}$:

$$a_{(FeS)} = \theta_{FeS}^{(FeO)} \, a_{Fe^{++}(O^{=})} \, a_{S^{=}(Fe^{++})} \tag{A50}$$

where $\theta_{FeS}^{(FeO)}$ is defined by equation (A50a):

$$\mu^{O}_{Fe^{++}(O^{=})} - \mu^{O}_{Fe^{++}(S^{=})} = RT \ln \theta_{FeS}^{(FeO)} \tag{A50a}$$

In the above, it has been shown that the standard state for ion activities should be related to neutral species. Temkin's rule, when applied to non-ideal solutions, is a special case in the present work, if the pure compound is the standard state for activities of both cation and anion, i.e. equation (A49a). If the standard states for cation and anion activities are chosen from different compounds, the conversion factor has to be introduced and Temkin's rule is thus modified.

The selection of standard state for ion activities is arbitrary. Once it is chosen, all ion activities in the solution should be uniquely defined.

A2-3 Evaluation of the Conversion Factors and Activity Coefficients of Ions

In order for our formulation to be useful, the conversion factors introduced above must be evaluated from experimental measurements of solutions. For this purpose, the following relationship in the solution of FeO-MnO will be derived. Following Grjotheim and Rosenblatt (1966), concentrations of FeO and MnO in the solution are taken as the products of cation and anion fractions:

$$N_{(FeO)} = N_{Fe^{++}} \, N_{O^{=}} \tag{A51}$$

$$N_{(MnO)} = N_{Mn^{++}} \, N_{O^{=}} \tag{A52}$$

Then, activity coefficient of FeO and MnO with pure FeO as the standard state can be expressed as:

$$\gamma_{(FeO)} = \gamma_{Fe^{++}(O^{=})}\ \gamma_{O^{=}(Fe^{++})} \tag{A53}$$

$$\gamma_{(MnO)} = \theta_{MnO}^{(FeO)}\ \gamma_{Mn^{++}(O^{=})}\ \gamma_{O^{=}(Fe^{++})} \tag{A54}$$

In these two equations, $\gamma_{(MnO)}$ and $\gamma_{(FeO)}$ are measurable quantities. There are four other unknowns including one conversion factor and three activity coefficients of ions, to be evaluated. It should be pointed out that activity coefficients are functions of the concentrations and the conversion factor $\theta_{MnO}^{(FeO)}$ is not.

Thus, we may consider a limiting case that ions Mn^{++} are infinitely dilute in the solution. In the pseudo-binary solution, the solute MnO and $Mn^{++}(O^{=})$ may be assumed to obey Henry's law and the solvent FeO, $Fe^{++}(O^{=})$ and $O^{=}(Fe^{++})$ obey Raoult's law, viz,

$$\lim_{N_{Mn^{++}} \to 0} \gamma_{(MnO)} \equiv \gamma^{O}_{(MnO)} \tag{A55}$$

$$\lim_{N_{Mn^{++}} \to 0} \gamma_{Mn^{++}(O^{=})} \equiv \gamma^{O}_{Mn^{++}(O^{=})} \tag{A56}$$

$$\lim_{N_{Mn^{++}} \to 0} \gamma_{O^{=}(Fe^{++})} \equiv 1 \tag{A57}$$

where $\gamma^{O}_{(MnO)}$ and $\gamma^{O}_{Mn^{++}(O^{=})}$ may be identified as Henrian constants which are independent of concentrations. From equations (A54) to (A57), following relationship is obtained in this special system, viz,

$$\gamma^{O}_{(MnO)} = \theta_{MnO}^{(FeO)}\ \gamma^{O}_{Mn^{++}(O^{=})} \tag{A58}$$

So that $\theta_{MnO}^{(FeO)}$ can be expressed as the ratio of Henrian constants of one compound and one ion in equation (A59).

$$\theta_{MnO}^{(FeO)} = \frac{\gamma^{O}_{(MnO)}}{\gamma^{O}_{Mn^{++}(O^{=})}} \tag{A59}$$

Substituting equation (A59) for $\theta_{MnO}^{(FeO)}$ in equation (A54), we have:

$$\frac{\gamma_{(MnO)}}{\gamma^{O}_{(MnO)}} = \frac{\gamma_{Mn^{++}(O^{=})}}{\gamma^{O}_{Mn^{++}(O^{=})}} \gamma_{O^{=}(Fe^{++})} \tag{A60}$$

In equation (A60), there are still three unknown activity coefficients of ions, including the Henrian constant $\gamma^{O}_{Mn^{++}(O^{=})}$, in one equation. To reduce the unknowns, two of them, $\gamma^{O}_{Mn^{++}(O^{=})}$ and $\gamma_{Mn^{++}(O^{=})}$, may be grouped into one. Thus, Henrian activity coefficient of Mn^{++} is defined:

$$f_{Mn^{++}(O^{=})} = \frac{\gamma_{Mn^{++}(O^{=})}}{\gamma^{O}_{Mn^{++}(O^{=})}} \tag{A61}$$

Similarly, Henrian activity coefficient of MnO, $f_{(MnO)}$ is also defined:

$$f_{(MnO)} = \frac{\gamma_{(MnO)}}{\gamma^{O}_{(MnO)}} \tag{A62}$$

Substituting equations (A61) and (A62) into equation (A60), a simple relationship among Henrian activity coefficients of MnO and Mn^{++} and Raoultian activity coefficient of $O^{=}$ is obtained, viz,

$$f_{(MnO)} = f_{Mn^{++}(O^{=})} \gamma_{O^{=}(Fe^{++})} \tag{A63}$$

In equation (A53) and (A63), there are five activity coefficients of ions and compounds. The corresponding activities can be expressed by activity coefficients and concentrations in the following equations, viz,

$$h_{(MnO)} = f_{(MnO)} N_{(MnO)} \tag{A64a}$$

$$a_{(FeO)} = \gamma_{(FeO)} N_{(FeO)} \tag{A64b}$$

$$h_{Mn^{++}(O^{=})} = f_{Mn^{++}(O^{=})} N_{Mn^{++}} \tag{A64c}$$

$$a_{Fe^{++}(O^{=})} = \gamma_{Fe^{++}(O^{=})} N_{Fe^{++}} \tag{A64d}$$

$$a_{O^{=}(Fe^{++})} = \gamma_{O^{=}(Fe^{++})}\ N_{O^{=}} \qquad \text{(A64e)}$$

Substituting equations (A51), (A52), (A64a) to (A64e) into equations (A53) and (A63), Henrian activity of MnO and Raoultian activity of FeO can be expressed as the products of ion activities:

$$h_{(MnO)} = h_{Mn^{++}(O^{=})}\ a_{O^{=}(Fe^{++})} \qquad \text{(A65)}$$

$$a_{(FeO)} = a_{Fe^{++}(O^{=})} a_{O^{=}(Fe)} \qquad \text{(A66)}$$

A2-4 A Reference State for Evaluation of Ion Activities

In equations (A53) and (A63) for MnO-FeO pseudo-binary system, there are two activity coefficients of compounds (γ_{FeO} and f_{MnO}) which can be experimentally measured and three activity coefficients of ions (i.e. $f_{Mn^{++}(O^{=})}$, $\gamma_{O^{=}(Fe^{++})}$ and $\gamma_{Fe^{++}(O^{=})}$) to be determined. To remove this extra degree of freedom, a reference state for evaluation of ion activities needs to be defined. In aqueous solutions, the potential of a reversible hydrogen electrode with hydrogen at one atmosphere pressure is taken to be zero at all temperatures (Grjotheim and Rosenblatt) and the activity of hydrogen ion is unity. In other ionic solutions where hydrogen ions do not exist, the reference state may be chosen accordingly by the convenience of studies. For instance, in MnO-FeO system, oxygen is the only anion in the solution. Then, we may choose $\gamma_{O^{=}(Fe^{++})} \equiv 1$. Then, activities of Fe^{++} and Mn^{++} can be evaluated, i.e. $a_{Fe^{++}(O^{=})} = a_{(FeO)}$ and $h_{Mn^{++}(O^{=})} = h_{(MnO)}$.

In a general system containing p ions, there will be p-1 independent measurements of activities of compounds. Similarly, when the reference state is chosen for one ion, activities of all other p-1 ions can be evaluated.

A3 Discussions

In this section, the consistency of our formulations of ion activities with the classical thermodynamics and some applications of these equations to the study of ionic solutions will be discussed.

A3-1. Internal Consistency with Classical Thermodynamics in the Formulation of Ion Activities

In the definition of standard state for ion activities, Temkin's rule has been modified by the conversion factors. In the system containing Mn^{++}, Fe^{++}, $O^{=}$ and $S^{=}$, activities of FeO, FeS and MnO have been expressed in equations (A47), (A49a) and (A50). Similarly, activity of MnS with FeO as the solvent which obeys Raoult's law can also be obtained, viz,

$$a_{(MnS)} = \theta_{MnS}^{(FeO)} \, a_{Mn^{++}(O^{=})} \, a_{S^{=}(Fe^{++})} \tag{A67}$$

Through the equilibrium of displacement reaction in the solution:

$$(MnO) + (FeS) = (MnS) + (FeO) \tag{A21}$$

the equilibrium constant can be expressed, i.e.

$$K_{A21} = \left[\frac{a_{(MnS)} a_{(FeO)}}{a_{(MnO)} a_{(FeS)}} \right]_{eq} = \frac{\theta_{MnS}^{(FeO)}}{\theta_{MnO}^{(FeO)} \, \theta_{FeS}^{(FeO)}} \tag{A68}$$

With equation (A68), these three conversion factors are related through the equilibrium constant K_{A21}.

On the other hand, comparing with equation (A29) which was demonstrated by Blander (1977), the ratio of activity coefficients of compounds may be expressed, considering equations (A54) and (A67), in the following way:

$$\frac{\gamma_{(FeO)}}{\gamma_{(MnO)}} = \frac{\gamma_{Fe^{++}(O^{=})}\,\gamma_{O^{=}(Fe^{++})}}{\gamma_{Mn^{++}(O^{=})}\,\gamma_{O^{=}(Fe^{++})}\,\theta_{MnO}^{(FeO)}} = \frac{\gamma_{Fe^{++}(O^{=})}}{\gamma_{Mn^{++}(O^{=})}\,\theta_{MnO}^{(FeO)}} \qquad (A69a)$$

and

$$\frac{\gamma_{(FeS)}}{\gamma_{(MnS)}} = \frac{\gamma_{Fe^{++}(O^{=})}\,\gamma_{S^{=}(Fe^{++})}\,\theta_{FeS}^{(FeO)}}{\gamma_{Mn^{++}(O^{=})}\,\gamma_{S^{=}(Fe^{++})}\,\theta_{MnS}^{(FeO)}} = \frac{\gamma_{Fe^{++}(O^{=})}\,\theta_{FeS}^{(FeO)}}{\gamma_{Mn^{++}(O^{=})}\,\theta_{MnS}^{(FeO)}} \qquad (A69b)$$

From (A69a) and (A69b), we have:

$$\frac{\gamma_{(FeO)}}{\gamma_{(MnO)}} = \frac{\gamma_{Fe^{++}(O^{=})}}{\gamma_{Mn^{++}(O^{=})}\,\theta_{MnO}^{(FeO)}} = \frac{\gamma_{(FeS)}}{\gamma_{(MnS)}}\left[\frac{\theta_{MnS}^{(FeO)}}{\theta_{MnO}^{(FeO)}\,\theta_{FeS}^{(FeO)}}\right] = \frac{\gamma_{(FeS)}}{\gamma_{(MnS)}}\,K_{A21} \qquad (A70)$$

This equation is to be compared with equation (A29). Therefore, the inconsistencies in the Temkin's rule when is applied to non-ideal solutions demonstrated by Blander (1977) and Forland and Grjotheim (1978) could be avoided in the present formulation.

A3-2 Two Type of Ideal Ionic Solutions

In the formulation of ion activities, the activity coefficients of both neutral species and ions may be properly defined. To satisfy the condition of ideality proposed by Temkin [equation (A6)], there might be two type of ideal solutions to describe one solution (e.g. FeO-MnO), by defining the activity coefficient of ions or neutral species to be unity.

Type 1: All activity coefficients of ions are unity.

From equations (A53) and (A54), following relationships are obtained:

$$\gamma_{(FeO)} = \gamma_{Fe^{++}(O^{=})}\,\gamma_{O^{=}(Fe^{++})} \equiv 1 \qquad (A71)$$

$$\gamma_{(MnO)} = \theta_{MnO}^{(FeO)}\,\gamma_{Mn^{++}(O^{=})}\,\gamma_{O^{=}(Fe^{++})} \equiv \theta_{MnO}^{(FeO)} \qquad (A72)$$

Type 2: All activity coefficients of neutral species are unity.

In this case, equation (A71) is still applicable to activity coefficient of FeO. For MnO, equation (A73) is assumed, viz,

$$\gamma_{(MnO)} = \theta_{MnO}^{(FeO)} \gamma_{Mn^{++}(O^{=})} \gamma_{O^{=}(Fe^{++})} \equiv 1 \qquad (A73)$$

In equation (A73), the product $(\gamma_{Mn^{++}(O^{=})} \gamma_{O^{=}(Fe^{++})})$ is $\left[\theta_{MnO}^{(FeO)}\right]^{-1}$ instead of unity in equation (A72).

From an experimentalist's point of view, activity coefficients of neutral species can be measured. It is usually recognized in the current practice that, when the value of activity coefficient of the neutral species is unity, e.g. $\gamma_{(MnO)} = 1$, MnO behaves ideal in a solution of oxides. For ionic solutions, the ideality may be considered that the activity coefficients of ions are unity, i.e. equations (A71) and (A72).

A3-3 Application of Gibbs-Duhem Relationship in Ionic Solutions

In ionic solutions, total Gibbs Free Energy may be expressed through the summation of chemical potential of ions, viz,

$$G = \sum_i n_i^+ \mu_i^+ + \sum_j n_j^- \mu_j^- \qquad (A74)$$

where μ_i^+ and μ_j^- are the chemical potential of cation and anion, respectively. By differentiating equation (A74) at constant temperature and pressure and considering the relationship:

$$dG = \sum_i \mu_i^+ dn_i^+ + \sum_j \mu_j^- dn_j^- \qquad (A75)$$

Gibbs-Duhem equation in ionic solutions is then obtained:

$$\sum_i n_i^+ d\mu_i^+ + \sum_j n_j^- d\mu_j^- \equiv 0 \qquad (A76)$$

For the ionic solution consisting of two cations Mn^{++} and Fe^{++} and two anions $O^=$ and $S^=$, Gibbs-Duhem equation (A76) becomes:

$$n_{Mn^{++}}\, d\mu_{Mn^{++}} + n_{Fe^{++}}\, d\mu_{Fe^{++}} + n_{O^=}\, d\mu_{O^=} + n_{S^=}\, d\mu_{S^=} \equiv 0 \qquad (A77)$$

By using compound MnO as the standard state for activities of Mn^{++}, FeO for activity of Fe^{++} and $O^=$ and FeS for activity of $S^=$, equation (A77) can be rearranged in form of ion activities:

$$n_{Mn^{++}}\, d\ln a_{Mn^{++}(O^=)} + n_{Fe^{++}}\, d\ln a_{Fe^{++}(O^=)}$$
$$+ n_{O^=}\, d\ln a_{O^=(Fe^{++})} + n_{S^=}\, d\ln a_{S^=(Fe^{++})} \equiv 0 \qquad (A78)$$

By substituting charge balance equation (A79):

$$n_{O^=} = n_{Mn^{++}} + n_{Fe^{++}} - n_{S^=} \qquad (A79)$$

into equation (A78), the Gibbs-Duhem equation can be further rearranged, viz,

$$(n_{Mn^{++}} - n_{S^=})\, d\ln \left[a_{Mn^{++}(O^=)} a_{O^=(Fe^{++})}\right] + n_{Fe^{++}}\, d\ln \left[a_{Fe^{++}(O^=)} a_{O^=(Fe^{++})}\right]$$
$$+ n_{S^=}\, d\ln \left[a_{Mn^{++}(O^=)} a_{S^=(Fe^{++})}\right] \equiv 0 \qquad (A80)$$

Considering that conversion factors are independent of concentrations, we have:

$$d\ln \theta_{MnO}^{(FeO)} = d\ln \theta_{MnS}^{(FeO)} = d\ln \theta_{FeS}^{(FeO)} = 0 \qquad (A81)$$

and equation (A80) can be rewritten in form of neutral species:

$$(n_{Mn^{++}} - n_{S^=})\, d\ln a_{MnO} + n_{Fe^{++}}\, d\ln a_{FeO} + n_{S^=}\, d\ln a_{MnS} = 0 \qquad (A82)$$

From equation (A82), we have:

$$-\, d\ln a_{MnS} = [(n_{Mn^{++}}/n_{S^=}) - 1]\, d\ln a_{MnO} + (n_{Fe^{++}}/n_{S^=})\, d\ln a_{FeO} \qquad (A83)$$

Similarly, activity of FeS can be calculated:

$$- d\ln a_{FeS} = [(n_{Fe^{++}}/n_{S^{=}}) - 1]\, d\ln a_{FeO} + (n_{Mn^{++}}/n_{S^{=}})\, d\ln a_{MnO} \qquad (A84)$$

Since it is usually more convenient to measure activities of oxides than to measure activities of sulfides, equations (A83) and (A84) provide an opportunity to calculate activities of sulfides from the measurements of oxides.

A4 Summary

It has been shown that the definition of standard states is the key issue for defining ion activities in ionic solutions, such as molten salts and slag. The Temkin's rule has been found to be leading to the inconsistencies in ideal ionic solutions (activity coefficients of compounds to be unity) by Temkin (1945) and to have similar difficulties in non-ideal solutions by Blander (1977) and Forland and Grjotheim (1978). The present work is aimed to solve these problems and is summarized as follows:

(1) In defining the chemical activity of one ion, the nature of co-existing ions of opposite charge must be recognized, equations (A30) and (A32). The conversion factor which converts the standard state of an ion activity in terms of one pure compound to another, equation (A46), is introduced. With this formulation, the inconsistencies in classical thermodynamics of ionic solutions demonstrated by Blander (1977) and Forland and Grjotheim (1978) may be avoided.

(2) Temkin's rule in the original form for molten salts is found to to be a limiting case in our formulation where the conversion factor is unity, equations (A42) and (A42a).

(3) The conversion factors, which are defined in terms of standard chemical potentials of ions in pure compounds, may be expressed in terms of Henrian activities of ions and compounds. The formulation becomes analogous with that used in the dilute aqueous solutions.

(4) A reference state for ion activities, similar to the definition of the standard hydrogen electrode for the study of aqueous solutions, needs to be selected for ionic solutions, e.g. unit activity of oxygen anion in oxide slags. Thus, activities of all ions in ionic solutions can be, in principle, evaluated based on the experimental data.

APPENDIX B

CALCULATIONS OF CONCENTRATION CHANGES IN THE REACTION ZONE DUE TO MULTIPLE AND SIMULTANEOUS INTERFACIAL REACTIONS

APPENDIX B

CALCULATIONS OF CONCENTRATION CHANGES IN THE REACTION ZONE DUE TO MULTIPLE AND SIMULTANEOUS INTERFACIAL REACTIONS

In this appendix, the details of calculations based on general reaction rate equations (3-5) and (3-8) for slag/metal system but limited to the reaction zone are presented. For a very short period of time, it is assumed that there is no mass fluxes across the boundaries between the reaction zone and the bulk phases. Therefore, masses of all reacting elements are conserved within the boundary of the reaction zone. The computed results will be used as the boundary conditions for computations of diffusion in slag and alloy (for details see Appendix C).

B1 General Equations

By substituting equation (3-5) into equation (3-8), the following equation is obtained:

$$\sum_{i=1}^{p} z_i k_i a_i \left[1 - L_i U^{z_i} \right] = 0 \qquad \text{(B1)}$$

In equation (B1), there is one equation with which one unknown may be determined, therefore, let it be the coupling factor U. Since the valence z_i of any element is an integer number (± 1, ± 2, ...), equation (B1) can be solved as a polynomial equation, i.e.

$$\sum_{i=1}^{p} z_i k_i a_i - \sum_{i=1}^{p} z_i k_i a_i L_i U^{z_i} = 0 \qquad \text{(B2)}$$

Using a special case for illustration that the system contains only divalent ions, e.g. A^{++}, B^{++}, C^{++}, $X^{=}$ and $Y^{=}$, equation (B1) becomes:

$$b_1 - b_2 U^2 + b_3 U^{-2} = 0 \qquad \text{(B3)}$$

or

$$b_2 U^4 - b_1 U^2 - b_3 = 0 \qquad \text{(B4)}$$

where

$$b_1 = k_A a_A + k_B a_B + k_C a_C - k_X a_X - k_Y a_Y \qquad \text{(B5)}$$

$$b_2 = L_A k_A a_A + L_B k_B a_B + L_C k_C a_C \qquad \text{(B6)}$$

$$b_3 = L_X k_X a_X + L_Y k_Y a_Y \qquad \text{(B7)}$$

Since the solution to the coupling factor U has to be non-zero and positive definite, U can then be uniquely calculated by the following equation:

$$U = \sqrt{\frac{b_1 + \sqrt{b_1^2 + 4b_2 b_3}}{2b_2}} \qquad \text{(B8)}$$

Another special case is the system containing ions of only single valence, e.g. A^{+}, B^{+}, C^{+}, X^{-} and Y^{-}, the coupling factor is then calculated in equation (B9), viz,

$$U = \frac{b_1 + \sqrt{b_1^2 + 4b_2 b_3}}{2b_2} \qquad \text{(B9)}$$

In general, ionic solutions usually contain ions of different valences, e.g. silicate slag. Thus, equation (B2) has to be solved through numerical methods which will be demonstrated in the next section.

B2 The Computation of Rates of Interfacial Reactions in Slag/Metal System

In our experimental system, there are six chemical elements, Al, Ca, Fe, Mn, Si and O. In alloy, iron is the solvent and the others are solutes. For convenience, activity of iron is expressed in Raoultian scale and those of solutes are in Henrian scale by using hypothetical one weight percent as the standard state. In slag, the standard states for activities of ions are chosen to be pure oxides in such a way that CaO is for activities of Ca^{++} and $O^{=}$ and other oxides for related cations only (Appendix A). Therefore, the term L_i in the rate equation (3-5) can be described as follows:

$$L_O = \frac{a_{O^{=}(Ca^{++})}}{K_O h_{[O]}} \tag{B10}$$

$$L_{Ca} = \frac{a_{Ca^{++}(O^{=})}}{K_{Ca} h_{[Ca]}} \tag{B11}$$

$$L_{Fe} = \frac{a_{Fe^{++}(O^{=})}}{K_{Fe} \gamma_{[Fe]} N_{[Fe]}} \tag{B12}$$

$$L_{Mn} = \frac{a_{Mn^{++}(O^{=})}}{K_{Mn} h_{[Mn]}} \tag{B13}$$

$$L_{Al} = \frac{a_{Al^{+++}(O^{=})}}{K_{Al} h_{[Al]}} \tag{B14}$$

$$L_{Si} = \frac{a_{Si^{4+}(O^{=})}}{K_{Si} h_{[Si]}} \tag{B15}$$

where $a_{O^{=}(Ca^{++})}$, $a_{Ca^{++}(O^{=})}$, etc are activities of anion $O^{=}$ and cations Ca^{++}, etc. in slag, $h_{[O]}$, etc. are Henrian activities of elements in alloy by using one weight percent as the standard state, e.g. $h_{[O]} = f_{[O]}[\%O]$, $\gamma_{[Fe]}$ is Raoultian activity coefficient of iron and K_O, etc. are the partition ratios between the ion activity in slag and activity of the element in alloy at equilibrium state.

Following Appendix A, these ion activities can be related to the activities of neutral species, i.e.

$$a_{(CaO)} = a_{Ca^{++}(O^{=})}\ a_{O^{=}(Ca^{++})} \tag{B16}$$

$$a_{(FeO)} = \theta_{FeO}^{(CaO)} a_{Fe^{++}(O^{=})}\ a_{O^{=}(Ca^{++})} \tag{B17}$$

$$a_{(MnO)} = \theta_{MnO}^{(CaO)} a_{Mn^{++}(O^{=})}\ a_{O^{=}(Ca^{++})} \tag{B18}$$

$$a_{(Al_2O_3)} = \theta_{Al_2O_3}^{(CaO)}\ a^2_{Al^{+++}(O^{=})}\ a^3_{O^{=}(Ca^{++})} \tag{B19}$$

$$a_{(SiO_2)} = \theta_{SiO_2}^{(CaO)} a_{Si^{4+}(O^{=})}\ a^2_{O^{=}(Ca^{++})} \tag{B20}$$

Then, from chemical reactions of formation of oxides, the equilibrium constants can be expressed by the products of partition ratios and the conversion factors, viz,

$$[Ca] + [O] = (CaO) \tag{B21}$$

$$K_{CaO} = \left[\frac{a_{(CaO)}}{h_{[Ca]}h_{[O]}}\right]_{eq} = \left[\frac{a_{Ca^{++}(O^{=})}\ a_{O^{=}(Ca^{++})}}{h_{[Ca]}h_{[O]}}\right]_{eq} = K_{Ca}K_{O} \tag{B22}$$

$$[Fe] + [O] = (FeO) \tag{B23}$$

$$K_{FeO} = \left[\frac{a_{(FeO)}}{\gamma_{[Fe]}N_{[Fe]}a_{[O]}}\right]_{eq} = \left[\frac{\theta_{FeO}^{(CaO)} a_{Fe^{++}(O^{=})}\ a_{O^{=}(Ca^{++})}}{\gamma_{[Fe]}N_{[Fe]}a_{[O]}}\right]_{eq} = \theta_{FeO}^{(CaO)}K_{Fe}K_{O} \tag{B24}$$

$$[Mn] + [O] = (MnO) \tag{B25}$$

$$K_{MnO} = \left[\frac{a_{(MnO)}}{h_{[Mn]}h_{[O]}}\right]_{eq} = \left[\frac{\theta_{MnO}^{(CaO)} a_{Mn^{++}(O^{=})} a_{O^{=}(Ca^{++})}}{h_{[Mn]}h_{[O]}}\right]_{eq} = \theta_{MnO}^{(CaO)}K_{Mn}K_{O} \tag{B26}$$

$$2\ [Al] + 3\ [O] = (Al_2O_3) \tag{B27}$$

$$K_{Al_2O_3} = \left[\frac{a_{(Al_2O_3)}}{h^2_{[Al]}h^3_{[O]}}\right]_{eq} = \left[\frac{\theta_{Al_2O_3}^{(CaO)} a^2_{Al^{+++}(O^{=})} a^3_{O^{=}(Ca^{++})}}{h^2_{[Al]}h^3_{[O]}}\right]_{eq} = \theta_{Al_2O_3}^{(CaO)}K^2_{Al}K^3_{O} \tag{B28}$$

$$[Si] + 2\,[O] = (SiO_2) \tag{B29}$$

$$K_{SiO_2} = \left[\frac{a_{(SiO_2)}}{h_{[Si]}h^2_{[O]}}\right]_{eq} = \left[\frac{\theta^{(CaO)}_{SiO_2} a_{Si^{4+}(O^=)} a^2_{O^=(Ca^{++})}}{h_{[Si]}h^2_{[O]}}\right]_{eq} = \theta^{(CaO)}_{SiO_2} K_{Si} K_O^2 \tag{B30}$$

By substituting equations (B16) to (B20) and (B22), (B24), (B26), (B28) and (B30) for cation activities and the partition ratios of cation elements in equations (B11) to (B15) and canceling the conversion factors, following relations are obtained:

$$L_{Ca} = \frac{a_{CaO}}{K_{CaO} h_{[Ca]}} \left[\frac{K_O}{a_{O^=(Ca^{++})}}\right] \tag{B31}$$

$$L_{Fe} = \frac{a_{FeO}}{K_{FeO} \gamma_{[Fe]} N_{[Fe]}} \left[\frac{K_O}{a_{O^=(Ca^{++})}}\right] \tag{B32}$$

$$L_{Mn} = \frac{a_{MnO}}{K_{MnO} h_{[Mn]}} \left[\frac{K_O}{a_{O^=(Ca^{++})}}\right] \tag{B33}$$

$$L_{Al} = \frac{a^{1/2}_{Al_2O_3}}{K^{1/2}_{Al_2O_3} h_{[Al]}} \left[\frac{K_O}{a_{O^=(Ca^{++})}}\right]^{3/2} \tag{B34}$$

$$L_{Si} = \frac{a_{SiO_2}}{K_{SiO} h_{[Si]}} \left[\frac{K_O}{a_{O^=(Ca^{++})}}\right]^{2} \tag{B35}$$

In the above equations, there are two unknown parameters, K_O and $a_{O^=(Ca^{++})}$ which are common in the expression of all L_i's. Therefore, these two parameters can be separated from the expression of L_i's and included in a new parameter U_O, viz,

$$U_O = U \left[\frac{K_O}{a_{O^=(Ca^{++})}}\right]^{1/2} \tag{B36}$$

Then, reaction rate equations for Ca, Fe, Mn, Al, Si and O can be written as:

$$\omega_{Ca} = \xi_{Ca} h_{[Ca]} \left[1 - \frac{a_{CaO}}{K_{CaO} h_{[Ca]}} U_O^2 \right] \tag{B37}$$

$$\omega_{Fe} = \xi_{Fe} \gamma_{[Fe]} N_{[Fe]} \left[1 - \frac{a_{FeO}}{K_{FeO} \gamma_{[Fe]} N_{[Fe]}} U_O^2 \right] \tag{B38}$$

$$\omega_{Mn} = \xi_{Mn} h_{[Mn]} \left[1 - \frac{a_{MnO}}{K_{MnO} h_{[Mn]}} U_O^2 \right] \tag{B39}$$

$$\omega_{Al} = \xi_{Al} h_{[Al]} \left[1 - \frac{a_{Al_2O_3}^{1/2}}{K_{Al_2O_3}^{1/2} h_{[Al]}} U_O^3 \right] \tag{B40}$$

$$\omega_{Si} = \xi_{Si} h_{[Si]} \left[1 - \frac{a_{SiO_2}}{K_{SiO_2} h_{[Si]}} U_O^4 \right] \tag{B41}$$

$$\omega_O = \xi_O h_{[O]} \left[1 - \frac{1}{h_{[O]}} U_O^{-2} \right] \tag{B42}$$

where for the solvent:

$$\xi_{Fe} = k_{Fe} C_{Fe} \qquad \text{in the unit of (cm/sec)(moles/cm}^3\text{)} \tag{B43}$$

and for the solutes with conversion of concentration unit to weight percent in h_i, then,

$$\xi_i = \frac{C_{alloy} \gamma_i^o}{M_i \sum_{j=1}^{p} ([\%j]/M_j)} \qquad (i = Al, Ca, O, Mn \text{ and } Si) \tag{B44}$$

where C_{alloy} is the density of alloy in moles per unit volume (mole/cm^3), γ_i^o is the Henrian constant of ith element, M_i is the molar weight of ith element and [%j] is the weight percent of jth element. Applying the constraint of no net electric current to the slag/metal system, we have:

$$2\omega_{Ca} + 2\omega_{Fe} + 2\omega_{Mn} + 3\omega_{Al} + 4\omega_{Si} - 2\omega_O \equiv 0 \tag{B45}$$

By substituting above rate equations (B37) to (B42) in (B45), following polynomial equation is obtained:

$$c_1 - c_2U_o^2 - c_3U_o^3 - c_4U_o^4 + c_5U_o^{-2} = 0 \qquad \text{(B46)}$$

where:

$$c_1 = 2\xi_{Ca}h_{[Ca]} + 2\xi_{Fe}\gamma_{[Fe]}N_{[Fe]} + 2\xi_{Mn}h_{[Mn]} + 3\xi_{Al}h_{[Al]} + 4\xi_{Si}h_{[Si]} - 2\xi_{O}h_{[O]} \qquad \text{(B47)}$$

$$c_2 = 2\left(\frac{\xi_{Ca}a_{CaO}}{K_{CaO}} + \frac{\xi_{Fe}a_{FeO}}{K_{FeO}} + \frac{\xi_{Mn}a_{MnO}}{K_{MnO}}\right) \qquad \text{(B48)}$$

$$c_3 = \frac{3\,\xi_{Al}a_{Al_2O_3}^{1/2}}{K_{Al_2O_3}^{1/2}} \qquad \text{(B49)}$$

$$c_4 = \frac{4\,\xi_{Si}a_{SiO_2}}{K_{SiO_2}} \qquad \text{(B50)}$$

$$c_5 = 2\,\xi_O \qquad \text{(B51)}$$

To solve for U_o in equation (B46), a numerical approach is applied. Since U_o is a non-zero parameter, the solution to equation (B46) is then identical to solving that $f(U_o) = 0$, viz,

$$f(U_o) = c_1U_o^2 - c_2U_o^4 - c_3U_o^5 - c_4U_o^6 + c_5 = 0 \qquad \text{(B52)}$$

With the first derivative of $f(U_o)$ with respect to U_o, i.e.

$$\frac{df(U_o)}{dU_o} = 2c_1U_o - 4c_2U_o^3 - 5c_3U_o^4 - 6c_4U_o^5 \qquad \text{(B53)}$$

Newtonian function is then built in such a way:

$$F(U_o) = U_o - \frac{f(U_o)}{df(U_o)/dU_o} \qquad \text{(B54)}$$

Therefore, the calculations are iterated through equation (B55):

$$U_{o,k+1} = U_{o,k} - \frac{f(U_{o,k})}{df(U_{o,k})/dU_{o,k}} \tag{B55}$$

The initial value for iterations has been chosen from the calculated result through equation (B56) by neglecting high order terms in equation (B52), which is corresponding to the system consisting of only divalent ions [equation (B8)]. This approach has been successful in obtaining numerical values of U_o for all cases computed in the present study.

$$U_{o,1} = \sqrt{\frac{c_1 + \sqrt{c_1^2 + 4c_2c_5}}{2c_2}} \tag{B56}$$

The iterations will stop when $U_{o,k+1}$-$U_{o,k}$ is less than the required precision ε, i.e.

$$|U_{o,k+1} - U_{o,k}| < \varepsilon \tag{B57}$$

In actual computations for slag/metal system, ε has been chosen to be $\varepsilon = 1\times10^{-4}$ $U_{o,k}$. Once U_o is obtained, reaction rates of all elements can be calculated according to equations (B37) to (B42).

B3 Mathematical Model of Kinetics of Interfacial Reactions

During the course of reaction, mass fluxes of each element across interface result in re-distributions of these elements between two phases and corresponding changes of concentrations and concentration gradients. The strategy of computation of this complex system has been outlined in Section 4-2, i.e. the simultaneous process of chemical reactions and diffusion in a physical system may be replaced by sequential steps, alternating between chemical reactions and diffusion.

The amount of elements transferred within a short time interval Δt_R can be calculated, viz,

$$\Delta n_i = \omega_i \, \Omega \, \Delta t_R \qquad (i=1,2,...,p) \qquad (B58)$$

where Ω is the interfacial area for reactions (cm^2) and ω_i is net reaction rate (mole/cm^2 sec.).

The computations may be carried out from the reaction rates determined at a time t (t=0 at initial state) and let it continue for a period of Δt_R. At the end of this period Δt_R, new concentrations in terms of mole fractions in metallic phase and cation and anion fractions in ionic phase at $t = t + \Delta t_R$, which are uniform in the reaction zone, are computed. The general expression for reactions take place for a duration of Δt_R, between t and $t + \Delta t_R$ are shown in the following equations:

for iron in metallic phase:

$$N_{Fe}^{t+\Delta t_R} = \frac{n_{Fe}^t - \Delta n_{Fe}}{\Sigma(n_j^t - \Delta n_j)} \qquad (B59)$$

and other elements:

$$[\%i]^{t+\Delta t_R} = \frac{(n_i^t - \Delta n_i)\, M_i}{\sum_j (n_j^t - \Delta n_j)\, M_j} \times 100 \qquad \text{(B60)}$$

where i = Al, Ca, O, Mn and Si, j = Al, Ca, O, Fe, Mn and Si and M_i is the molar weight of ith element;

for mole fractions of oxides in slag:

$$N_{ko}^{t+\Delta t_R} = \frac{n_{ko}^t + \Delta n_k}{\sum_l (n_{lo}^t + \Delta n_l) + (n_{Al_2O_3}^t + 1/2\ \Delta n_{Al})} \qquad \text{(B61)}$$

$$N_{Al_2O_3}^{t+\Delta t_R} = \frac{n_{Al_2O_3}^t + 1/2 \Delta n_{Al}}{\sum_l (n_{lo}^t + \Delta n_l) + (n_{Al_2O_3}^t + 1/2\ \Delta n_{Al})} \qquad \text{(B62)}$$

where k, l = Ca, Fe, Mn and Si and kO, lO represents oxides of CaO, FeO, MnO and SiO_2.

When new concentrations at time $t+\Delta t_R$ are obtained, activities of each component will be re-calculated. Another round of computations of reaction rates for a duration of Δt_R will continue. The flow chart is shown in Fig. B1. This repetitive calculations of the chemical state in the reaction zone may be stopped after certain required changes made or after certain time of reaction. Then, the chemical reactions will be switched off and diffusion switched on.

One of important parameters in computations is the selection of time interval Δt_R. If Δt_R is too large, computations may not be converged or errors in numerical results may be large. If Δt_R is too small, computing time may be unnecessarily long. The value of Δt_R should be adjusted in computations. In our system, it has been selected to be 1.0 millisecond in the computations (Chapter Six).

APPENDIX C

NUMERICAL SOLUTION OF DIFFUSION EQUATIONS BY FINITE DIFFERENCE METHOD

APPENDIX C

NUMERICAL SOLUTION OF DIFFUSION EQUATIONS BY FINITE DIFFERENCE METHOD

In order to solve diffusion equations (4-2) and (4-6) in metallic and ionic phases, the total length of specimen L may be divided by n nodes. In each spatial interval, Δx, which is equal to L/n. In computations, the time interval Δt_D is also chosen. In this way, diffusion distance and time become discontinuous. Therefore, all the derivatives in equations (4-2) and (4-6) can be replaced by the equation of finite difference approximation using a taylor series expansion, viz,

$$C_i(k+i,\ell) = C_i(k,\ell) + \frac{\Delta t_D}{(\Delta x)^2} \sum_{j=1}^{p} \Big[\Big[C_j(k,\ell) - C_j(k+1,\ell-1) \Big] \times \Big[D_{ij}(k,\ell) - D_{ij}(k+1,\ell-1) \Big] + D_{ij}(k,\ell) \times \Big[C_j(k,\ell+1) - 2C_j(k,\ell) + C_j(k+1,\ell-1) \Big] \Big] \quad \text{(C1)}$$

where i=1,2,...,p, k represents time intervals starting from zero and ℓ for the spatial intervals starting from one to n-1. Since equations (4-2) and (4-6) have identical formulations, equations (C1) may be used for computations of diffusion in both ionic and metallic phase by changing values of diffusion coefficients and concentrations.

In computations, the application of boundary conditions given in Chapter

Four is described as follows. At time zero, i.e. $k = 0$, initial condition is used, i.e. $C_i(0,\ell) = C_i^o$. When reactions start, e.g. $k = 1$, boundary conditions are used, where $C_i(1,0)$ is computed through the model of kinetics for interfacial reactions and $C_i(1,m)$ will be kept a constant value, i.e. C_i^o. In this way, iterations will continue until the time m Δt_D for the model computations (see Chapter Four) is reached.

APPENDIX D

TABLES OF CHEMICAL ANALYSIS OF REAGENTS AND Fe-Mn ALLOY

APPENDIX D

TABLES OF CHEMICAL ANALYSIS OF REAGENTS AND Fe-Mn ALLOY

Table D1: Lot Analysis of Silicon Oxide, SiO_2, 99.995+%
Lot Number: 02207 JV

Appearance:	White crystalline powder			
Loss on Ignition:	0.37			
Trace Analysis (ICP):	Element	ppm	Element	ppm
	Na	35	Mn	0.3
	Al	20	Mg	0.1
	Fe	3	Ti	0.1
	Ca	1		

Table D2: Lot Analysis of Fe lump, Electrolytic, 99.9+%
Lot Number: 00329 LK

Appearance:	Shiny grey-black chips		
Trace Analysis (X-ray):	Al	350	ppm
	Zn	25	ppm
	Si	20	ppm
	Cu	5	ppm
	Ca	2	ppm
	Mg	0.4	ppm

Table D3: Lot Analysis of Manganese, Mn Flake, 99.98%

Lot Number: 01611 PT

Appearance:	Metallic grey chunks		
Trace analysis (ICP):	Pb	95	ppm
	Co	35	ppm
	Mg	30	ppm
	Cr	25	ppm
	Ca	9	ppm

Table D4: Chemical Analysis of Fe-Mn Alloy

Mn: 22.33%

Trace analysis (ppm):

P	Si	Cu	Co	Pb	As	Sn	Nb	B	Ca	Mg
850	23	28	23	166	219	84	21	16	3	4

APPENDIX F

LIST OF MEASURED CONCENTRATION PROFILES BY USING EPMA

APPENDIX E

LIST OF MEASURED CONCENTRATION PROFILES BY USING EPMA

TABLE E1: MEASURED CONCENTRATION PROFILES IN SPECIMEN 1a

Distance from Interface	Slag Phase					Metal Phase	
x (μm)	(%CaO)	(%Al_2O_3)	(%SiO_2)	(%MnO)	(%FeO)	[%Si]	[%Mn]
0*	32.5	20.5	45.6	1.41	0.20	2.00	0.39
10	31.8	20.0	46.8	1.40	0.16	1.93	0.40
20	31.9	20.0	46.7	1.41	0.15	1.89	0.49
30	31.9	20.0	46.6	1.45	0.14	1.93	0.53
40	31.8	19.9	46.9	1.45	0.12	1.88	0.54
50	32.0	20.1	46.7	1.27	0.10	1.91	0.55
60	31.9	20.0	46.8	1.36	0.10	1.88	0.62
70	31.9	20.0	46.8	1.28	0.10	1.92	0.68
80	32.1	20.1	46.7	1.15	-	1.91	0.72
90	31.9	20.0	46.9	1.13	0.07	1.82	0.76
100	32.0	20.1	46.9	1.08	-	1.92	0.83
150	32.0	20.0	47.0	0.93	0.04	1.73	1.04
200	32.3	20.2	46.6	0.82	0.05	1.80	1.19
250	32.5	20.3	46.5	0.64	-	1.74	1.24
300	32.4	20.2	47.0	0.41	0.03	1.72	1.33
350	32.3	20.2	47.1	0.41	-	1.76	1.52
400	32.3	20.1	47.3	0.32	-	1.64	1.50
450	32.2	20.0	47.5	0.20	-	1.71	1.50
500	32.2	20.0	47.5	0.19	-	1.68	1.47
550	32.1	20.0	47.7	0.19	-	1.67	1.53
600	31.9	19.8	48.1	0.09	-	1.70	1.47
Far end	31.6	19.9	48.3	-	-	1.65	1.46

where * indicates that the measurd data are in the vicinity of interface through the control of the electron beam.

TABLE E2: MEASURED CONCENTRATION PROFILES IN SPECIMEN 1b

Distance from Interface	Slag Phase					Metal Phase	
x (μm)	(%CaO)	(%Al_2O_3)	(%SiO_2)	(%MnO)	(%FeO)	[%Si]	[%Mn]
0*	30.8	20.2	47.3	1.72	0.44	1.68	0.33
10	30.7	20.1	47.4	1.79	0.28	1.73	0.39
20	30.7	20.1	47.5	1.66	0.37	1.76	0.31
30	30.6	20.1	47.6	1.70	0.26	1.71	0.31
40	30.6	20.0	47.6	1.79	0.33	1.68	0.36
50	30.7	20.1	47.6	1.62	0.26	1.72	0.31
60	30.6	20.0	47.9	1.60	0.24	1.72	0.37
70	30.6	20.0	47.7	1.72	0.24	1.71	0.34
80	30.7	20.1	47.7	1.56	0.21	1.71	0.41
90	30.7	20.1	47.7	1.56	-	1.66	0.42
100	30.5	19.9	47.8	1.77	0.18	1.71	0.48
150	30.5	19.9	48.0	1.54	0.16	1.65	0.55
200	30.6	20.0	48.0	1.49	0.18	1.69	0.63
250	30.6	20.0	48.5	1.38	0.17	1.68	0.69
300	30.7	20.1	47.7	1.42	0.15	1.73	0.79
350	30.9	20.2	47.9	1.09	-	1.58	0.90
400	30.6	19.9	48.3	1.08	0.13	1.64	0.88
450	30.8	20.1	48.1	1.03	-	1.69	1.06
500	30.8	20.1	48.1	0.96	0.11	1.66	1.08
550	30.9	20.2	48.2	0.75	-	1.72	1.11
600	31.1	20.2	47.9	0.78	-	1.61	1.19
Far end	30.6	20.3	49.1	-	-	1.62	1.45

where * indicates that the measurd data are in the vicinity of interface through the control of the electron beam.

TABLE E3: MEASURED CONCENTRATION PROFILES IN SPECIMEN 2a

Distance from Interface	Slag Phase					Metal Phase	
x (μm)	(%CaO)	(%Al_2O_3)	(%SiO_2)	(%MnO)	(%FeO)	[%Si]	[%Mn]
0*	39.1	18.7	41.4	0.79	0.61	1.43	0.51
10	40.0	20.0	39.1	0.98	0.43	1.48	0.51
20	40.1	19.4	39.6	0.95	0.31	1.49	0.55
30	39.7	19.4	40.0	0.87	0.26	1.52	0.57
40	39.8	19.4	40.0	0.86	0.17	1.44	0.61
50	40.1	19.8	39.3	0.83	0.18	1.48	0.67
60	39.6	19.4	40.3	0.73	0.18	1.52	0.74
70	39.8	19.5	39.9	0.82	0.20	1.49	0.74
80	40.3	19.6	39.3	0.82	0.18	1.50	0.79
90	40.4	19.7	39.1	0.77	0.15	1.44	0.86
100	39.8	19.6	39.8	0.74	-		
150	39.8	19.2	40.2	0.76	0.14	1.43	1.03
200	40.6	19.9	38.8	0.73	0.08	1.40	1.10
250	39.4	19.3	40.7	0.62	0.06		
300	40.0	19.7	39.7	0.63	0.06	1.41	1.29
350	39.9	19.8	39.9	0.46	0.08	1.37	1.28
400	40.0	19.4	40.1	0.48	0.05	1.39	1.27
450	40.3	19.5	39.7	0.49	-		
500	40.7	19.5	39.4	0.33	0.08	1.31	1.32
550	40.8	19.9	39.0	0.30	-		
600	39.6	19.3	40.8	0.25	-	1.33	1.31
Far end	39.8	19.8	48.4	-	-	1.41	1.46

where * indicates that the measurd data are in the vicinity of interface through the control of the electron beam.

TABLE E4: MEASURED CONCENTRATION PROFILES IN SPECIMEN 2b

Distance from Interface	Slag Phase					Metal Phase	
x (μm)	(%CaO)	(%Al_2O_3)	(%SiO_2)	(%MnO)	(%FeO)	[%Si]	[%Mn]
0*	31.1	25.9	39.5	0.84	0.66	1.44	0.23
10	35.6	27.2	35.8	0.96	0.46	1.41	0.38
20	36.8	25.6	36.6	0.97	0.26	1.47	0.40
30	37.2	26.3	35.5	1.03	0.35	1.50	0.36
40	36.9	25.7	36.7	0.91	0.11	1.38	0.46
50	37.1	25.8	36.4	0.90	0.06	1.47	0.36
60	37.5	26.3	35.5	0.99	0.08	1.40	0.43
70	37.6	26.1	35.7	0.93	0.02	1.46	0.42
80	36.7	25.6	36.9	0.95	0.13	1.45	0.48
90	38.2	26.1	34.9	0.98	0.18	1.47	0.50
100	37.1	25.5	36.8	0.89	0.08	1.44	0.43
150	37.8	26.0	35.6	0.93	0.06	1.46	0.49
200	36.9	25.7	36.8	0.87	0.08	1.37	0.69
250	35.9	25.3	38.2	0.82	-	1.41	0.76
300	36.1	25.1	38.3	0.77	0.05	1.39	0.79
350	36.1	25.3	37.8	0.74	0.03	1.39	0.88
450	36.6	25.6	37.1	0.72	0.02	1.30	0.85
550	36.0	25.6	37.8	0.68	0.03	1.43	1.11
Far end	36.2	25.5	38.3	-	-	1.43	1.45

where * indicates that the measurd data are in the vicinity of interface through the control of the electron beam.

APPENDIX F

THE COMPUTER PROGRAM FOR COMPUTATIONS OF CHANGES IN COUPLED INTERFACIAL REACTIONS AND DIFFUSION IN THE SLAG/METAL SYSTEM

APPENDIX F

THE COMPUTER PROGRAM FOR COMPUTATIONS OF CHANGES IN COUPLED INTERFACIAL REACTIONS AND DIFFUSION IN THE SLAG/METAL SYSTEM

```
      IMPLICIT REAL*8 (A-H,O-Z)

      DOUBLE PRECISION  DENSM,DENSS,AREA,DDT,DT,ENS,TD,TDR,TG,TP,
     *        TEMP,ACCU,SO,SP,SQ,YS,YZ,XM,XS,DXM,DXS,DYM,DYYM,DYS,
     *        DYYS,U,YB,YC,ZB,ZC,ZD,ZZ,WCOP,WMETAL,WSLAG,WIRON,YD

      DOUBLE PRECISION ACTM(8),ACTS(8),CE(8),CCM(8),CK(8),CS(8),
     *    CTM(8),DN(8),DM(8),DS(8),ELCHE(8),FA(8),HREF(8),ONS(8),
     *    Q(8),Q1(8),RATE(8),SREF(8),TNS(8),TWM(8),W1(8),WTPC(8),
     *    XMO(8),YMO(8,0:150),YY(0:150),YYMO(8),ZM(8)

      DOUBLE PRECISION ACTM1(8,0:150),CATAN(8,0:150),EE(8,8),
     &       FB(8,0:150),SACT(8,0:150),WT(0:150),WTP(8,0:150),
     &       XCATAN(8,0:150),XMET(8,0:150),YION(8,0:150),ZION(8,0:150)

      DOUBLE PRECISION  DVM(8,8,0:150),DVS(8,8,0:150),E(2,8,8),
     *        ONSV(8,8,0:150),W(2,8,8)

      INTEGER   U1(8),V1(8), VAL(8)
      PRINT*, 'PROGRAM START'

      OPEN(UNIT=3, STATUS='OLD')
      OPEN(UNIT=4, STATUS='NEW')
      OPEN(UNIT=7, STATUS='NEW')
      REWIND 3

C     Input Data
      FARADY=23063
      R=1.987
      IONS=6
      ICAT=5
      TI=0.
      TDR=0.0
      TII=0.
      TIME=0.
      TQ=9.9
      GAMN=0.5
```

```
      READ(3,*) (CS(I), I=1, 5)
      READ(3,*) (CCM(I), I=2, 6), PT
      READ(3,*) DENSM,DENSS,AREA,DDT,DT,TD,TG,TP,TEMP,NB,NC,
     *          NF,NH,ACCU,NS,NM,XM,XS,DXM,DXS
      DO 100 I=1,IONS
      READ(3,*) CK(I), CE(I), VAL(I), ZM(I), DM(I), DS(I)
  100 CONTINUE

      DO 20 I=1, IONS
      READ(3,*) (EE(I,J), J=1,IONS)
   20 CONTINUE
      DO 30 I=1, ICAT
      READ(3,*) U1(I), V1(I), HREF(I), SREF(I)
   30 CONTINUE

      DO 70 I=1, ICAT-1
      DO 60 J=I+1, ICAT
      READ(3,*) W(1,I,J), W(2,I,J), E(1,I,J), E(2,I,J)
   60 CONTINUE
   70 CONTINUE
      CLOSE(UNIT=3)
C
C     Initialization
C
      WMETAL=DENSM*AREA*DXM
      WSLAG=DENSS*AREA*DXS
      DYS=XS/NS
      DYM=XM/NM
      WS=DENSS*AREA*DYS
      WM=DENSM*AREA*DYM
      DO 10 I=1,IONS
      Q(I)=0
   10 CONTINUE
C
C  Computing Initial Comp. & Activities in Metal Phase
C
      WIRON=0
      DO 35 I=2, IONS
      WIRON=WIRON+CCM(I)
   35 CONTINUE
      CCM(1)=.1D3-WIRON

      DO 15 K=0, NM
      DO 15 I=1, IONS
      WTPC(I)=CCM(I)
   15 CONTINUE

      PRINT*, (CCM(I), I=1, IONS)
      PRINT*, (CS(I), I=1, ICAT)
      PRINT*, (VAL(I), I=1, IONS)
```

```
      WRITE(4,110)
110   FORMAT(1X,' I',5X,'Ui',2X,'  MO ',2X,'Vi',5X,/)

      DO 710 I=1, IONS
      TWM(I)=WTPC(I)*WMETAL/.1D3
      FA(I)=0.0
710   CONTINUE
      DO 910 I=2, IONS
      DO 810 J=2, IONS
      FA(I)=EE(I,J)*WTPC(J)+FA(I)
810   CONTINUE
      ACTM(I)=EXP(FA(I)*2.303)*WTPC(I)
910   CONTINUE
      ACTM(1)=.1D1

      YZ=0.D0
      DO 305 I=1, IONS
      YZ=YZ+CCM(I)/ZM(I)
305   CONTINUE

      DO 312 I=1, IONS
      DO 312 J=0, NM
      XMET(I,J)=CCM(I)/ZM(I)/YZ
312   CONTINUE
C
C   COMPUTING COMP. & ACTIVITIES OF IONS IN SLAG PHASE
C
      YS=0
      DO 11 I=1, ICAT
      CTM(I)=ZM(I)*U1(I)+ZM(IONS)*V1(I)
      YS=YS+CS(I)/CTM(I)
11    CONTINUE

      DO 17 I=1, ICAT
      XMO(I)=CS(I)/CTM(I)/YS
17    CONTINUE

      DO 130 I=1, ICAT
      WRITE(4,120) I,U1(I),XMO(I),V1(I)
130   CONTINUE
120   FORMAT(1X,I2,5X,I2,2X,F7.2,2X,I2,5X)

      CALL ACTSLAG (XMO, ACTS, WSLAG,TEMP,U1,V1,HREF,SREF,W,E,ICAT)
      IF(XMO(2).LE.0.05) THEN
      ACTS(2)=GAMN*XMO(2)
      ENDIF
      ACTS(IONS)=1.0D0

      SO=0.0
      SQ=0.0
      SP=0.0
```

```
      DO 40 I=1,ICAT
      SO=SO+CS(I)/CTM(I)*WSLAG*V1(I)/.1D3
      SQ=SQ+CS(I)/CTM(I)*WS*V1(I)/.1D3
      SP=SP+XMO(I)*U1(I)
40    CONTINUE
      CATAN(IONS,0)=SO
      DO 50 I=1, ICAT
      CATAN(I,0)=XMO(I)*(WSLAG*YS/.1D3)*U1(I)
50    CONTINUE
      DO 55 I=1, ICAT
      DO 55 K=1, NS
      CATAN(I,K)=XMO(I)*(WS*YS/.1D3)*U1(I)
55    CONTINUE
      DO 57 K=0, NS
      CATAN(IONS,K)=SQ
      XCATAN(IONS,K)=1.0
      DO 57 I=1, ICAT
      XCATAN(I,K)=XMO(I)*U1(I)/SP
57    CONTINUE

      PRINT*,'ELEMENTAL MOLE WEIGHT: ',(ZM(I), I=1, IONS)
      PRINT*, (ACTS(K), K=1, IONS)

      CALL ELECTRO (CK, CE, IONS, NB, NC, NF, NH, VAL,
     &        ACTM,ACTS,TEMP,U,R,FARADY)

      PRINT*, U

      WRITE(4,920) TIME, U

      WRITE(4,200)
200   FORMAT(1X,'IONS=',7X,'[ Fe ]',4X,'[ Mn ]',4X,'[ Ca ]',4X,'[ Al ]',
     &     4X,'[ Si ]',4X,'[ O ] ',/)

      WRITE(4,240) (VAL(I), I=1,IONS)
240   FORMAT(1X,'VAL.=',4X,6(2X,I6,2X))

      WRITE(4,260) (CK(I), I=1,IONS)
260   FORMAT(/,1X,' KK =',4X,6(1X,D8.3,1X))

      WRITE(4,280) (CE(I), I=1,IONS)
280   FORMAT(1X,' KE =',1X,6(1X,D8.3,1x),/)

      DO 300 I=1, IONS
      Q1(I)=ACTS(I)/CE(I)
      IF(U1(I).EQ.2) THEN
      Q1(I)=SQRT(ACTS(I)/CE(I))
      ENDIF
      IF(ACTM(I).EQ.0) GOTO 300
      Q(I)=Q1(I)/ACTM(I)
300   CONTINUE
```

```
      WRITE(4,940) (XMO(I), I=1,ICAT)
      WRITE(4,950) (ACTS(I), I=1,ICAT)
      WRITE(4,960) (WTPC(I), I=1,IONS)
      WRITE(4,980) (ACTM(I), I=1,IONS)

      DO 420 I=1, IONS
      IF(ACTM(IONS).EQ.0.D0) GOTO 420
      ELCHE(I)=Q(I)*EXP(LOG(U)*VAL(I))
420   CONTINUE

      WRITE(4,1280) (ELCHE(I), I=1, IONS)
      WRITE(4,360) (Q(I), I=1,IONS)
      ENS=0.0
      DO 350 I=1, IONS
      RATE(I)=CK(I)*(ACTM(I)-Q1(I)*EXP(VAL(I)*LOG(U)))
      IF(ELCHE(I).EQ.O) THEN
      ELCHE(I)=1E-10
      ENDIF
      ENS=ENS+RATE(I)*AREA*R*TEMP*LOG(ELCHE(I))*1000
350   CONTINUE
360   FORMAT(1X,' L(I)=',3X,6(D9.3,1X),/)
      WRITE(4,1240) (RATE(i), I=1,IONS)
      WRITE(4,1350) ENS

      DO 520 I=1,IONS
      TNS(I)=CATAN(I,0)
520   CONTINUE
C
C     COMPUTING REACTION RATES
C
  1   DO 1100 I=1, IONS
      Q1(I)=ACTS(I)/CE(I)
      IF(U1(I).EQ.2) THEN
      Q1(I)=SQRT(ACTS(I)/CE(I))
      ENDIF
      RATE(I)=CK(I)*(ACTM(I)-Q1(I)*EXP(VAL(I)*LOG(U)))
      W1(I)=ABS(RATE(I))
1100  CONTINUE

      WCOP=W1(1)
      DO 1120 I=2, IONS
      IF(WCOP.LT.W1(I)) THEN
      WCOP=W1(I)
      ELSE
      ENDIF
1120  CONTINUE
C
C  COMPUTING NEW COMP. & ACTIVITIES IN SLAG
C
      DO 1200 I=1, IONS
      DN(I)=RATE(I)*AREA*DT
```

```
      TNS(I)=TNS(I)+DN(I)
      IF(TNS(I).LE.0.D0) THEN
      TNS(I)=0.D0
      ENDIF
1200   CONTINUE

      CAT2=0.0
      CAT1=0.0
      DO 1300 I=1, ICAT
      CAT2=CAT2+TNS(I)/U1(I)
      CAT1=CAT1+TNS(I)
1300   CONTINUE
      DO 1500 I=1, ICAT
      XMO(I)=TNS(I)/U1(I)/CAT2
      XCATAN(I,0)=TNS(I)/CAT1
1500   CONTINUE

      DO 1600 I=1, IONS
      WSLAG=WSLAG+DN(I)*ZM(I)
1600   CONTINUE

      CALL ACTSLAG (XMO, ACTS, WSLAG,TEMP,U1,V1,HREF,SREF,W,E,ICAT)
      IF(XMO(2).LE.0.05) THEN
      ACTS(2)=GAMN*XMO(2)
      ENDIF
      ACTS(IONS)=1.0
      XCATAN(IONS,0)=1.0

      YD=0.0
      DO 2230 I=1, ICAT
      YD=YD+XMO(I)*CTM(I)
2230   CONTINUE
      DO 2235 I=1, ICAT
      CATAN(I,0)=XMO(I)*CTM(I)*.1D3/YD
2235   CONTINUE
C
C      COMPUTING NEW COMPOSITIONS IN METAL PHASE
C
      DO 1700 I=1, IONS
      TWM(I)=TWM(I)-DN(I)*ZM(I)
      IF(TWM(I).LE.0.D0) THEN
      TWM(I)=0.D0
      ENDIF
1700   CONTINUE

      DO 1800 I=1, IONS
      WMETAL=WMETAL-DN(I)*ZM(I)
1800   CONTINUE
      DO 1900 I=1, IONS
      WTPC(I)=TWM(I)/WMETAL*1.0D2
1900   CONTINUE
```

```
      YC=0.0
      DO 1910 I=1, IONS
      YC=YC+WTPC(I)/ZM(I)
1910   CONTINUE
      DO 1920 I=1, IONS
      XMET(I,0)=WTPC(I)/ZM(I)/YC
1920   CONTINUE
C      COMPUTING THE ACTIVITIES IN METAL PHASE
C
      DO 900 I=2, IONS
      FA(I)=0.D0
      DO 800 J=2, IONS
      FA(I)=EE(I,J)*WTPC(J)+FA(I)
 800   CONTINUE
      ACTM(I)=EXP(FA(I)*.2303D1)*WTPC(I)
 900   CONTINUE
      ACTM(1)=1.0D0

      CALL ELECTRO (CK,CE,IONS,NB,NC,NF,NH,VAL,
     &        ACTM,ACTS, TEMP, U, R, FARADY)
      TI=TI+DT
      IF(TI.GE.TD) GOTO 2000
      GOTO 1
C
C     Computing Diffusion in Slag Phase
C
2000   DO 2050 J=0, NS
      YY(J)=0.D0
      DO 2040 I=1, ICAT
      YY(J)=YY(J)+VAL(I)*VAL(I)*XCATAN(I,J)*DS(I)
2040   CONTINUE
2050   CONTINUE
      DO 2100 K=0, NS
      DO 2100 I=1, ICAT
      DO 2100 J=1, ICAT
      IF(J.EQ.I) THEN
      DVS(I,J,K)=DS(I)*(YY(K)-DS(I)*XCATAN(I,K)*VAL(I)*VAL(I))/YY(K)
      ELSE
      DVS(I,J,K)=-DS(I)*DS(J)*XCATAN(I,K)*VAL(J)/YY(K)
      ENDIF
2100   CONTINUE
      DYYS=DDT/DYS/DYS
      DO 2150 K=1, NS-1
      DO 2150 I=1, ICAT
      YB=0
      DO 2140 J=1, ICAT
       YB=YB+(DVS(I,J,K)-DVS(I,J,K-1))*(XCATAN(J,K)-XCATAN(J,K-1))
     *      +DVS(I,J,K)*(XCATAN(J,K+1)-XCATAN(J,K)*2+XCATAN(J,K-1))
2140   CONTINUE
       YION(I,K)=XCATAN(I,K)+DYYS*YB
      IF(YION(I,K).LE.0.0) THEN
```

```
      YION(I,K)=0.0
      ENDIF
2150   CONTINUE

      DO 2200 I=1, ICAT
      DO 2200 J=1, NS-1
      XCATAN(I,J)=YION(I,J)
2200   CONTINUE
C
C     Computing Diffusion in Metal Phase
C
      DO 3040 K=0, NM
      DO 3030 J=1, IONS
      DO 3020 I=1, IONS
      DVM(I,J,K)=0.D0
3020   CONTINUE
3030   CONTINUE
3040   CONTINUE
      DO 3000 I=1,IONS
      ONS(I)=DM(I)/R/TEMP
3000   CONTINUE
      ZG=0.D0
      DO 3060 I=1, IONS
      ZG=ZG+ONS(I)
3060   CONTINUE
      DO 3150 K=0, NM
      DO 3150 I=2, IONS
      DO 3150 J=2, IONS
      IF(XMET(J,K).LT.0.1D-3) THEN
       GOTO 3150
      ENDIF
      IF(J.EQ.I) THEN
      ONSV(I,J,K)=(1-2*XMET(J,K))*ONS(J)+XMET(J,K)*XMET(J,K)*ZG
      ELSE
      ONSV(I,J,K)=-XMET(I,K)*ONS(J)-XMET(J,K)*ONS(I)
     &          +XMET(I,K)*XMET(J,K)*ZG
      ENDIF
      DVM(I,J,K)=R*TEMP*(1+EE(I,J)*ZM(J)*XMET(J,K)/.2425)
     &           *ONSV(I,J,K)/XMET(J,K)
3150   CONTINUE
      DYYM=DDT/DYM/DYM
      DO 3270 K=1, NM-1
      DO 3270 I=2, IONS
      ZB=0.0
      DO 3250 J=2, IONS
      ZB=ZB+DVM(I,J,K)*(XMET(J,K+1)-2*XMET(J,K)+XMET(J,K-1))+
     *    (DVM(I,J,K)-DVM(I,J,K-1))*(XMET(J,K)-XMET(J,K-1))
3250   CONTINUE
      ZION(I,K)=XMET(I,K)+DYYM*ZB
      IF(ZION(I,K).LE.0.D0) THEN
      ZION(I,K)=0.0
```

```
      ENDIF
3270  CONTINUE

      DO 3400 K=1, NM-1
      DO 3320 I=2, IONS
      XMET(I,K)=ZION(I,K)
3320  CONTINUE
      ZC=0.0
      ZD=0.0
      DO 3350 I=2, IONS
      ZC=ZC+XMET(I,K)*ZM(I)
      ZD=ZD+XMET(I,K)
3350  CONTINUE
      XMET(1,K)=1-ZD
3400  CONTINUE

      TII=TII+DDT
      TDR=TDR+DDT
      IF(TDR.GE.TG) GOTO 3900
      IF(TII.LE.TD) GOTO 2000
      IF(WCOP.LE.ACCU) GOTO 2000
      TI=0.0
      TII=0.0
      GOTO 1

3900  TIME=TIME+TDR
      TG=TG+TP

      TIME1=TIME/.6D2

      DO 4000 I=1, IONS
      IF(ACTM(I).EQ.0.D0) GOTO 4000
      Q(I)=ACTS(I)/CE(I)/ACTM(I)
      IF(U1(I).EQ.2) THEN
      Q(I)=SQRT(ACTS(I)/CE(I))/ACTM(I)
      ENDIF
4000  CONTINUE

      PRINT*, 'Reaction Time: ',TIME1,'  min.'
      WRITE(4,920) TIME1, U
 920  FORMAT(//,10X,'TIME = ',F10.4,3X,'min.',6X,'COUPLING (Do)=',
     &          3X,D14.4,3X,/)

      WRITE(4,930) WMETAL, WSLAG
 930  FORMAT(2X,'WEIGHT OF METAL=',2X,D10.5,'  g',
     &          6X,'WEIGHT OF SLAG=',2X,D10.5,2X,' g',/)
      WRITE(4,200)
      WRITE(4,240) (VAL(I), I=1,IONS)

      WRITE(4,940) (XMO(I), I=1,ICAT)
      WRITE(4,945) (CATAN(I,0), I=1,ICAT)
```

```
      WRITE(4,950) (ACTS(I), I=1,IONS)
940   FORMAT(/,1X,'X(I)=',4X,5(1X,F9.6))
945   FORMAT(/,1X,'(wt%)=',3X,5(1X,F9.6))
950   FORMAT(/,1X,'ACTS=',4X,6(1X,F9.6))
      WRITE(4,960) (WTPC(I), I=1,IONS)
960   FORMAT(1X,'[wt%]=',3X,6(1X,F9.6))

      WRITE(4,980) (ACTM(I), I=1,IONS)
980   FORMAT(1X,'ACT=',5X,6(1X,F9.6))
      WRITE(4,1240) (RATE(I), I=1,IONS)
1240  FORMAT(1X,'R  TE=',4X,6(D9.3,1X))
      DO 1260 I=1, IONS
      IF(ACTS(I).EQ.0.D0) GOTO 1260
      IF(ACTM(I).EQ.0.D0) GOTO 1260
      ELCHE(I)=Q(I)*EXP(LOG(U)*VAL(I))
1260  CONTINUE
      WRITE(4,360) (Q(I), I=1,IONS)
      WRITE(4,1280) (ELCHE(I), I=1, IONS)
1280  FORMAT(1X,'L*D  =',2X,6(F9.3,1X))
      ENS=0.0
      DO 1320 I=1, IONS
      IF(ELCHE(I).EQ.O) THEN
      ELCHE(I)=1E-10
      ENDIF
      ENS=ENS+RATE(I)*AREA*R*TEMP*LOG(ELCHE(I))*1000
1320  CONTINUE
      WRITE(4,1350) ENS
1350  FORMAT(1H,'Free Energy Rate:',8X,F14.6,3X,'mili-cal/sec.',/)
      IF(TIME1.LT.TQ) GOTO 4900
      PRINT*, 'Writing Diffusion Profile'
      TQ=79
      DO 4400 K=0, NS
      ZZ=2/(2-XCATAN(4,K))
      DO 4400 I=1, ICAT
      IF(I.EQ.4) THEN
      YMO(I,K)=XCATAN(I,K)*ZZ/2
      ELSE
      YMO(I,K)=XCATAN(I,K)*ZZ
      ENDIF
4400  CONTINUE
      DO 4450 K=1, NS
      YD=0.0
      DO 4410 I=1, ICAT
      YD=YD+YMO(I,K)*CTM(I)
4410  CONTINUE
      DO 4420 I=1, ICAT
      CATAN(I,K)=YMO(I,K)*CTM(I)/YD*100
4420  CONTINUE
4450  CONTINUE
      WRITE (7,920) TIME1, U
      VV=XM/NM*.1D5
```

```
      DO 4125 K=0,NS
      WT(K)=0.0
      DO 4120 I=1,IONS
      WT(K)=WT(K)+XMET(I,K)*ZM(I)
4120  CONTINUE
      DO 4125 J=1,IONS
      WTP(J,K)=XMET(J,K)*ZM(J)/WT(K)*100
4125  CONTINUE

      WRITE(7,4130)
4130  FORMAT(///,2X,'Compositions in Metal Phase:',//)

      WRITE(7,4100)
4100  FORMAT(1X,'X (micro)',5X,'     Fe ',5x,'     Mn ',5x,'     Ca ',
     &        5x,'     Al ',5x,'     Si ',5x,'      O ',/)

      DO 4150 K=0, 100
      WRITE(7,4170) VV*K, (WTP(I,K), I=1, IONS)
4150  CONTINUE

4170  FORMAT(3X,F5.0,7X,6(F10.5,3X))

      VW=XS/NS*.1D5

      WRITE(7,4185)
4185  FORMAT(///,2X,'Compositions in Slag Phase:',//)

      WRITE(7,4100)
      DO 4200 K=0, 100
      WRITE(7,4170) VW*K, (CATAN(I,K), I=1, ICAT)
4200  CONTINUE

4245  FORMAT(5X,'Element',3x,'  Fe(1) ',5x,'  Mn(2) ',5x,'  Ca(3) ',
     &        5x,'  Al(4) ',5x,'  Si(5) ',5x,'   O(6) ',/)

4180  FORMAT(8X,I3,4X,6(D9.3,4X))

4900  TI=0.0
      TII=0.0
      IF(TIME1.GT.PT) GOTO 5000
      IF(WCOP.LE.ACCU) GOTO 2000
      GOTO 1

5000  STOP
      END
C     END MAIN


      SUBROUTINE ELECTRO(CK,CE,IONS,NB,NC,NF,NH,VAL,ACTM,
     &                   AS,TEMP, U, R, FARADY)
```

```
      IMPLICIT REAL*8 (A-H, O-Z)
      DOUBLE PRECISION CK(8), CE(8), ACTM(8), AS(8)
      DOUBLE PRECISION A, B1, B2, B3, B4, B5, B6, B7, DFUNC,
     &       FF, FU, FUNC, U, U1, U2, U3, U4
      INTEGER VAL(8)
      A=0.D0
      B1=0.D0
      B2=0.D0
      B3=0.D0
      B4=0.D0
      B5=0.D0
      B6=0.D0
      B7=0.D0

      DO 100 I=1, IONS
      A=A+VAL(I)*CK(I)*ACTM(I)
100   CONTINUE
      DO 200 I=1,NB
      B1=B1+VAL(I)*CK(I)*AS(I)/CE(I)
200   CONTINUE
      DO 300 I=NB+1,NC
      B2=B2+VAL(I)*CK(I)*SQRT(AS(I)/CE(I))
300   CONTINUE
      DO 400 I=NC+1,NF
      B3=B3+VAL(I)*CK(I)*AS(I)/CE(I)
400   CONTINUE
      DO 800 I=NF+1,NH
      B7=B7+VAL(I)*CK(I)*AS(I)/CE(I)
800   CONTINUE

      FF=ABS(B2)+ABS(B3)
      U1=SQRT(A*A-4.*B1*B7)
      U=SQRT((A+U1)/2/B1)

      IF(FF.NE.0.0) GOTO 1100
      GOTO 2000

1100  U2=U*U
      U3=U2*U
      U4=U2*U2

      FUNC=A*U2-B1*U4-B2*U3*U2-B3*U3*U3-B4*U3*U4-B5*U3-B6*U-B7
      DFUNC=2*A*U-4*B1*U3-5*B2*U4-6*B3*U3*U2-7*B4*U3*U3-3*B5*U2-B6

      U=U-FUNC/DFUNC

      IF(U.LT.0.D0) THEN
      PRINT*, 'U is less than zero, check initial value'
      GOTO 2000
      ELSE
      ENDIF
```

```
      FUNT=FUNC/DFUNC
      FU=ABS(FUNT)

      IF(FU.LE.1.0D-7) GOTO 2000

      GOTO 1100

2000  RETURN
      END
C     END ELECTRO

      SUBROUTINE ACTSLAG (X,ACTS,WSLAG,TEMP,U,V,HREF,SREF,W,E,M)
      IMPLICIT REAL*8 (A-H, O-Z)

      DOUBLE PRECISION ACT(8),X(8),HREF(8),SREF(8),ACTS(8),CEREF(8),
     *     W(2,8,8),E(2,8,8),HR(8),SR(8),XX(8)

      DOUBLE PRECISION WSLAG, TEMP

      INTEGER U(8), V(8), UU(8), VV(8)

      LOGICAL SNV, SOK

      DO 100 I=1, M
      UU(I)=U(M+1-I)
      VV(I)=V(M+1-I)
      HR(I)=HREF(M+1-I)
      SR(I)=SREF(M+1-I)
      XX(I)=X(M+1-I)
100   CONTINUE

      DO 200 I=1, M
      U(I)=UU(I)
      V(I)=VV(I)
      HREF(I)=HR(I)
      SREF(I)=SR(I)
      X(I)=XX(I)
200   CONTINUE

      CALL CTHMKF (M,U,V,W,E,TEMP,X,4,.1D3,SNV,SOK,ACT)

      IF (SNV) WRITE(6,300)
300   FORMAT(/2X,'SNV')
      IF (SNV) GO TO 700

      DO 400 J=1,M
      CEREF(J)=EXP((HREF(J)-TEMP*SREF(J))/1.987/TEMP)
      HR(J)=ACT(J)*CEREF(J)
      IF (HR(J).GE.1) HR(J)=1.
400   CONTINUE
```

```
      DO 500 I=1, M
      ACTS(I)=HR(M+1-I)
500   CONTINUE

      DO 600 I=1, M
      UU(I)=U(M+1-I)
      VV(I)=V(M+1-I)
      HR(I)=HREF(M+1-I)
      SR(I)=SREF(M+1-I)
      XX(I)=X(M+1-I)

600   CONTINUE

      DO 650 I=1, M
      U(I)=UU(I)
      V(I)=VV(I)
      HREF(I)=HR(I)
      SREF(I)=SR(I)
      X(I)=XX(I)
650   CONTINUE

      GOTO 1000

700   PRINT*, 'Not Logic Computation'
      STOP

1000  RETURN
      END
C     END ACTSLAG

      SUBROUTINE CTHMKF (M,U,V,W,E,T,X,INDEX,PREC,SNV,SOK,ACT)

      IMPLICIT REAL*8 (A-H, O-Z)

      DOUBLE PRECISION W(2,8,8),E(2,8,8),X(8),R(8,8),ACT(8),
     *          WR(2,8,8),ER(2,8,8),XR(8),RR(8,8),
     *          XM(8),XP(8),RM(8,8),RP(8,8),DG(8)

      DOUBLE PRECISION PREC, T, GM, HM, SE, GE, GEM, GEP, TM, TP
      INTEGER U(8),UR(8), V(8),VR(8), IR(8)

      LOGICAL    SNV,SOK,SOKP
C     PRINT *,'START  OF  CTHMKF'

C     INITIALISITION
C     A)

      SNV=.FALSE.
      SOK=.TRUE.
      GM=0.D0
```

```
      GE=0.D0
      HM=0.D0
      SE=0.D0

      DO  1   I=1,M
      ACT(I)=0.D0
      DO  1   J=1,M
    1 R(I,J)=0.D0

C          B)  INDEXATION
C

      MR=0
      DO  5  I=1,M
      IF  (X(I)-.1D-4)  5,5,6
    6 MR=MR+1
      IR(MR)=I
    5 CONTINUE

C     C) STOP CALCULATION FOR SINGLE CONSTITUENT
      IF  (MR-1)  11,10,14
   10 I=IR(MR)
      ACT(I)=1.0
      R(I,I)=V(I)*X(I)
   11 RETURN

C     D) INITIALISITION OF REDUCED SYSTEM VARIABLES

   14 DO  15  I=1,MR
      DO  15  J=1,MR
      DO  15  IO=1,2
      WR(IO,I,J)=0.0
   15 ER(IO,I,J)=0.0

      DO  16  I=1,MR
      K=IR(I)
      UR(I)=U(K)
      VR(I)=V(K)
      XR(I)=X(K)

      DO 18  J=I,MR
      L=IR(J)
      DO  18  IO=1,2
      WR(IO,I,J)=W(IO,K,L)
   18 ER(IO,I,J)=E(IO,K,L)

   16 CONTINUE

C     CALCULATION OF THERMODYNAMICS MAGNITUDES
C     A) CELL FRACTIONS AT POINT T,XR
```

```
      CALL  RIJ  (MR,UR,VR,WR,ER,T,XR,1,PREC,SNV,SOK,RR)
      IF  (SNV)  RETURN
      DO   20  I=1,MR
      K=IR(I)
      DO   20  J=I,MR
      L=IR(J)
      R(K,L)=RR(I,J)
   20 R(L,K)=R(K,L)

C       B)-  CALCULATION  OF  EXCESS MIXING FREE ENTHALPY

      CALL  GFROH (MR,UR,VR,WR,ER,T,XR,RR,GM,GE)
      GO TO  (11,25,30,25),INDEX

C       D)-  CALCULATION  OF  MIXNG  ENTHALPY  AND  EXCESS  ENTROPY

   25 TM=T-10
      TP=T+10
      DO  26  I=1,MR
      DO  26  J=1,MR
      RM(I,J)=RR(I,J)
   26 RP(I,J)=RR(I,J)

      CALL  RIJ  (MR,UR,VR,WR,ER,TM,XR,2,PREC,SNV,SOKP,RM)

      IF  (SNV)  RETURN
      SOK=SOK  .AND.  SOKP

      CALL  RIJ  (MR,UR,VR,WR,ER,TP,XR,2,PREC,SNV,SOKP,RP)

      IF  (SNV)  RETURN
      SOK=SOK  .AND.  SOKP

      CALL  GFROH  (MR,UR,VR,WR,ER,TM,XR,RM,GMM,GEM)
      CALL  GFROH  (MR,UR,VR,WR,ER,TP,XR,RP,GMP,GEP)

      SE=(GEM-GEP)/.2D2
      HM=GE+T*SE
      GO  TO  (11,11,30,30)  INDEX

C       E)-  CALCULATION  OF  ACTIVITY  OF  CONPONENT

   30 DO  31  ID=2,MR
      Z=DMIN1(.1D-4,XR(1),(1-XR(1)),XR(ID),(1-XR(ID)))/.1D2

      DO  32  I=1,MR
      XM(I)=XR(I)
   32 XP(I)=XR(I)

      XM(ID)=XM(ID)-Z
```

```
      XM(1)=XM(1)+Z
      XP(ID)=XP(ID)+Z
      XP(1)=XP(1)-Z

      CALL  RIJ  (MR,UR,VR,WR,ER,T,XM,2,PREC,SNV,SOKP,RM)

      IF  (SNV)  RETURN
      SOK=SOK  .AND.  SOKP

      CALL  RIJ  (MR,UR,VR,WR,ER,T,XP,2,PREC,SNV,SOKP,RP)

      IF  (SNV)  RETURN
      SOK=SOK  .AND.  SOKP

      CALL  GFROH  (MR,UR,VR,WR,ER,T,XM,RM,GMM,GEM)
      CALL  GFROH  (MR,UR,VR,WR,ER,T,XP,RP,GMP,GEP)

      DG(ID)=(GMM-GMP)/(XM(ID)-XP(ID))
   31 CONTINUE

      K=IR(1)
      ACT(K)=GM
      DO  42  I=2,MR
      L=IR(I)
   42 ACT(K)=ACT(K)-X(L)*DG(I)

      DO  43  I=2,MR
      L=IR(I)
   43 ACT(L)=ACT(K)+DG(I)

      DO  44  I=1,MR
      K=IR(I)
      ACT(K)=EXP(ACT(K)/1.987/T)
   44 IF  (ACT(K) .GE. 1.D0)  ACT(K)=1.D0

      RETURN
      END
C     END  CTHMKF


      SUBROUTINE  GFROH  (M,U,V,W,E,T,X,R,GM,GE)

      IMPLICIT REAL*8 (A-H, O-Z)

      DOUBLE PRECISION  W(2,8,8),E(2,8,8),X(8),R(8,8),Z0(8),Z1(8),
     *          Z2(8),RS(8,8)
      DOUBLE PRECISION T,GM,GE,GLN,PLN,UUSLN,ES,EF,EI,S

      INTEGER U(8), V(8)
C
C     I)-  CALCULATION OF  DIVERSE  PARAMETERS
```

```
C       PRINT *,'BEGINNING OF GFROH'

        DO  50  I=1,M
        Z0(I)=0.D0
        DO  50  J=I,M
  50    Z0(I)=Z0(I)+V(J)*X(J)

        DO  51  I=1,M-1
        Z1(I)=Z0(I)*LOG(Z0(I)/V(I)/X(I))
  51    Z2(I)=Z0(I+1)*LOG(Z0(I+1)/V(I)/X(I))

        DO  52  I=1,M
        DO  52  J=1,M
  52    RS(I,J)=V(I)*X(I)*V(J)*X(J)/Z0(1)

C       II)-  CALCULATION OF SYSTEM DEGENERATION
C       A)-  CALCULATION OF LN(P) (LOGARITHM OF TOTAL PERMUTATION
C            NUMBER OF METALLIC ATOMS

        PLN=0.D0
        DO  60  I=1,M-1
  60    PLN=PLN+U(I)*(Z1(I)-Z2(I))/V(I)

C       B)- CALCULATION OF LN(U/U*) (LOGARITHM OF PERMUTATIONS
C           DISTINCTES NUMBER BETWEEN CELLS

        UUSLN=0.D0
        DO  65  I=1,M
        DO  65  J=1,M
  65    UUSLN=UUSLN+RS(I,J)*LOG(RS(I,J))-R(I,J)*LOG(R(I,J))
C
C       C)- CALCULATION OF LOGARITHM OF DEGENERESCENCE

        GLN=PLN+UUSLN

C       III)-  CALCULATION OF TOTAL SYSTEM ENERGE
C       A)- CELLS FORMATION ENERGE

        EF=0.D0
        DO  70  I=1,M-1
        DO  70  J=I+1,M
  70    EF=EF+2.D0*R(I,J)*(W(1,I,J)+X(I)*W(2,I,J))

C       B)- CELLS INTERACTION ENERGE

        EI=0.D0
        DO  75 I=1,M-1
        S=0.D0
        DO  76 J=I+1,M
  76    S=S+V(J)*X(J)*(E(1,I,J)+X(I)*E(2,I,J))
```

```
 75     EI=EI+2.0*R(I,I)*S/Z0(1)
C       TOTAL  ENERGE
        ES=EF+EI
C       IV)-  CALCULATION  OF  FREE  ENTHALPY
        GM=ES-1.987*T*GLN
C       V)-  CALCULATION  OF  EXESS  FREE  ENERGE
        GE=GM
        DO  80  I=1,M
 80     GE=GE-1.987*T*X(I)*LOG(X(I))
        RETURN
        END
C       END  GFROH
C **********************
C  CALCULATION  0F  CELL  FRACTIONS
C**********************
        SUBROUTINE  RIJ  (M,U,V,W,E,T,X,IND,PREC,SNV,SOK,R)
        DOUBLE PRECISION  W(2,8,8),E(2,8,8),X(8),R(8,8),P(8,8),Y(8),
     *            PZ(8,8),A(8,8),AI(8,8),B(8),DY(8),D2Y(8),Q(8)
        DOUBLE PRECISION T, PREC, AD, DZ, Z
        INTEGER U(8), V(8)
        LOGICAL    SNV,SOK
C       PRINT *,'BEGINNING  OF  RIJ'
C       INITIALISATION  OF  P  AND  Y  IN  RIJ
        AD=V(M)*X(M)
        P(M,M)=1.D0
        Q(M)=0.D0
        DO 50  I=1,M-1
        AD=AD+V(I)*X(I)
        P(I,I)=1.D0
        Q(I)=0.D0
        DO  51  J=I+1,M
 51     Q(I)=Q(I)+V(J)*X(J)*(E(1,I,J)+X(I)*E(2,I,J))
 50     CONTINUE
        DO 52  I=1,M-1
        DO 52  J=I+1,M
        P(I,J)=EXP((-W(1,I,J)-X(I)*W(2,I,J)+(Q(I)+Q(J))/AD)/1.987D0/T)
 52     P(J,I)=P(I,J)
```

```
      GO TO (1,2),IND

    1 DO 3 I=1,M
    3 Y(I)=V(I)*X(I)/SQRT(AD)

      Z=0.D0
      GO TO 5

    2 DO 4 I=1,M
    4 Y(I)=SQRT(R(I,I))

      GO TO 20

C     CALCULATION OF Y BY DEVELOPMENTS LIMITS
C 1)_ CALCULATION OF MATRIX PZ

    5 DO 6 I=1,M
      DO 6 J=1,M
    6 PZ(I,J)=P(I,J)**Z

C 2)- CALCULATION OF MATRIX A

      DO 7 I=1,M
      A(I,I)=2*Y(I)
      DO 7 J=1,M
      IF (I-J) 8,7,8
    8 A(I,J)=PZ(I,J)*Y(I)
      A(I,I)=A(I,I)+PZ(I,J)*Y(J)
    7 CONTINUE
C 3)- INVERSION OF MATRIX A

      CALL GAUINV (M,A,SNV,AI)

      IF (SNV) RETURN

C 4)- CALCULATION OF DY


      DO 10 I=1,M
      B(I)=0
      DO 10 J=1,M
   10 B(I)=B(I)-PZ(I,J)*LOG(P(I,J))*Y(I)*Y(J)

      DO 11 I=1,M
      DY(I)=0
      DO 11 J=1,M
   11 DY(I)=DY(I)+AI(I,J)*B(J)

C 5)- CALCULATION OF D2Y

      DO 12 I=1,M
```

```
      B(I)=0
      DO  12  J=1,M
   12 B(I)=B(I)-PZ(I,J)*(2*DY(I)*DY(J)+2*LOG(P(I,J))*(Y(I)*DY(J)+
     *       Y(J)*DY(I))+Y(I)*Y(J)*LOG(P(I,J))**2)

      DO  13  I=1,M
      D2Y(I)=0
      DO  13  J=1,M
   13 D2Y(I)=D2Y(I)+AI(I,J)*B(J)

C 6)- CALCULATION OF Z AND Y NEW VALUE

      DZ=0.5D0

      DO  15  I=1,M
      IF  (DY(I))  16,17,16
   16 DZ=DMIN1(DZ,ABS(.1*Y(I)/DY(I)))
   17 IF  (D2Y(I))  18,15,18
   18 DZ=DMIN1(DZ,SQRT(ABS(.05*Y(I)/D2Y(I))))
   15 CONTINUE

      DZ=DMAX1(DZ,.1D-2)
      DZ=DMIN1(DZ,(1-Z))
      Z=Z+DZ

      DO  19  I=1,M
   19 Y(I)=Y(I)+DY(I)*DZ+D2Y(I)*DZ*DZ/2

      IF (Z-1)  5,20,20

C       VALUES IMPROVEMENT OF Y BY ITERATION

   20 NITER=0
C 1)- CALCULATIPON OF MATRIX A

   30 DO  21  I=1,M
      A(I,I)=2*Y(I)
      DO  21  J=1,M
      IF (I-J)  22,21,22
   22 A(I,J)=P(I,J)*Y(I)
      A(I,I)=A(I,I)+P(I,J)*Y(J)
   21 CONTINUE

C 2)- INVERSION OF MATRIX A

      CALL  GAUINV  (M,A,SNV,AI)

      IF  (SNV)  RETURN

C 3)- CALCULATION OF DY
```

```
      DO  23  I=1,M
      B(I)=V(I)*X(I)
      DO  23  J=1,M
23    B(I)=B(I)-P(I,J)*Y(I)*Y(J)

      DO  34  I=1,M
      DY(I)=0

      DO  24  J=1,M
24    DY(I)=DY(I)+AI(I,J)*B(J)

34    CONTINUE

      SOK=.TRUE.

      DO  25  I=1,M
      IF  (Y(I))  26,25,26
26    SOK=SOK  .AND.  (ABS(DY(I)/Y(I))  .LT.  PREC)
25    CONTINUE
      DO  27  I=1,M
27    Y(I)=Y(I)+DY(I)
      NITER=NITER+1
      IF (SOK) GO  TO  40
      IF (NITER-10)  30,40,40

C     CALCULATION  OF  CELL  FRACTIONS

40    DO  41  I=1,M
      DO  42  J=1,M
42    R(I,J)=P(I,J)*Y(I)*Y(J)
41    CONTINUE

      RETURN
      END
C     END  RIJ


C***************
C     INVERSION  OF  MATRIX  BY  GAUSS  METHOD
C***************
      SUBROUTINE  GAUINV  (N,A,ASINGL,U)

      IMPLICIT REAL*8 (A-H, O-Z)
      DOUBLE PRECISION  A(8,8), U(8,8)
      DOUBLE PRECISION S, UMAX
      INTEGER IL(8), JL(8)
      LOGICAL   ASINGL

C  INITIALISATION  OF  U
```

```
      DO  1  I=1,N
      DO  1  J=1,N
1     U(I,J)=A(I,J)

      ASINGL=.FALSE.
      DO  3  L=1,N
      UMAX=0.
      IF  (ASINGL)  GO  TO  3

C SELECTION  OF  ELEMENT

      DO  4  I=L,N
      DO  4  J=L,N
      IF  (ABS(UMAX)-ABS(U(I,J)))  5,4,4
5     UMAX=U(I,J)
      IL(L)=I
      JL(L)=J
4     CONTINUE

C CALCULATION  OF  PARTIAL  DETERMINANT

      ASINGL=ABS(UMAX)  .LT.  1.0D-8
      IF  (ASINGL)  GO  TO  3

C DISPLACEMENT  OF  ROWS  AND  COLUMNS

      I=IL(L)
      IF  (I-L)  8,10,8

8     DO  6  J=1,N
      S=U(L,J)
      U(L,J)=U(I,J)
6     U(I,J)=-S

10    J=JL(L)
      IF  (J-L)  12,15,12

12    DO  11  I=1,N
      S=U(I,L)
      U(I,L)=U(I,J)
11    U(I,J)=-S
15    DO  16  I=1,N
      IF  (I-L)  17,16,17
17    U(I,L)=-U(I,L)/UMAX
16    CONTINUE

      DO  20  I=1,N
      DO  20  J=1,N
      IF  ((I-L)*(J-L))  21,20,21
21    U(I,J)=U(I,J)+U(I,L)*U(L,J)
20    CONTINUE
```

```
      DO  25  J=1,N
      IF  (J-L)  26,25,26
   26 U(L,J)=U(L,J)/UMAX
   25 CONTINUE

      U(L,L)=1.0/UMAX
    3 CONTINUE

C STOP CALCULATION WHEN A IS SINGULAR

      IF (ASINGL) RETURN

C ORDERING OF INVERSE MATRIX

      DO  30  L1=1,N
      L=N-L1+1
      J=IL(L)
      IF  (J-L)  35,35,32

   32 DO  31  I=1,N
      S=U(I,L)
      U(I,L)=-U(I,J)
   31 U(I,J)=S

   35 I=JL(L)
      IF  (I-L)  30,30,37
   37 DO  36  J=1,N
      S=U(L,J)
      U(L,J)=-U(I,J)
   36 U(I,J)=S
   30 CONTINUE
      RETURN
      END
C      END  GAUINV
```

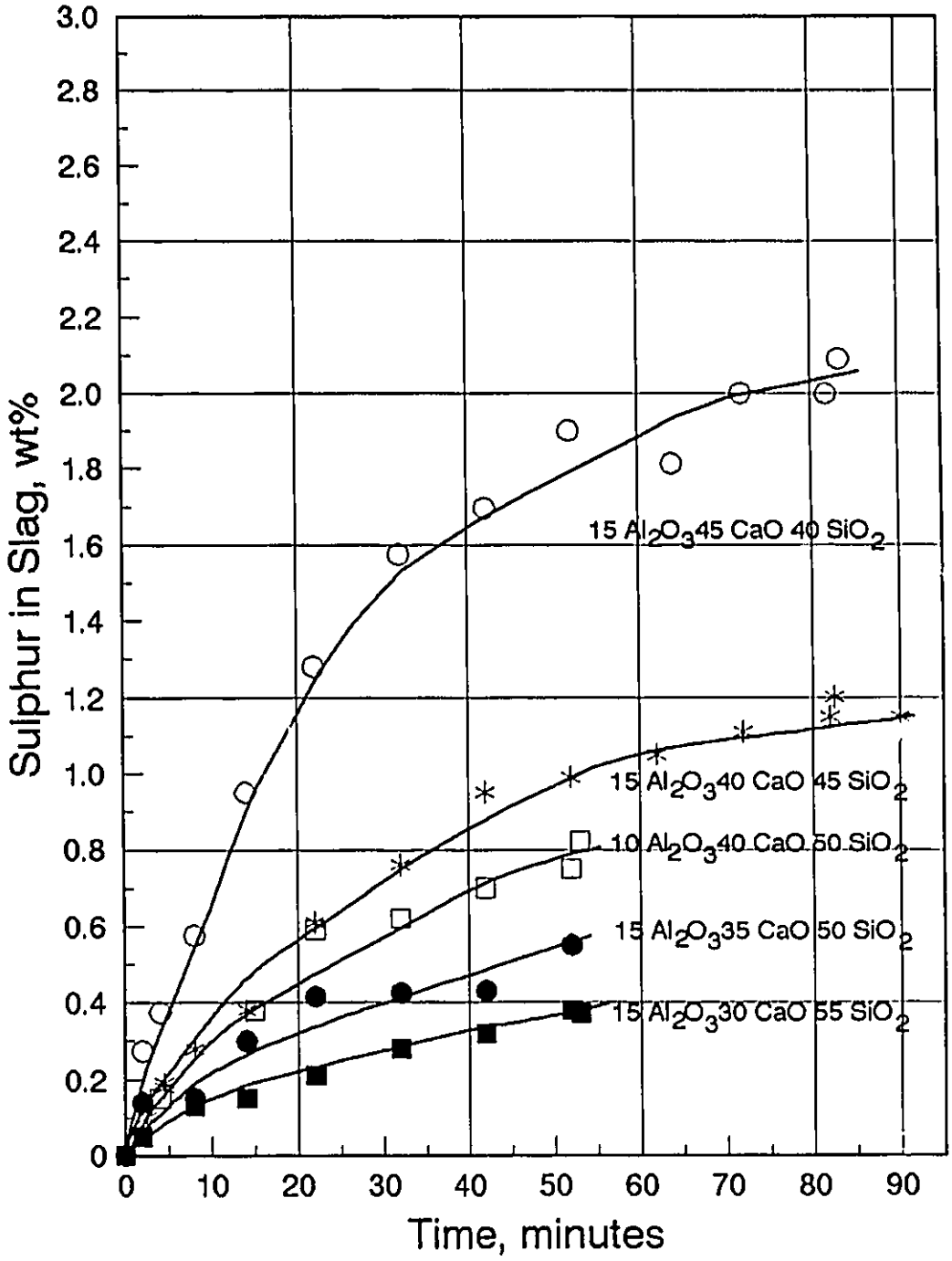

Fig. 2-1: Rate Curves for five slags at 1540 °C
(reproduced Fig. 6 from Chang and Goldman, 1948)

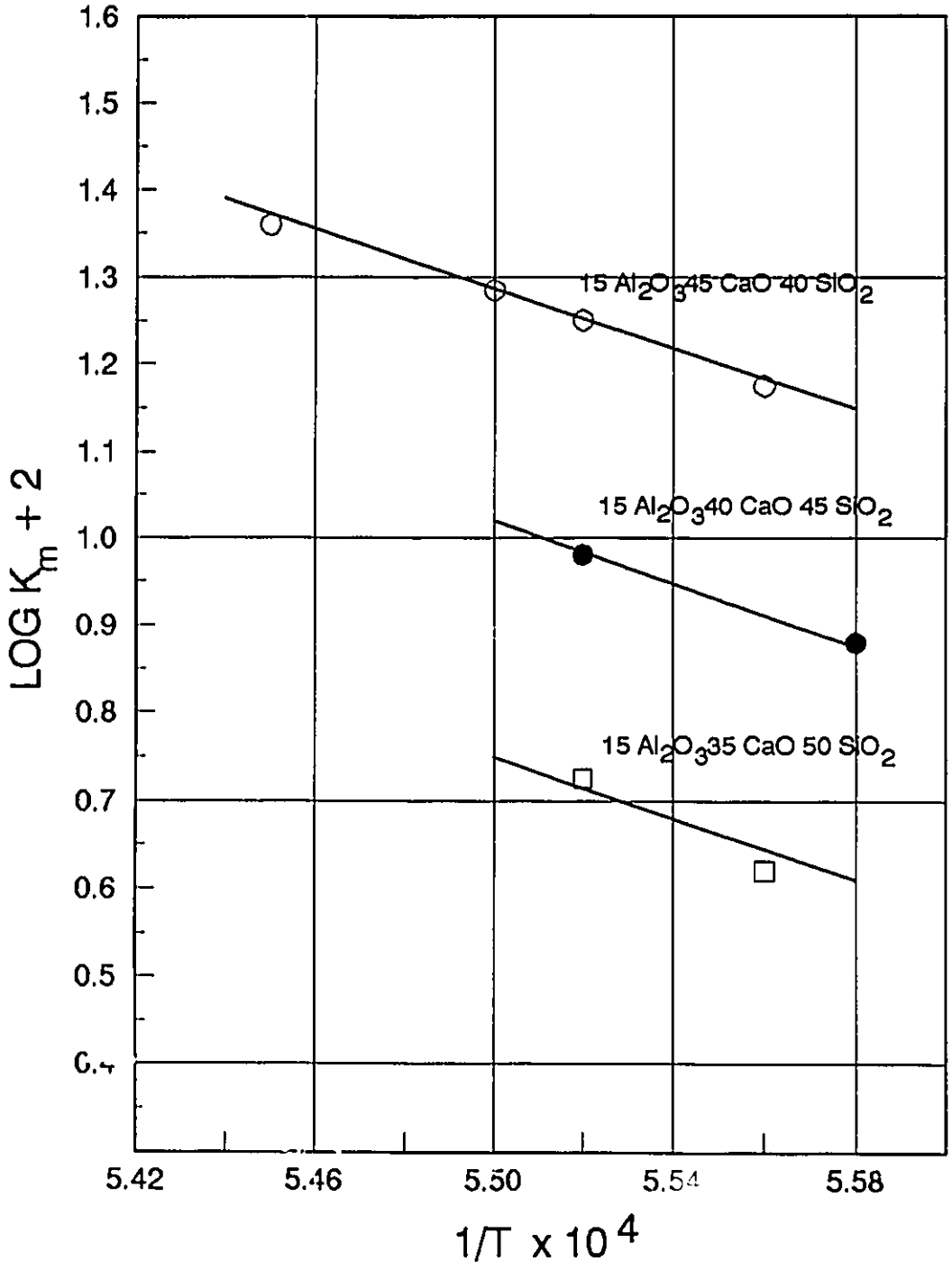

Fig. 2-2: Log K_m vs. 1/T plot for three slags
(reproduced Fig. 10 from Chang and Goldman, 1948)

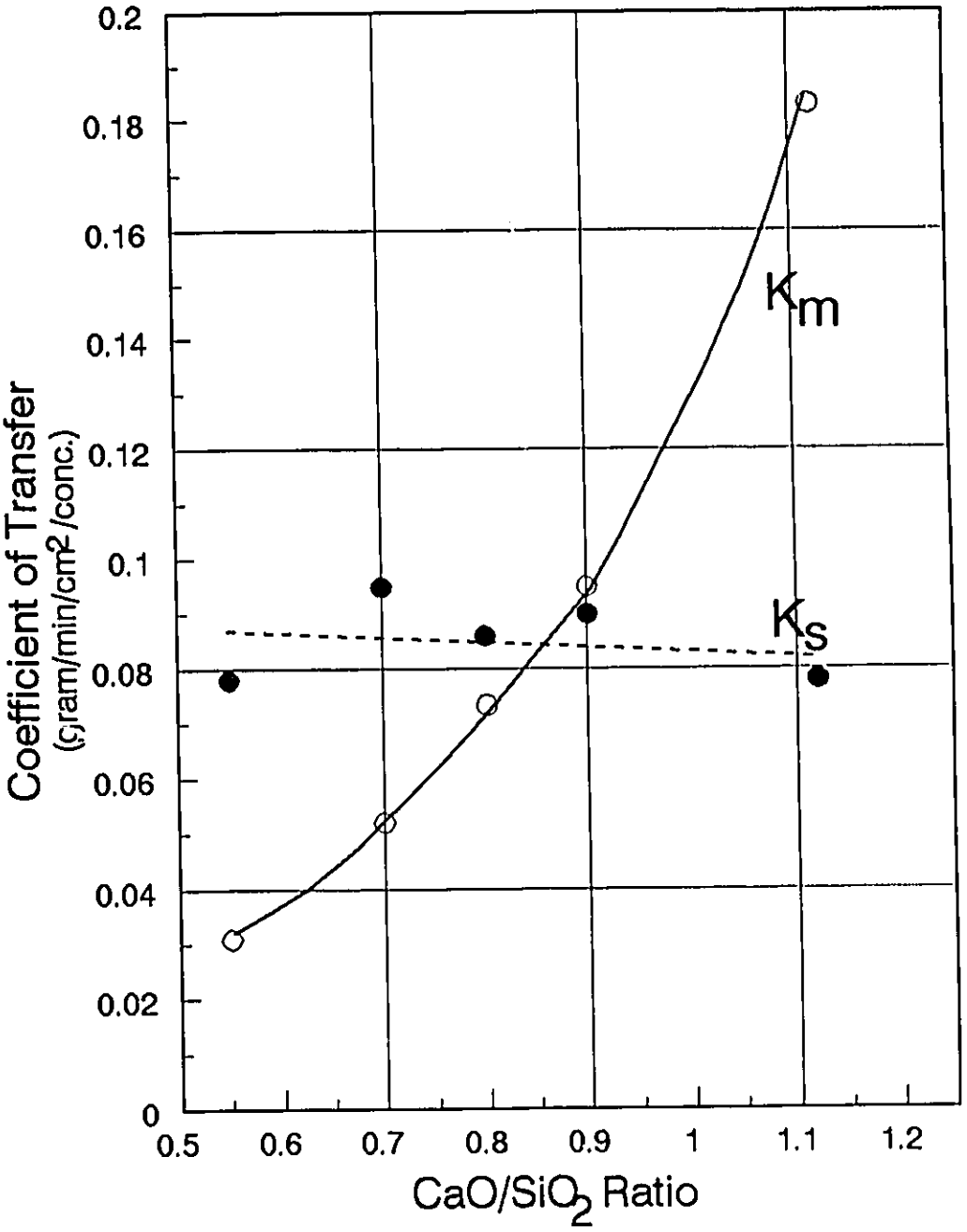

Fig. 2-3: Coefficients of transfer vs. CaO/SiO_2 weight ratio for five slags at 1540 °C

(reproduced Fig. 11 from Chang and Goldman, 1948)

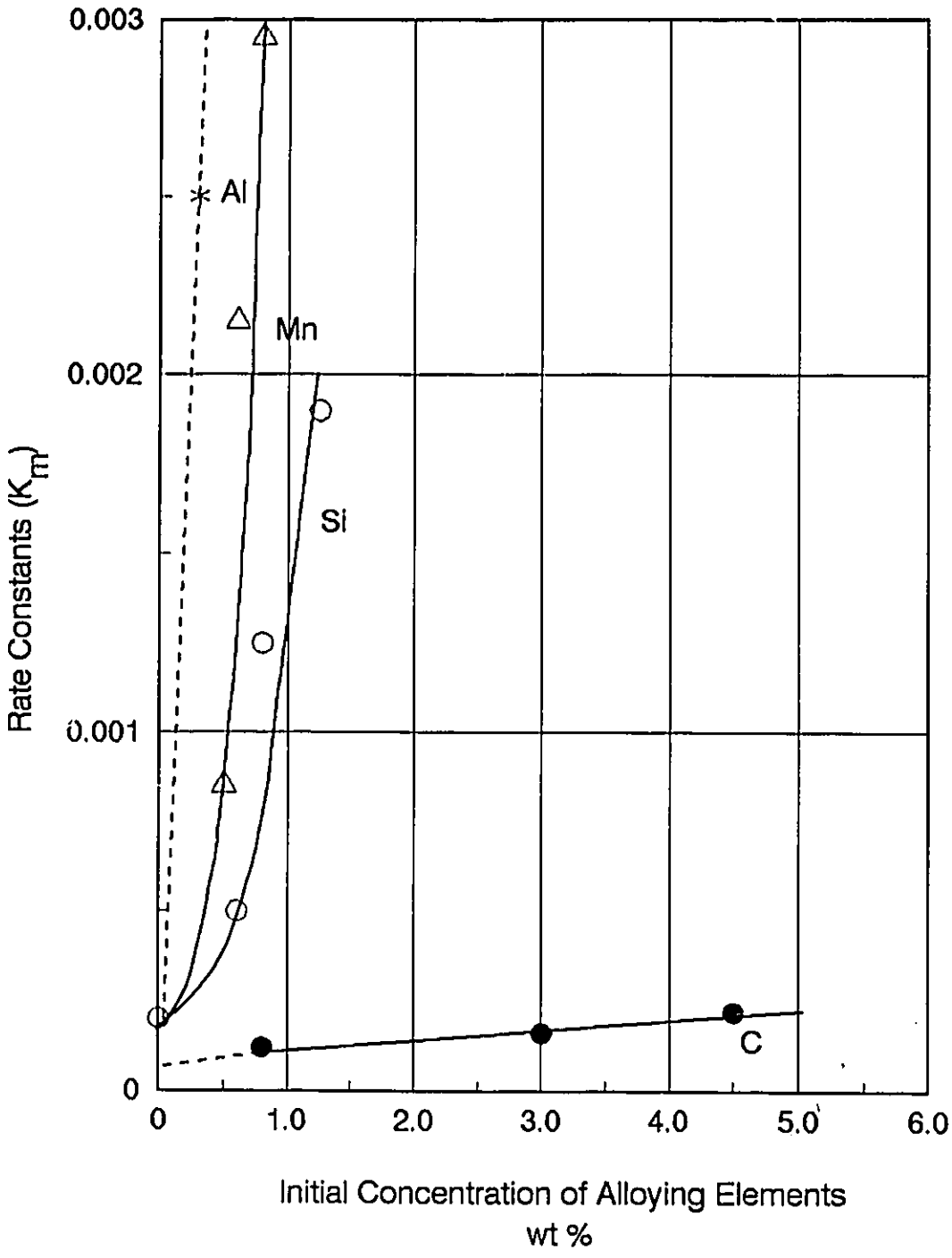

Fig. 2-4: Comparison of the effect of alloying elements on rate constants for sulphur transfer with acid slags.
(reproduced Fig. 18 from Goldman, Derge and Philbrook, 1954)

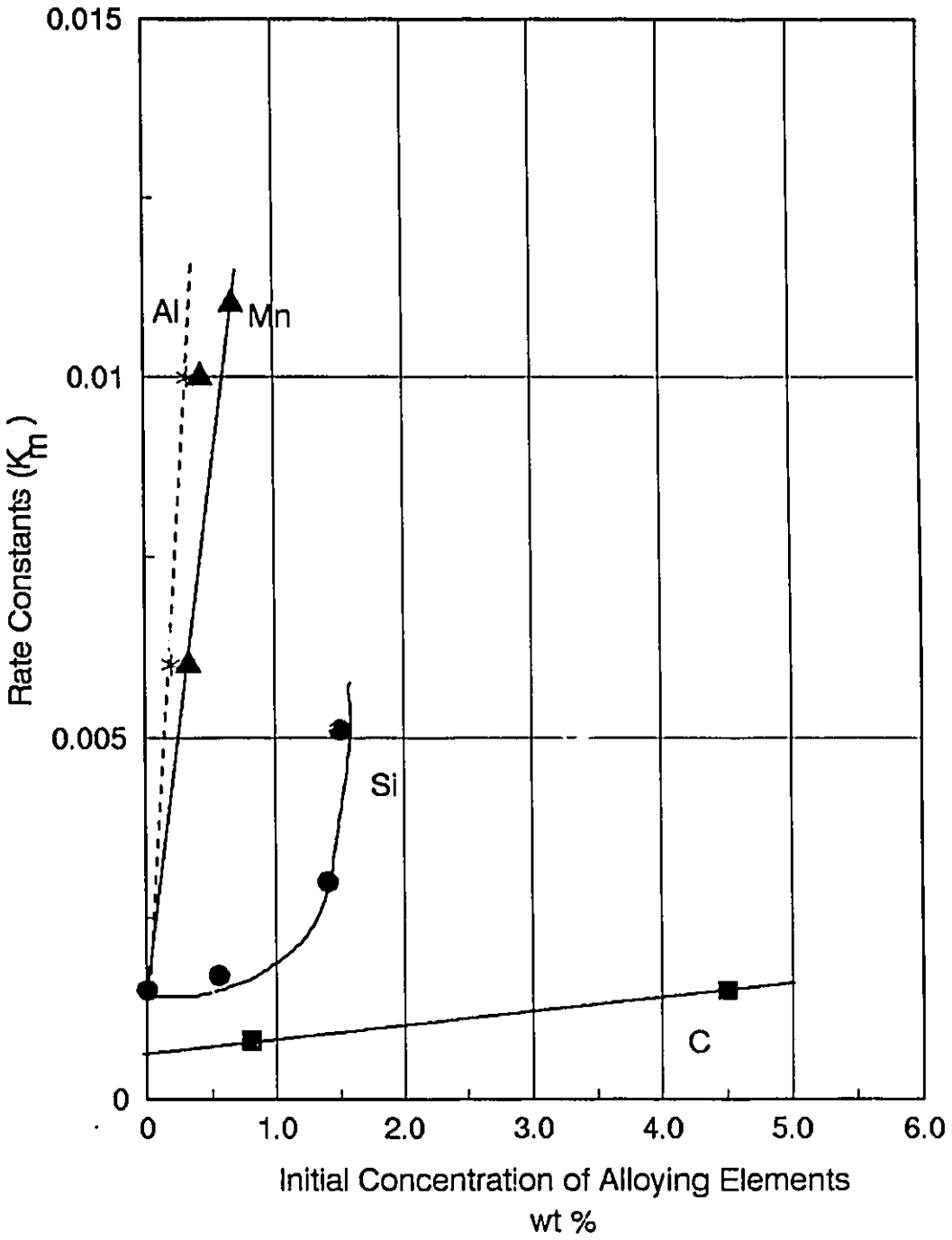

Fig. 2-5: Comparison of the effect of alloying elements on rate constants for sulphur transfer with basic slag.
(reproduced Fig. 19 from Goldman, Derge and Philbrook, 1954)

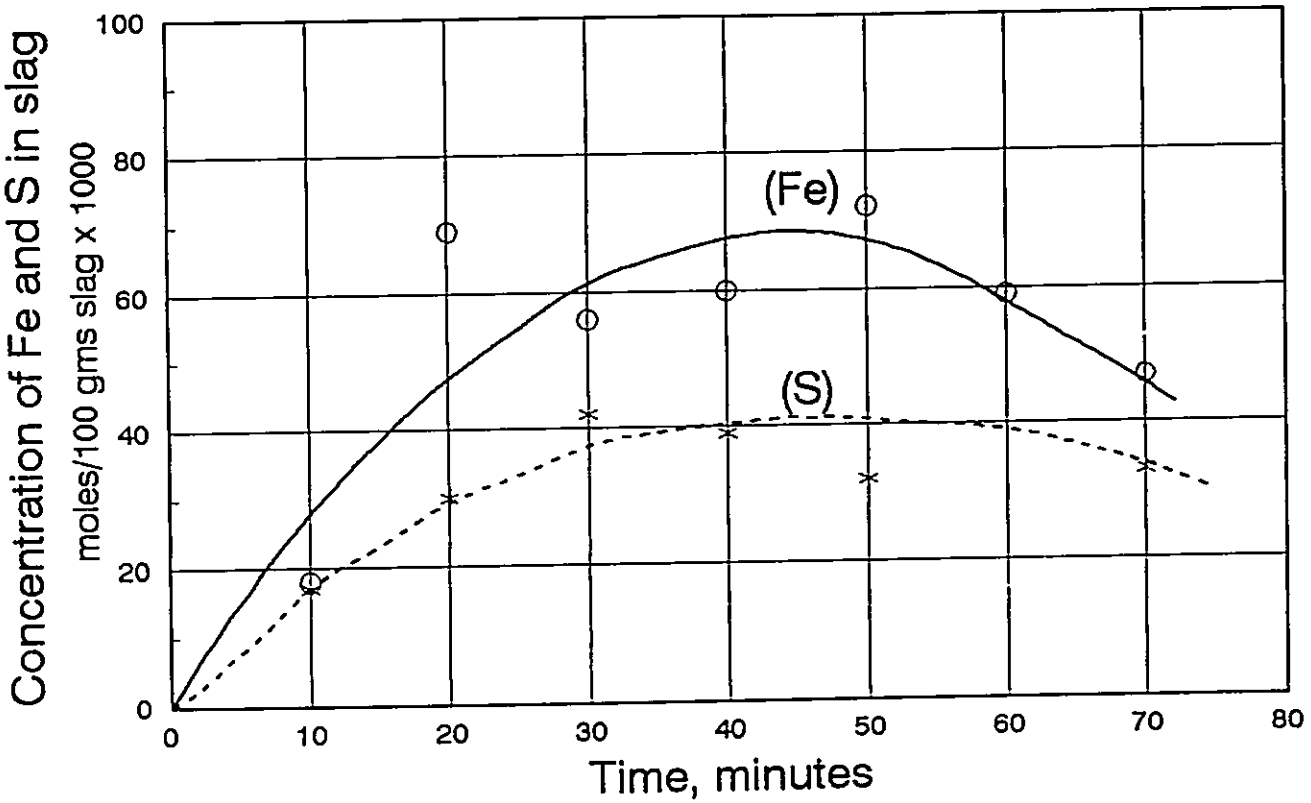

Fig. 2-6: Rate curves for iron and sulphur in slags.

(reproduced Fig. 3a from Derge, Philbrook and Goldman, 1950)

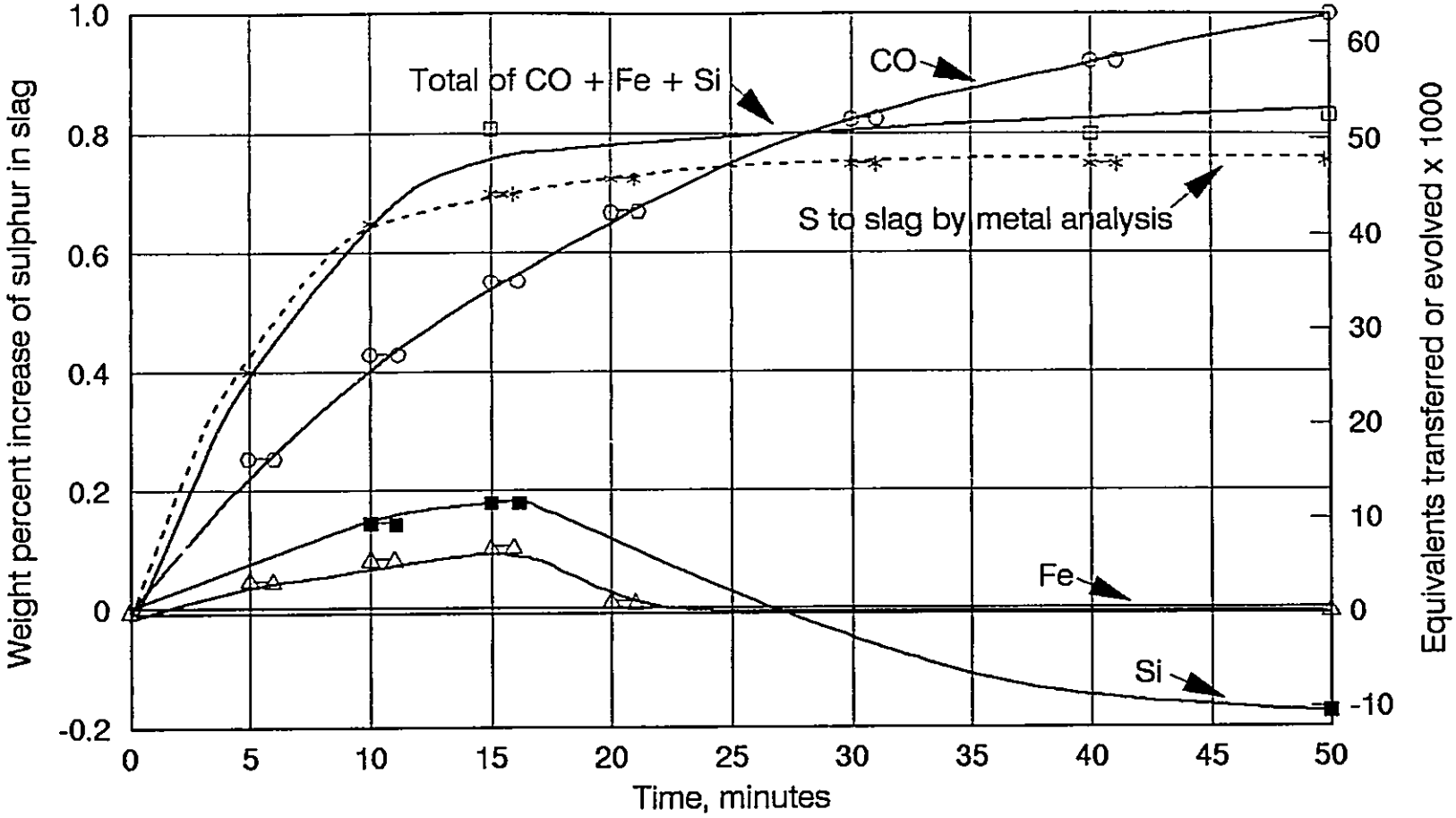

Fig. 2-7: Equivalents of S, Fe and Si transferred from metal to slag and equivalents of CO evolved.

(reproduced Fig. 2 from King and Ramanchandran, 1956)

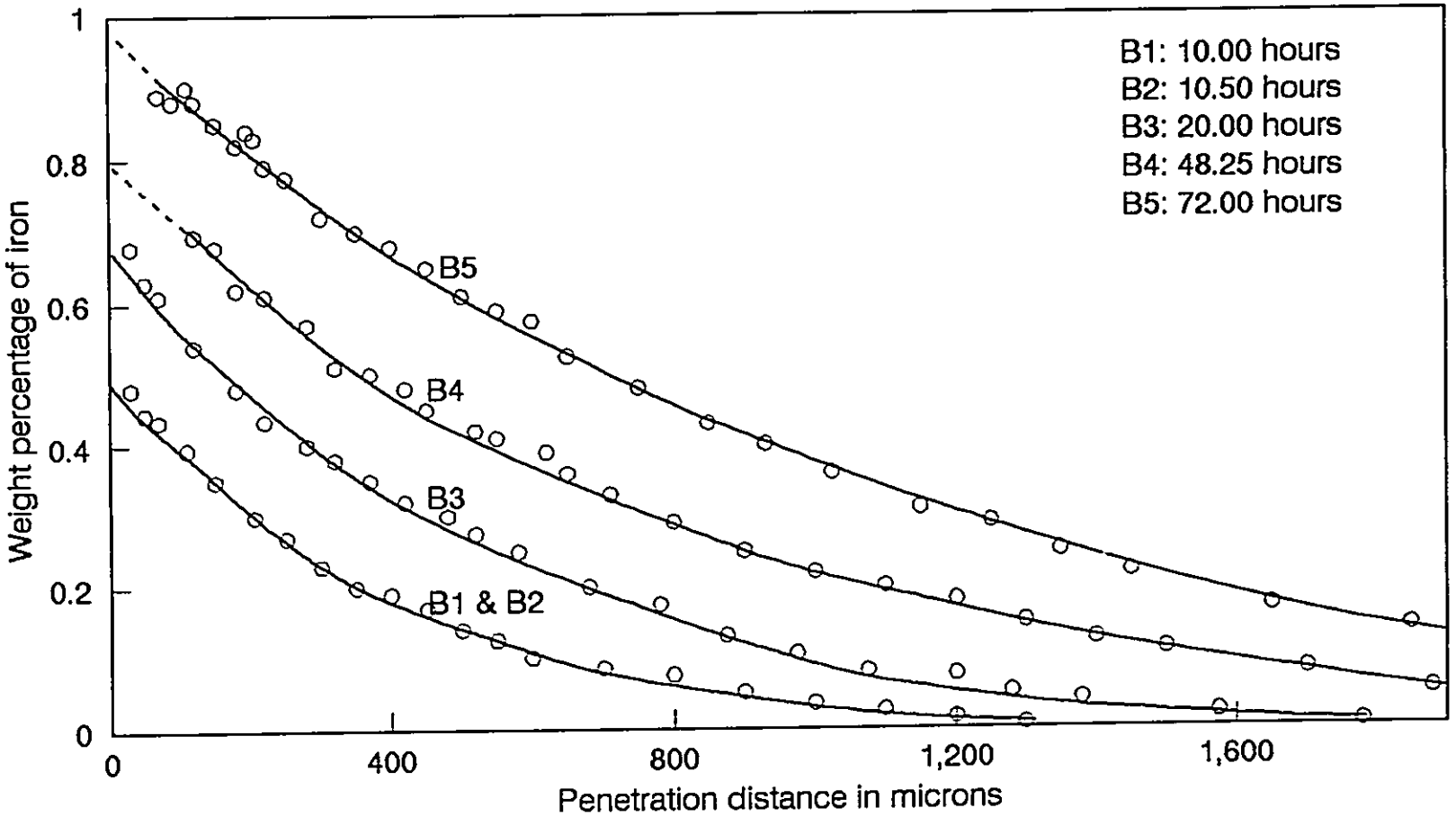

Fig. 2-8: Diffusion profiles of iron in sodium disilicate glass obtained at approximately 950 °C.

(reproduced Fig. 1 from Borom and Pask, 1967)

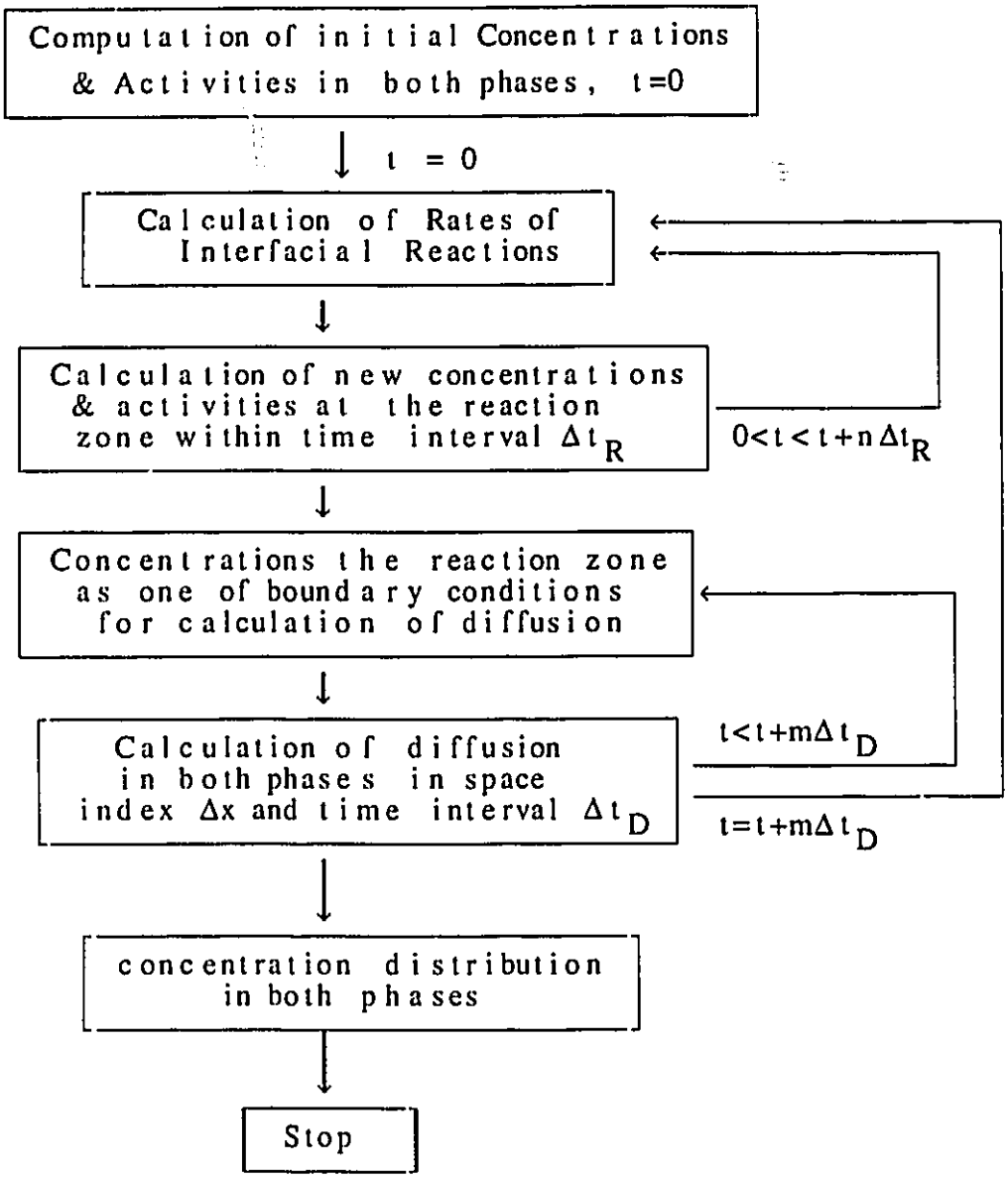

Fig. 4-1 The flow chart for the computations of coupling of diffusion and interfacial reactions in slag/metal system

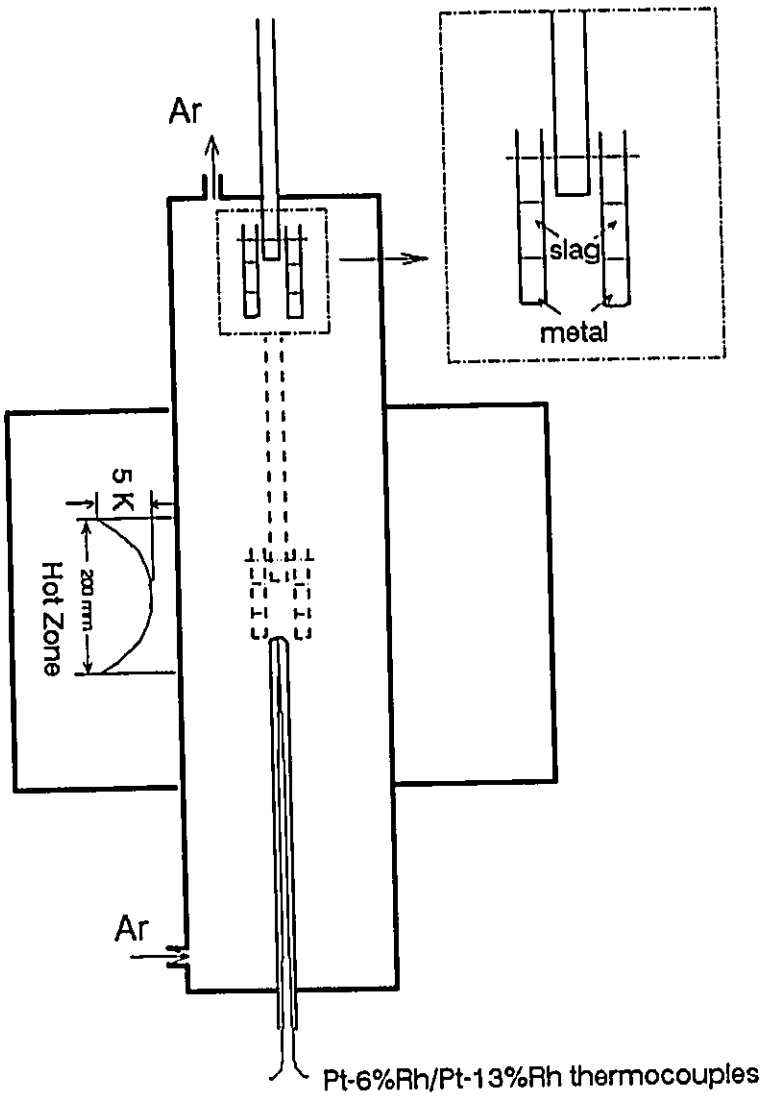

Fig. 5-1: Schematic furnace and assembly for slag/metal reactions in the experiments.

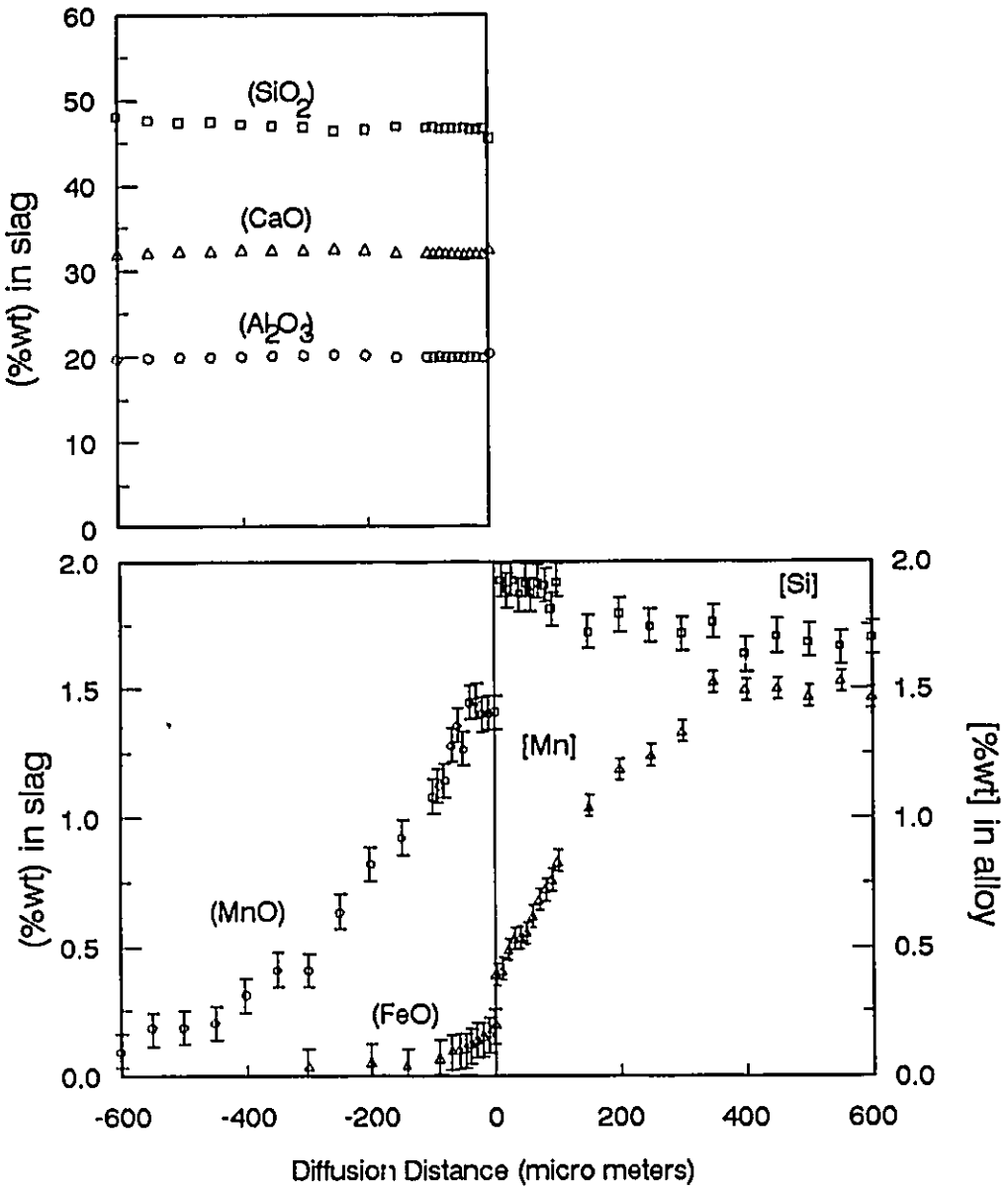

Fig. 5-2: Measured concentration profiles in specimen 1a.

(T = 1763 K, t = 10 min)

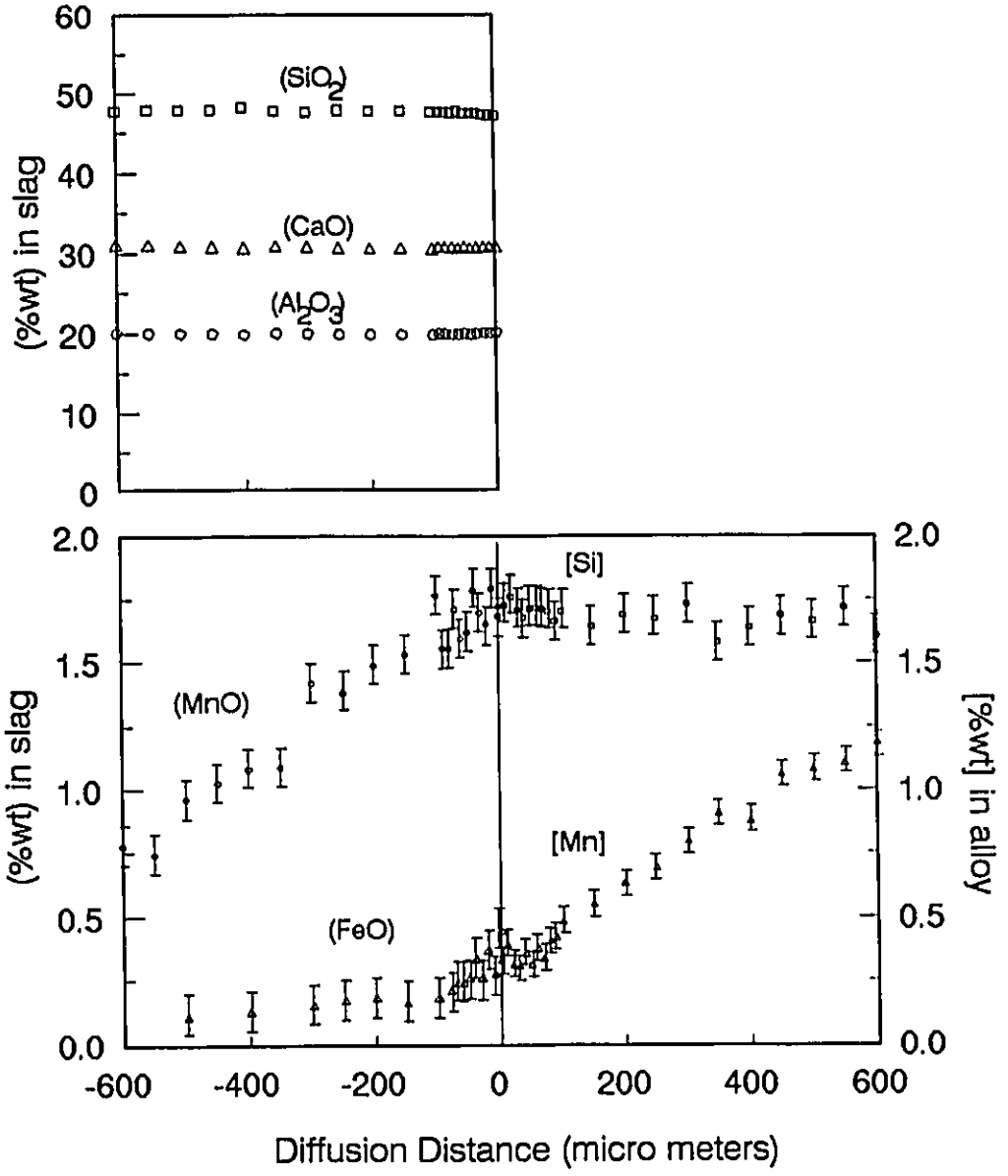

Fig. 5-3: Measured concentration profiles in specimen 1b
(T = 1763 K, t = 80 min)

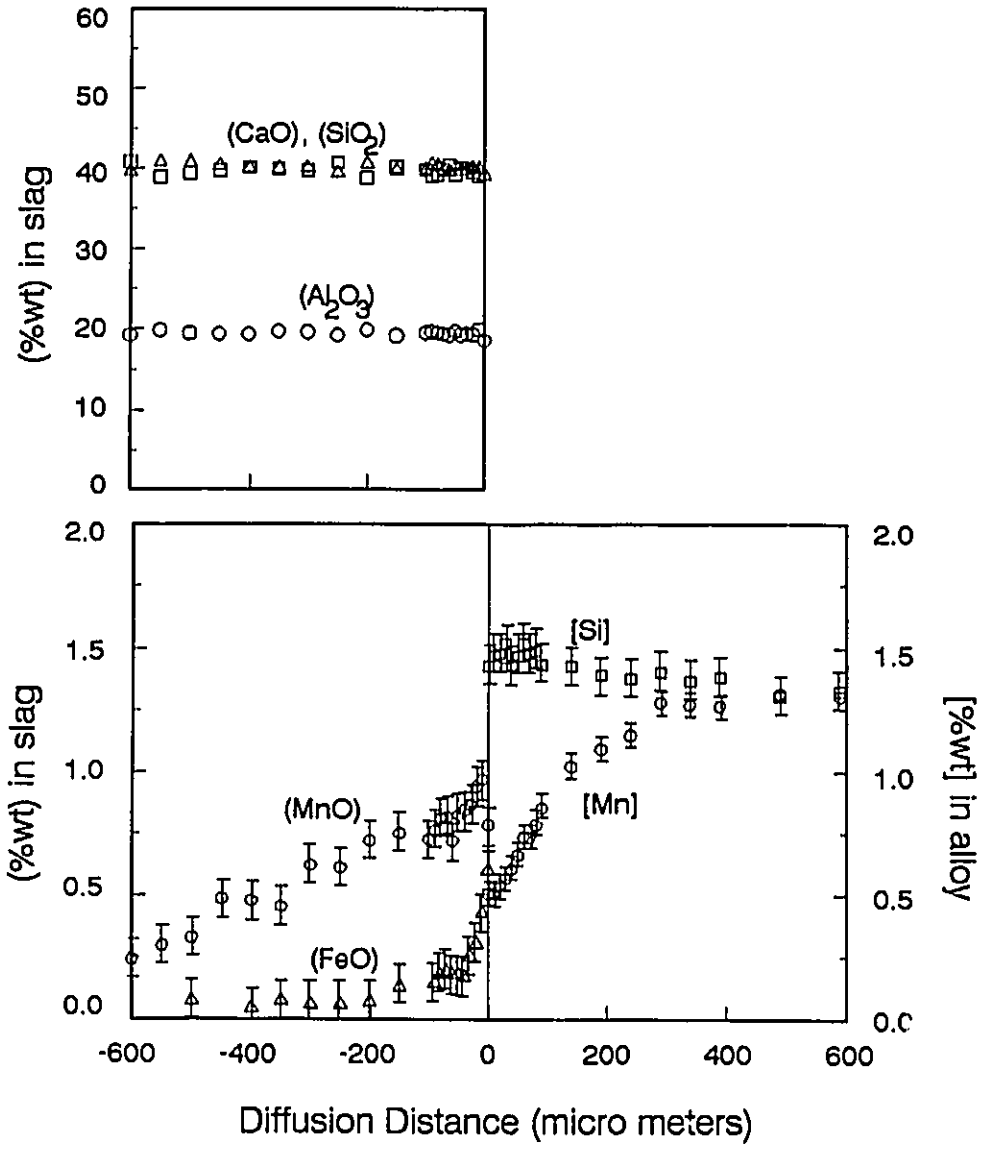

Fig. 5-4: Measured concentration profiles in specimen 2a
(T = 1763 K, t = 10 min.)

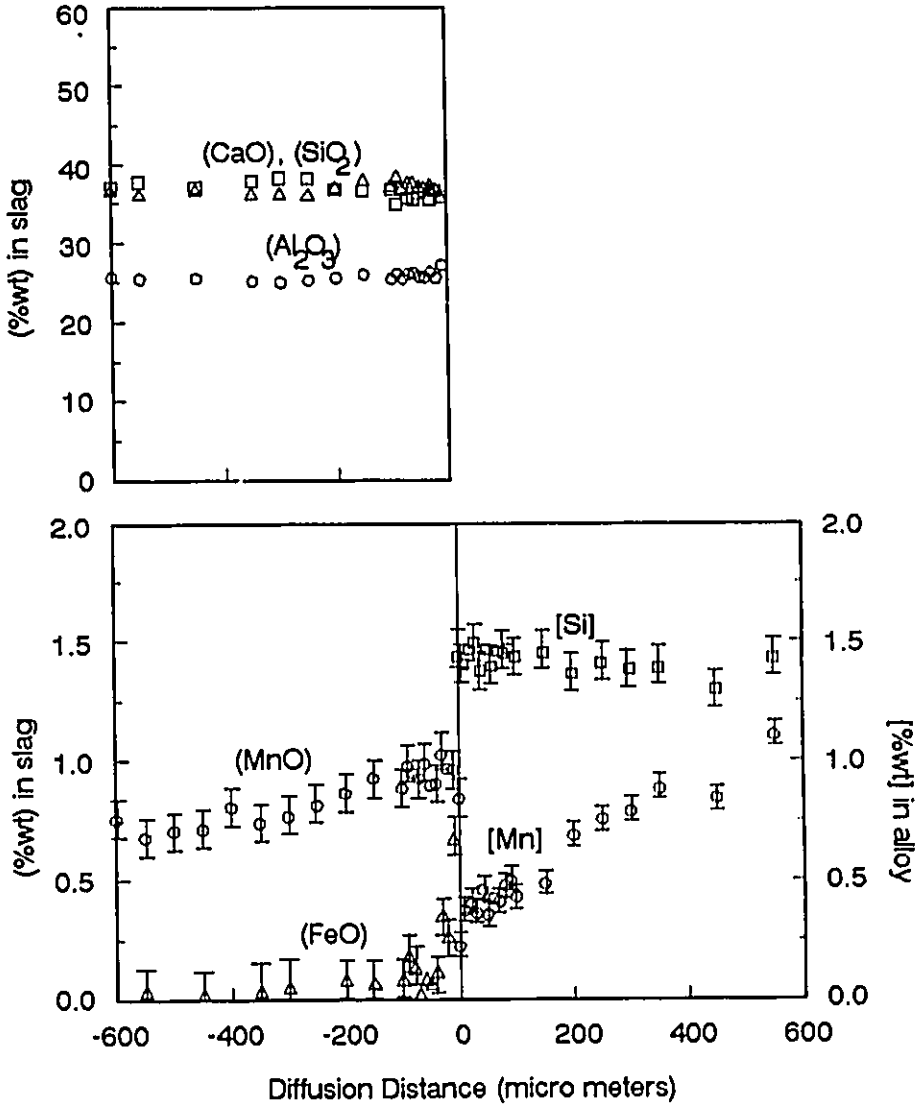

Fig. 5-5: Measured concentration profiles in specimen 2b
(T = 1763 K, t = 80 min.)

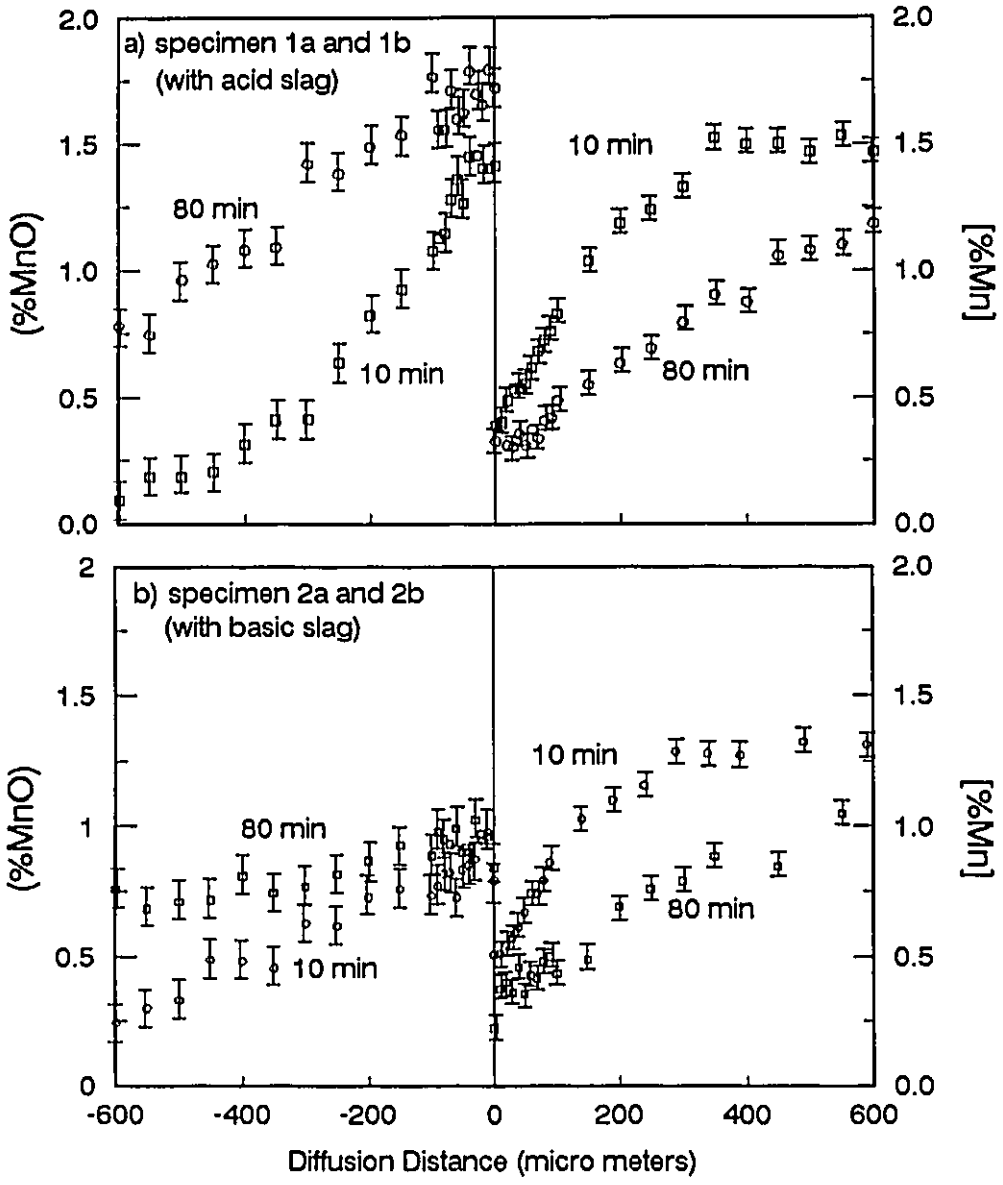

Fig. 5-6: Measured concentration profiles of Mn in alloy and MnO in slag

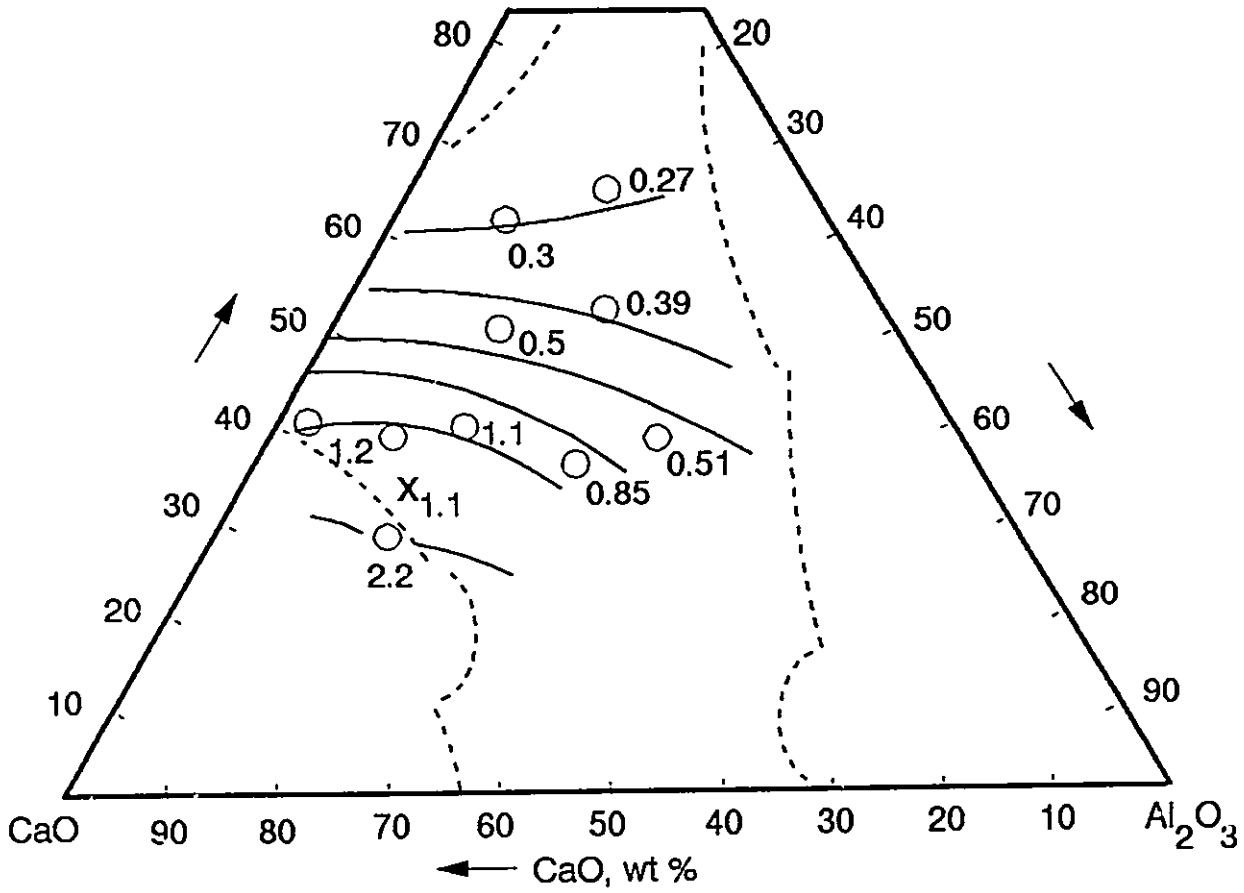

Fig. 6-1: Activity coefficient of manganese oxide (on molar basis) at concentration up 0.07 molar (about 8 wt%) in MnO $CaO+SiO_2+Al_2O_3$ melts at 1873 K (marked by x) and 1923 K (reproduced from Abraham, Davis and Richardson, 1960)

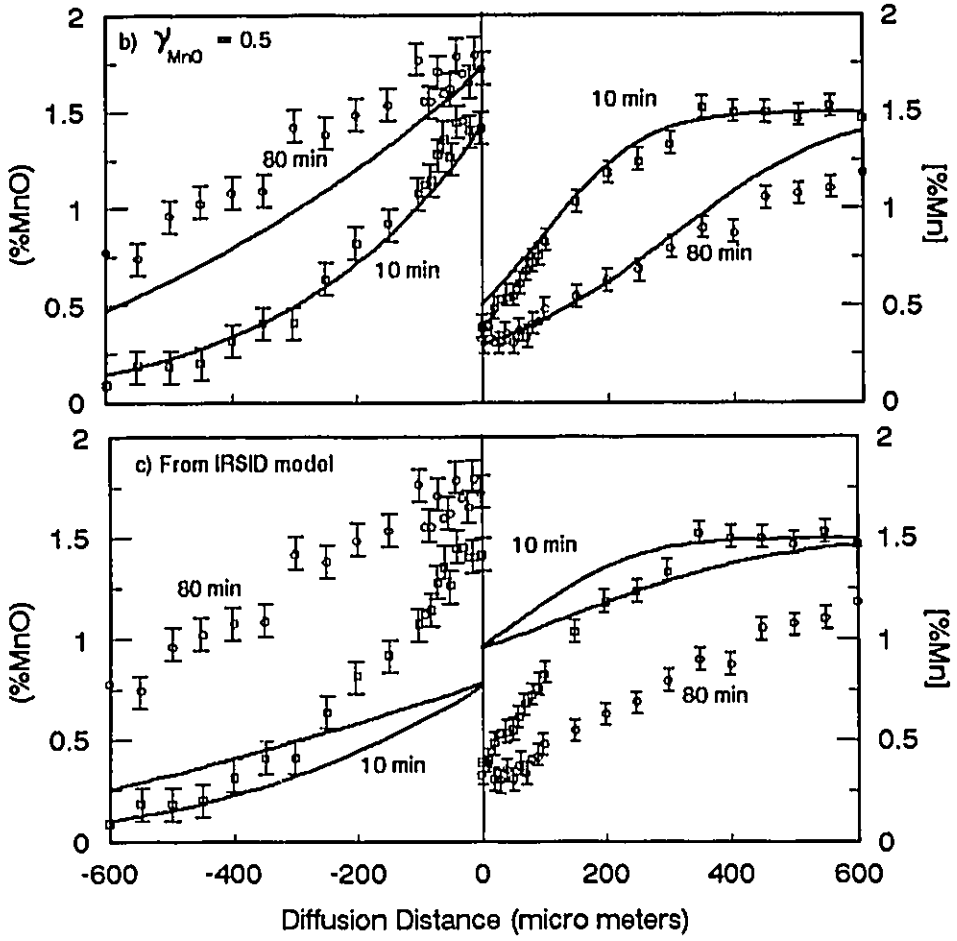

Fig. 6-2: Influence of activity coefficient of MnO on computed results comparing with experimental data in 1a and 1b (see Table 6-9 for other thermochemical parameters)

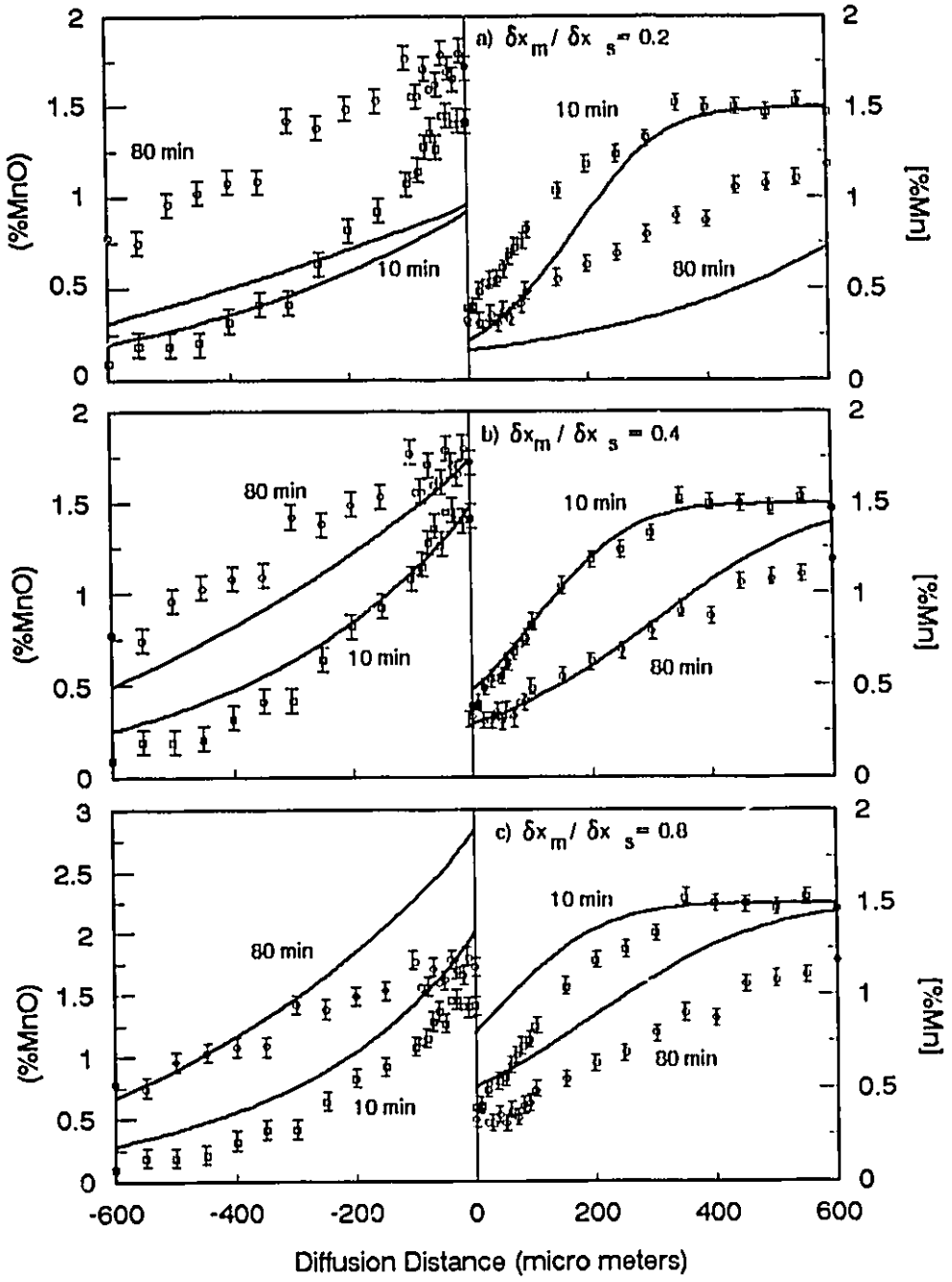

Fig. 6-3: Influence of varying values of the ratio $\delta x_m / \delta x_s$ on computed results comparing with experimental data of manganese and manganese oxide in specimens 1a and 1b. (see Table 6-9 for other thermochemical parameters)

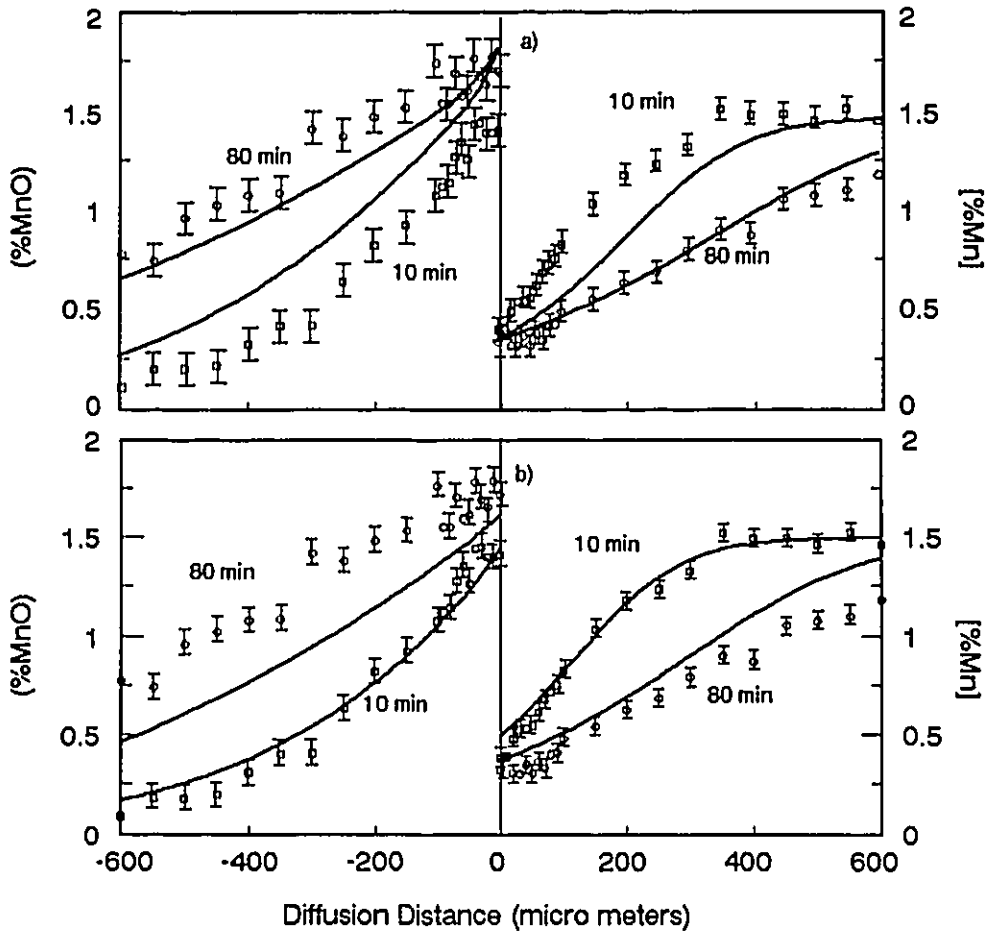

Fig. 6-4: Comparison between computed and experimental results of Mn in alloy and MnO in slag at different values of chemical reaction rate constant for transfer of iron, manganese and silicon.

a) $k_{Fe} = 6.0 \times 10^{-4}$, $k_{Mn} = 2.2 \times 10^{-3}$, $k_{Si} = 2.2 \times 10^{-3}$ cm/sec;
b) $k_{Fe} = 1.0 \times 10^{-8}$, $k_{Mn} = 8.0 \times 10^{-7}$, $k_{Si} = 1.3 \times 10^{-3}$ cm/sec.

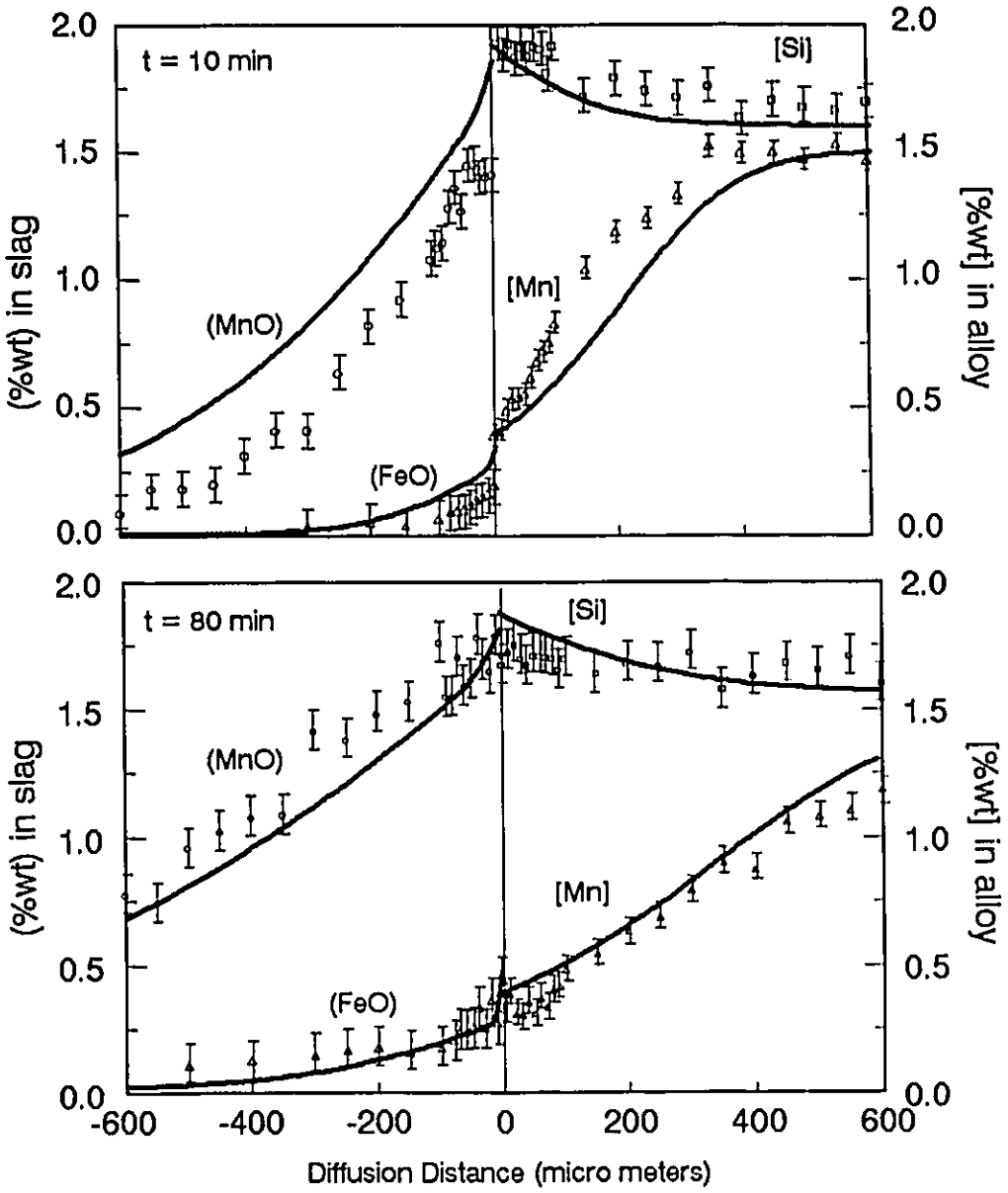

Fig. 6-5: Comparison between computed and experimental results based on initial values of thermochemical parameters in Table 6-8.

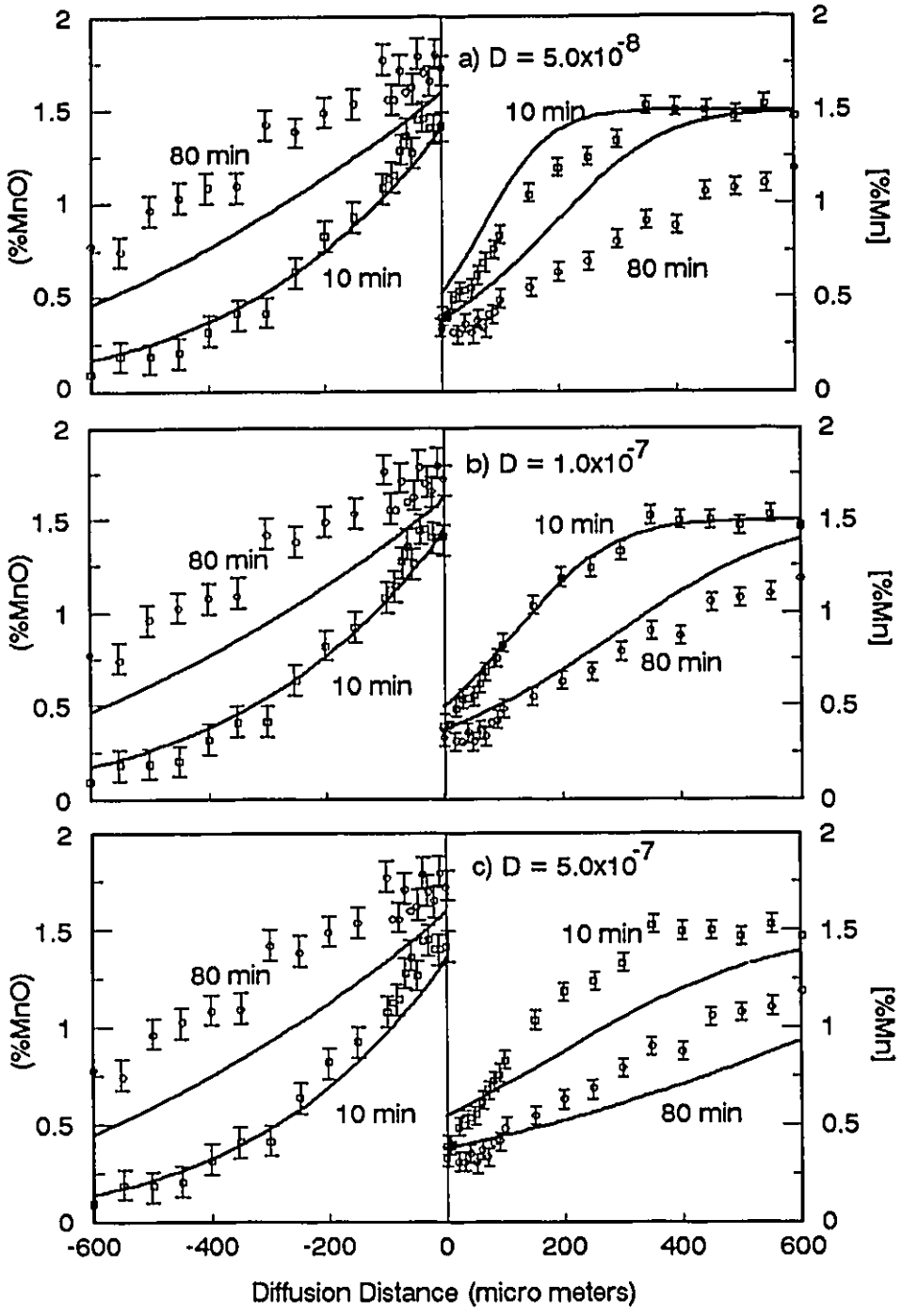

Fig. 6-6: influence of variation of diffusion coefficient of manganese (cm^2/sec) in alloy on computed results comparing with measured concentration profiles of manganese in alloy of specimens 1a and 1b (on right side of the figure).

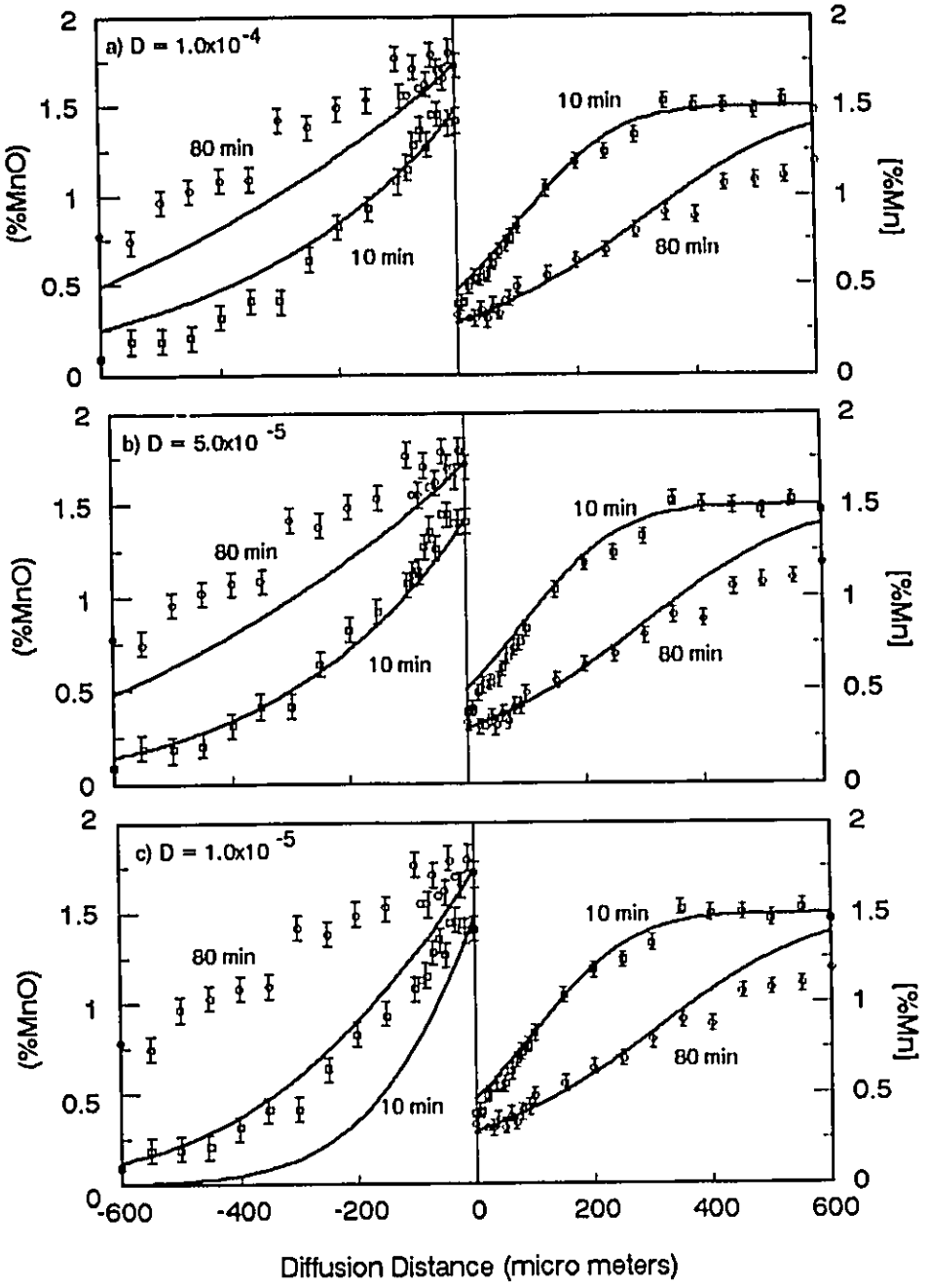

Fig. 6-7: Influence of variation of diffusion coefficient of manganese ion (cm^2/sec) in slag on computed results comparing with measured concentration profiles of MnO in slag of specimens 1a and 1b (on left side of the figure).

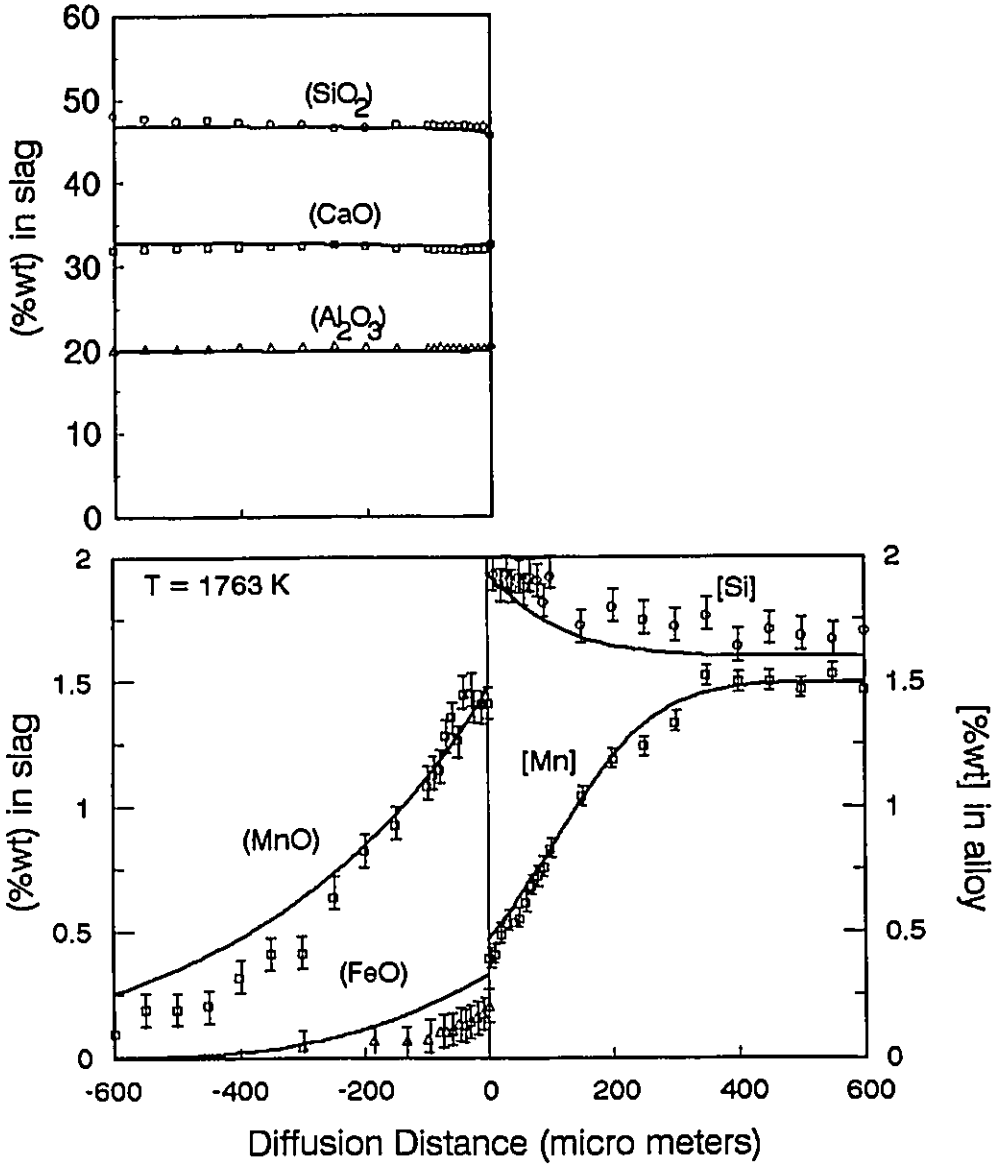

Fig. 6-8: Comparison between experimental data and computed results with recommended values of thermochemical parameters in Table 6-9 for specimen 1a (10 min).

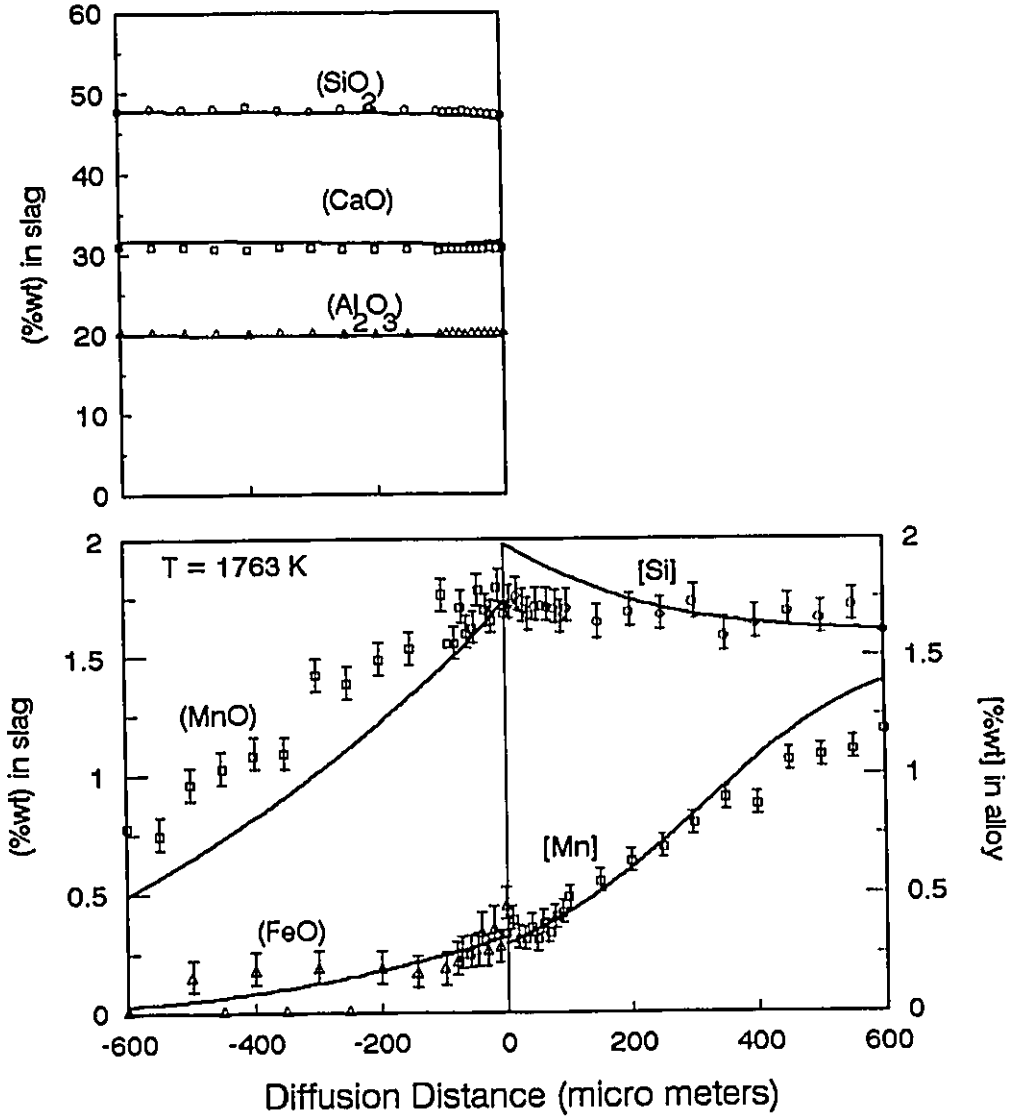

Fig. 6-9: Comparison between experimental data and computed results with recommended values of thermochemical parameters in Table 6-9 for specimen 1b (80 min).

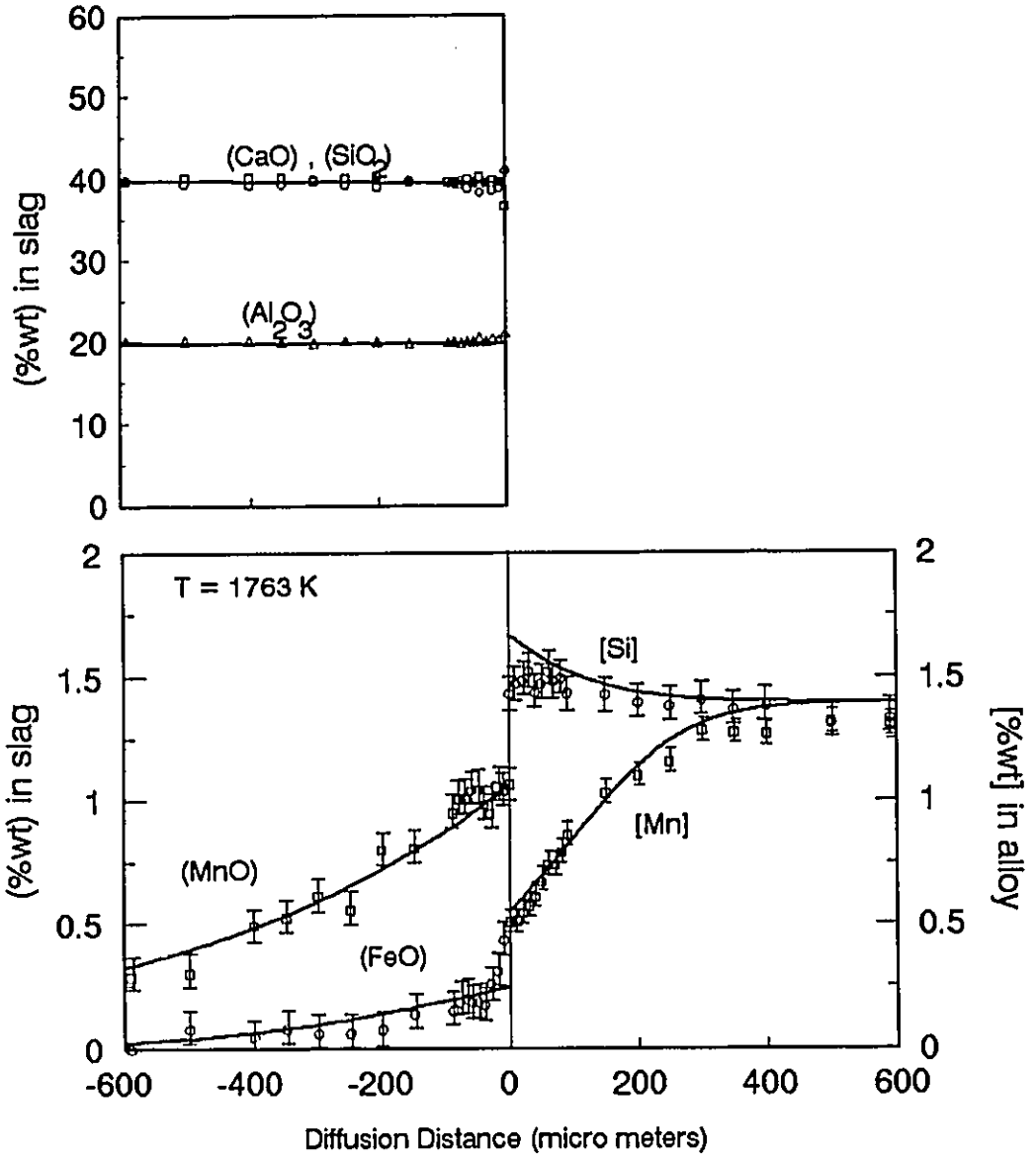

Fig. 6-10: Comparison between computed results with recommended thermochemical parameters in Table 6-9 and experimental data in speciemn 2a (10 min).

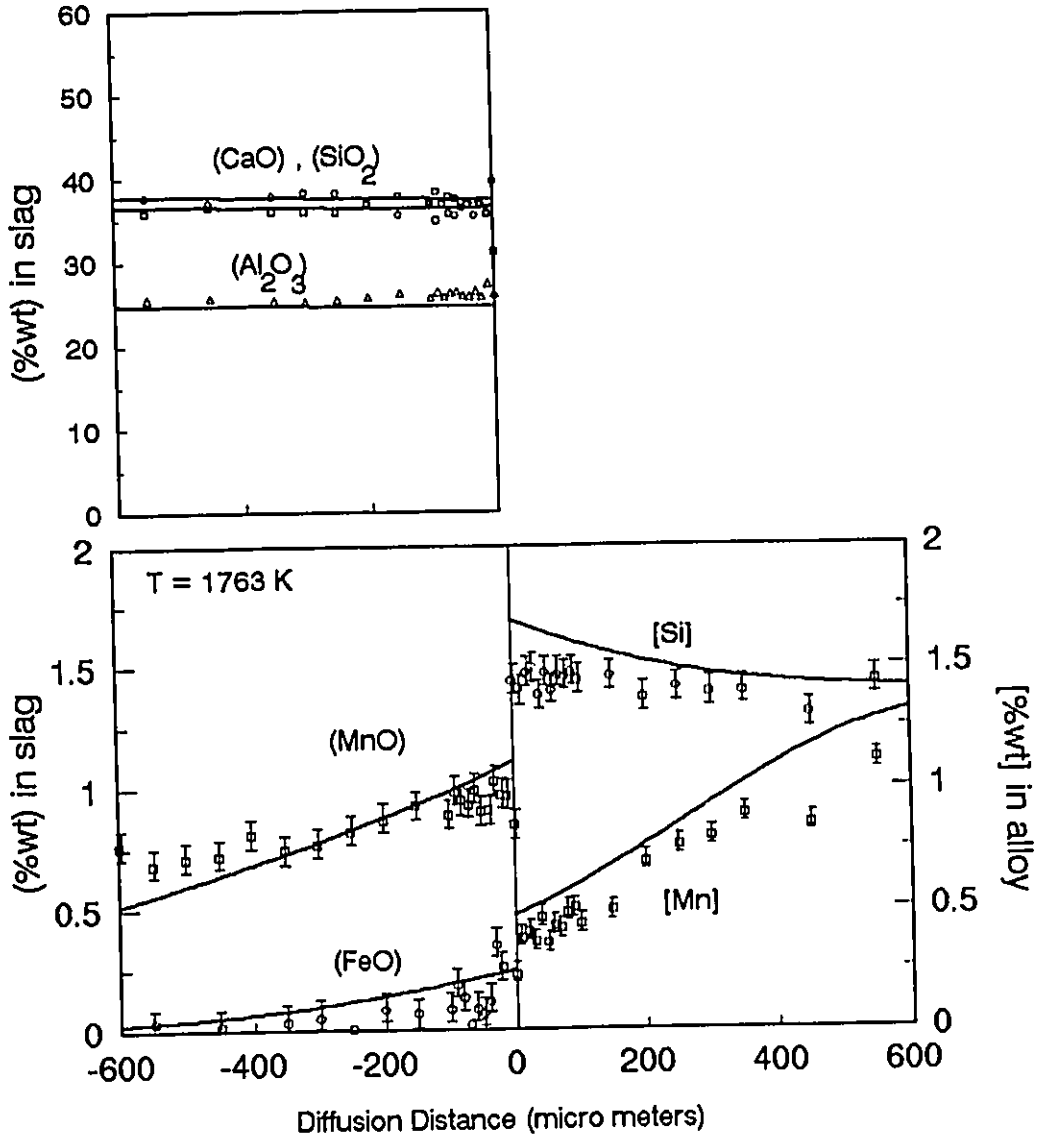

Fig. 6-11: Comparison between computed results with recommended thermochemical parameters in Table 6-9 and experimental data in specimen 2b (80 min).

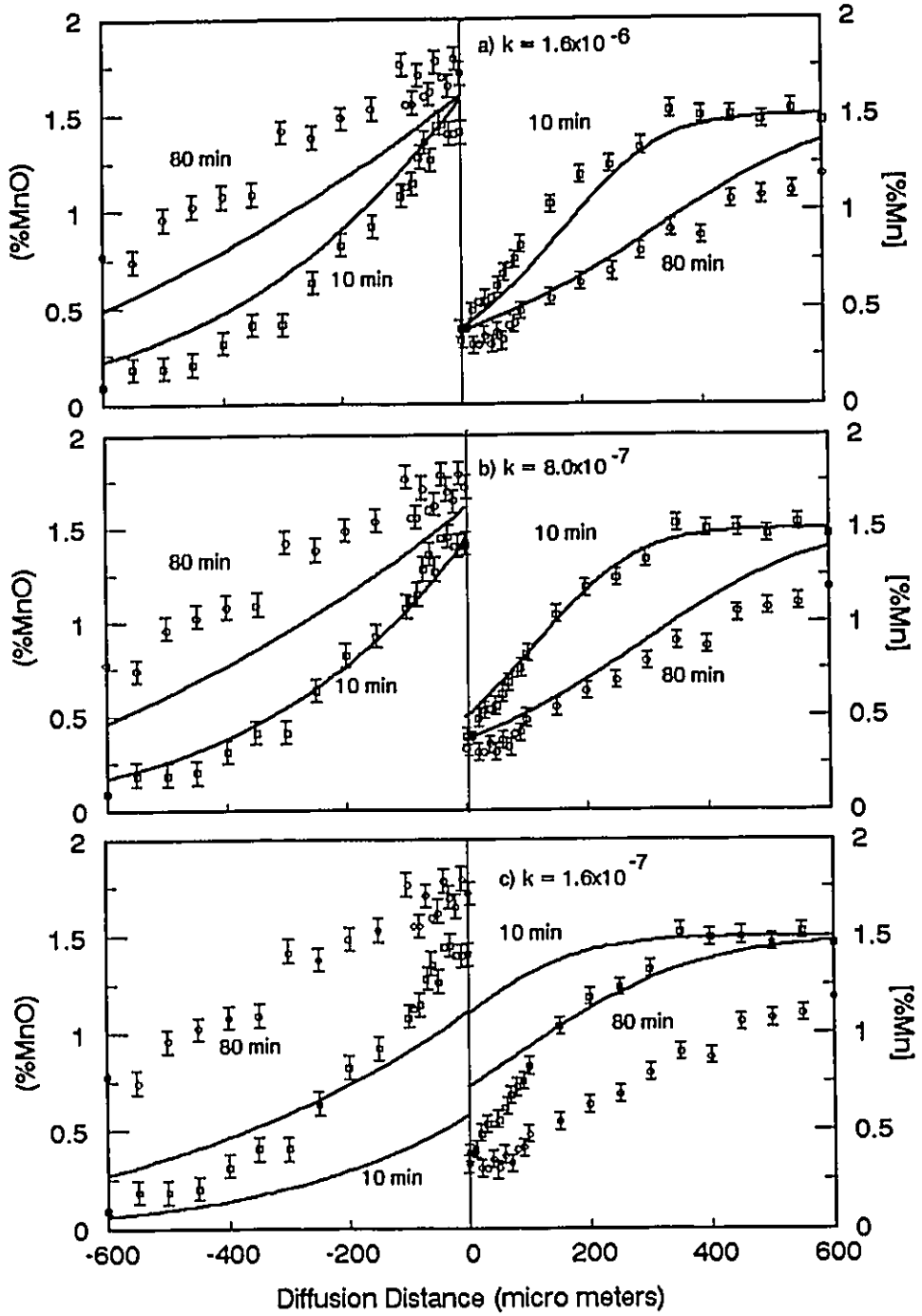

Fig. 6-12: Influence of variation of reaction rate constant of manganese transfer (cm/sec) on computed results comparing with measured concentration profiles of Mn and MnO in 1a and 1b (see Table 6-9 for other parameters).

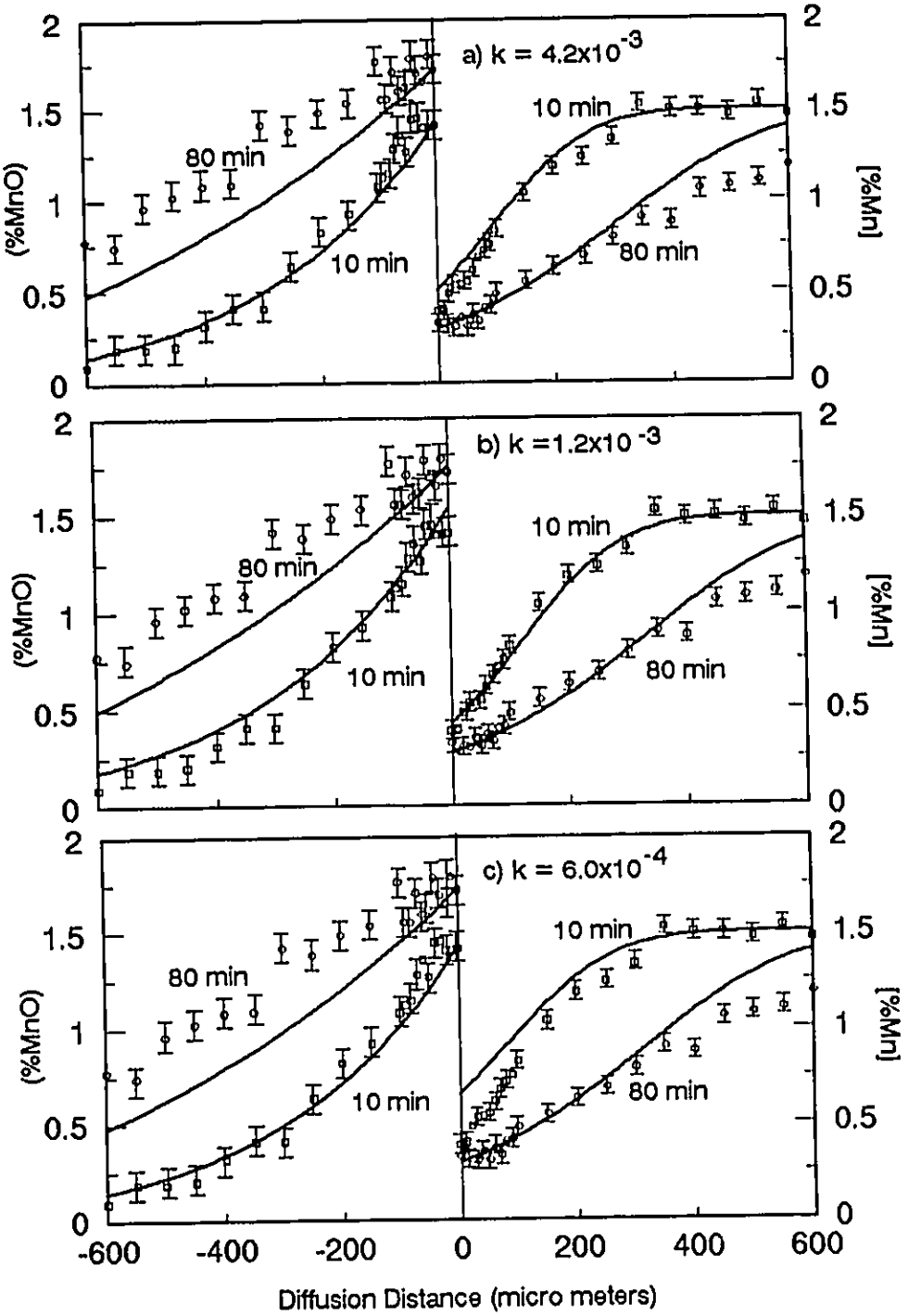

Fig. 6-13: Influence of variation of reaction rate constant of silicon transfer (cm/sec) on computed results comparing with measured concentration profiles of Mn and MnO in 1a and 1b (see Table 6-9 for other parameters).

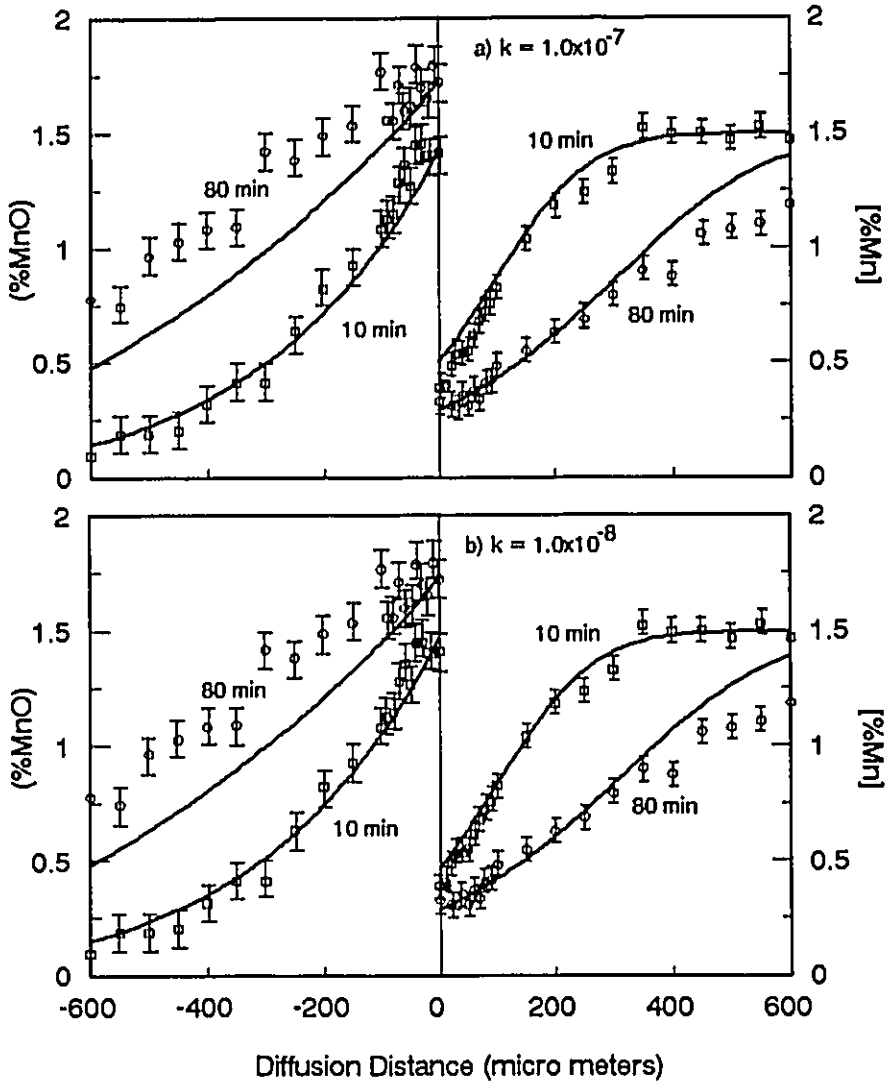

Fig. 6-14: Influence of variation of reaction rate constant of iron transfer (cm/sec) on computed results comparing with measured concentration profiles of Mn and MnO in 1a and 1b (see Table 6-9 for other parameters).

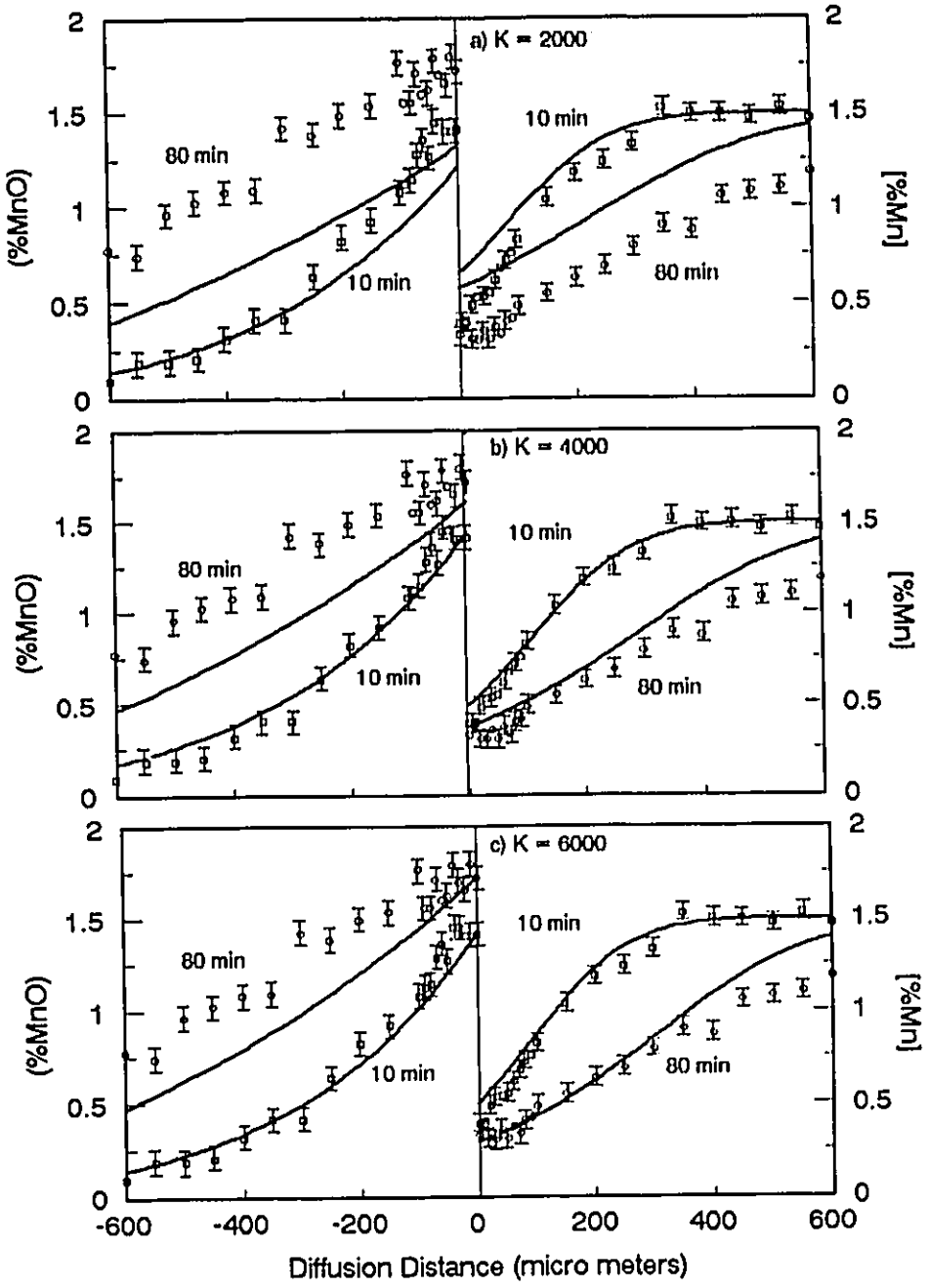

Fig. 6-15: Influence of varying values of equilibrium constant for formation of MnO on computed results comparing with measured concentration profiles of Mn and MnO in 1a and 1b (see Table 6-9 for other parameters).

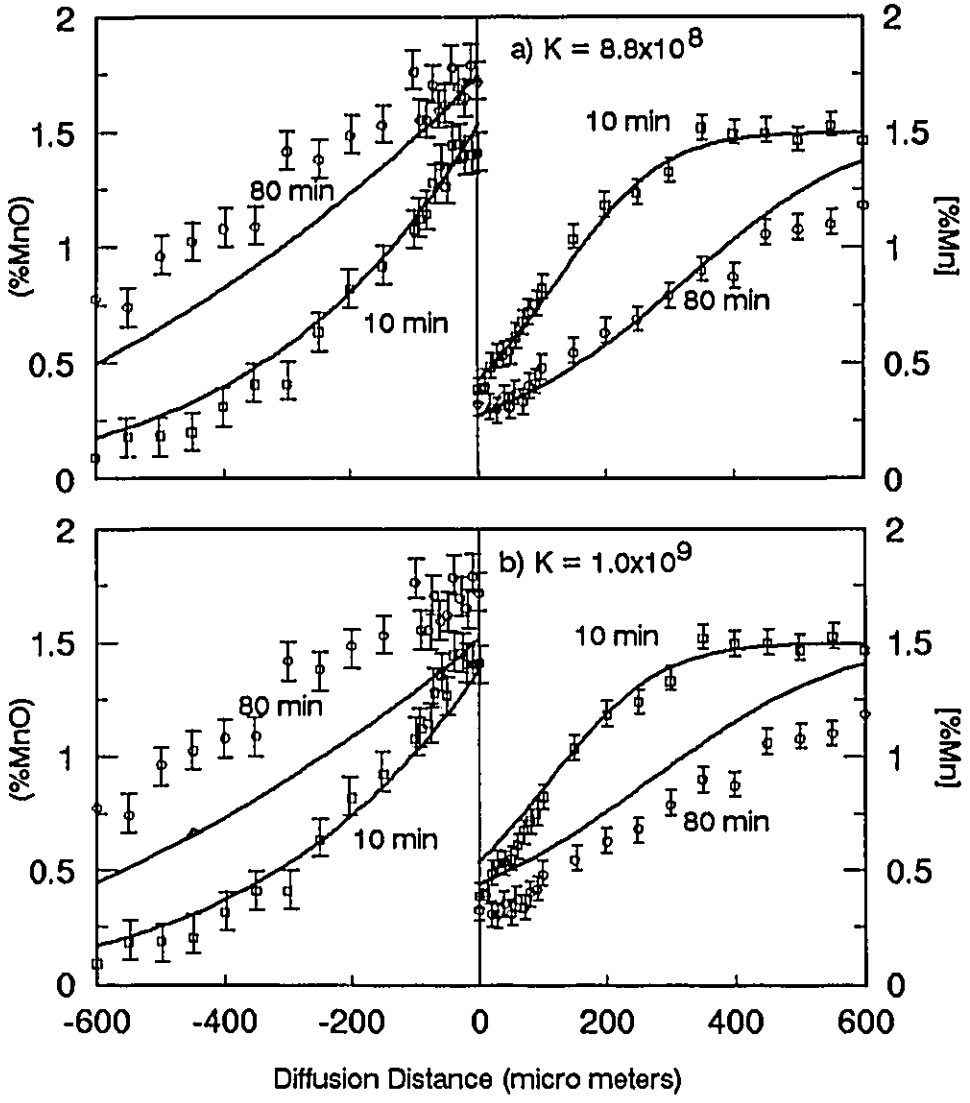

Fig. 6-16: Influence of varying values of equilibrium constant for formation of silicon oxide on computed results comparing with measured concentration profiles of Mn and MnO in 1a and 1b (see Table 6-9 for other parameters).

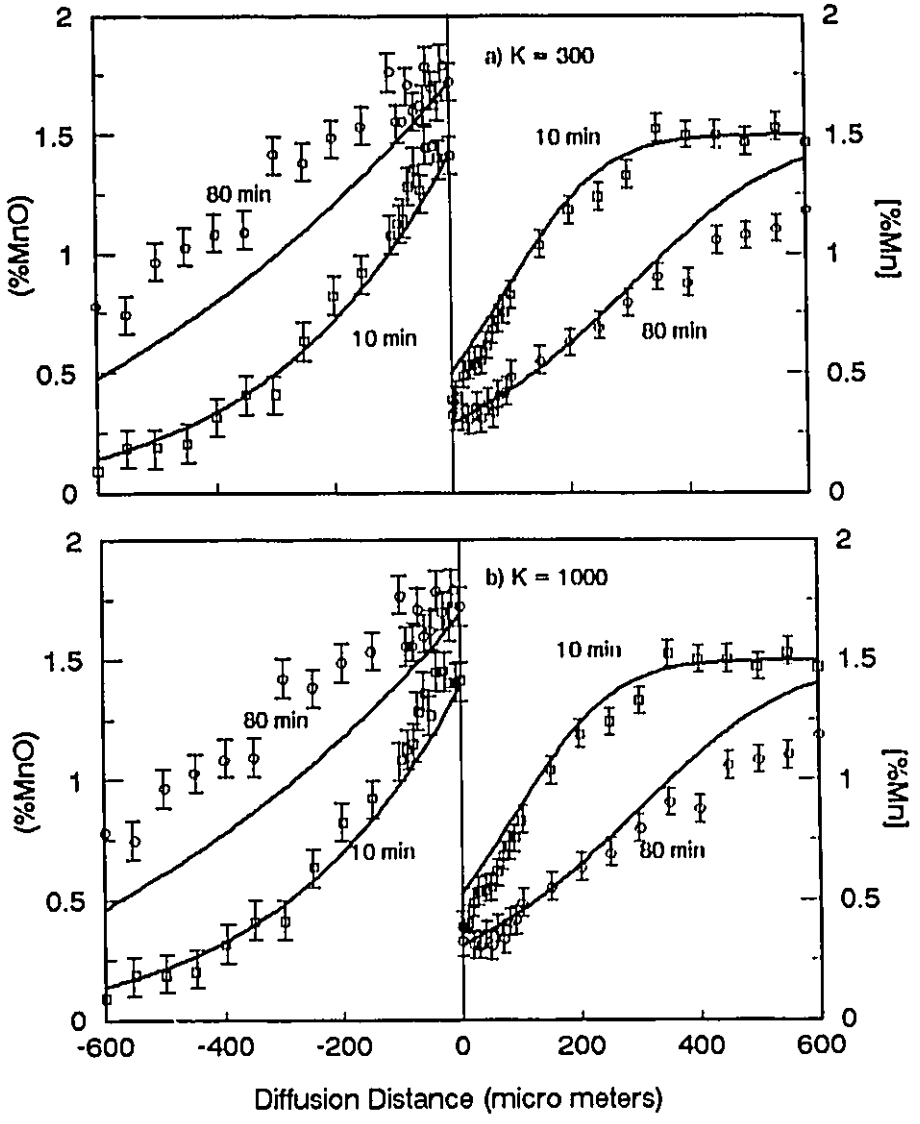

Fig. 6-17: Influence of varying values of equilibrium constant for formation of FeO on computed results comparing with measured concentration profiles of Mn and MnO in 1a and 1b (see Table 6-9 for other parameters).

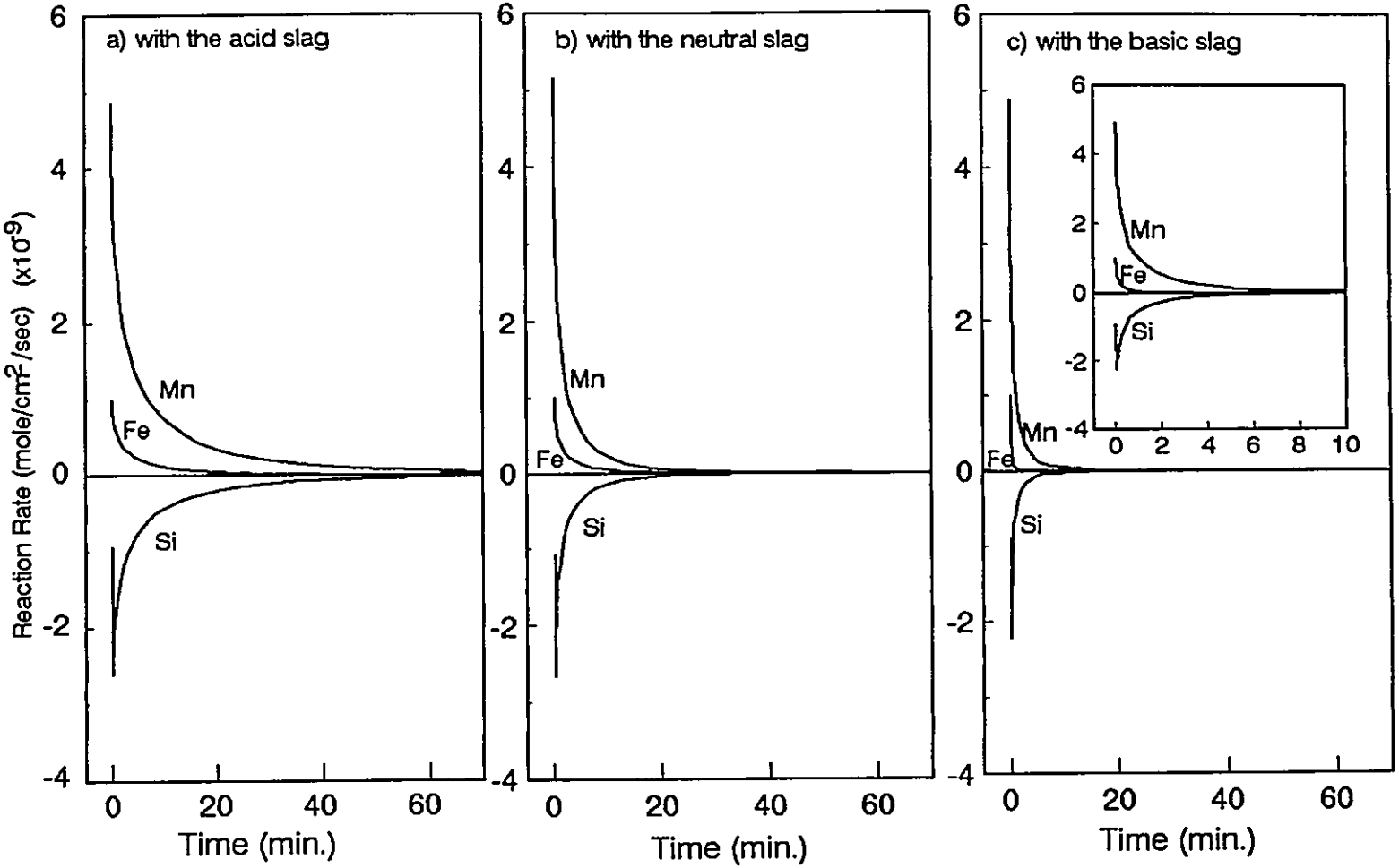

Fig. 7-1: Change in values of computed reaction rates for transfer of Fe, Mn and Si.

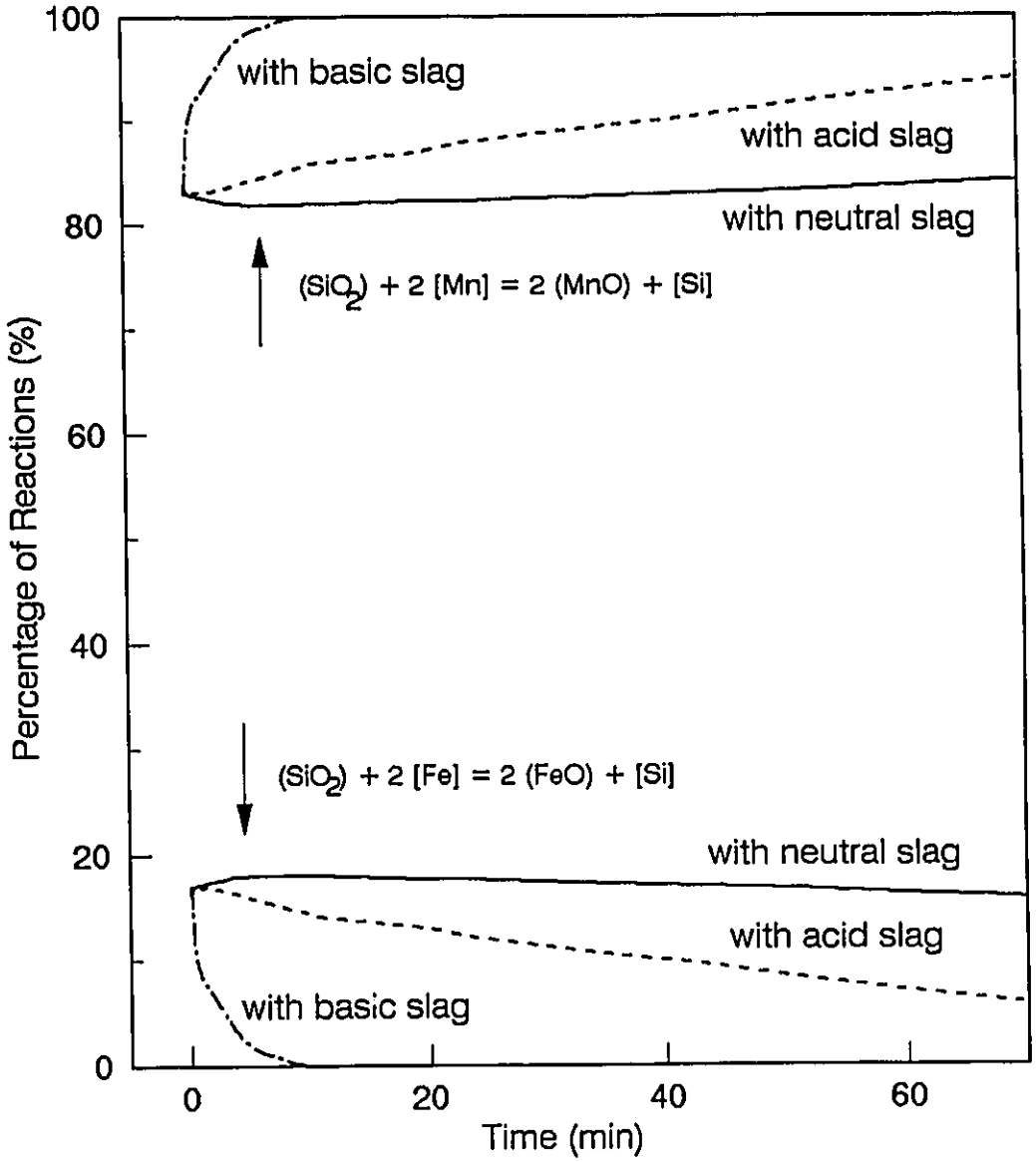

Fig. 7-2: Demonstration of distribution in simultaneous reduction of SiO_2 by manganese and iron in alloy.

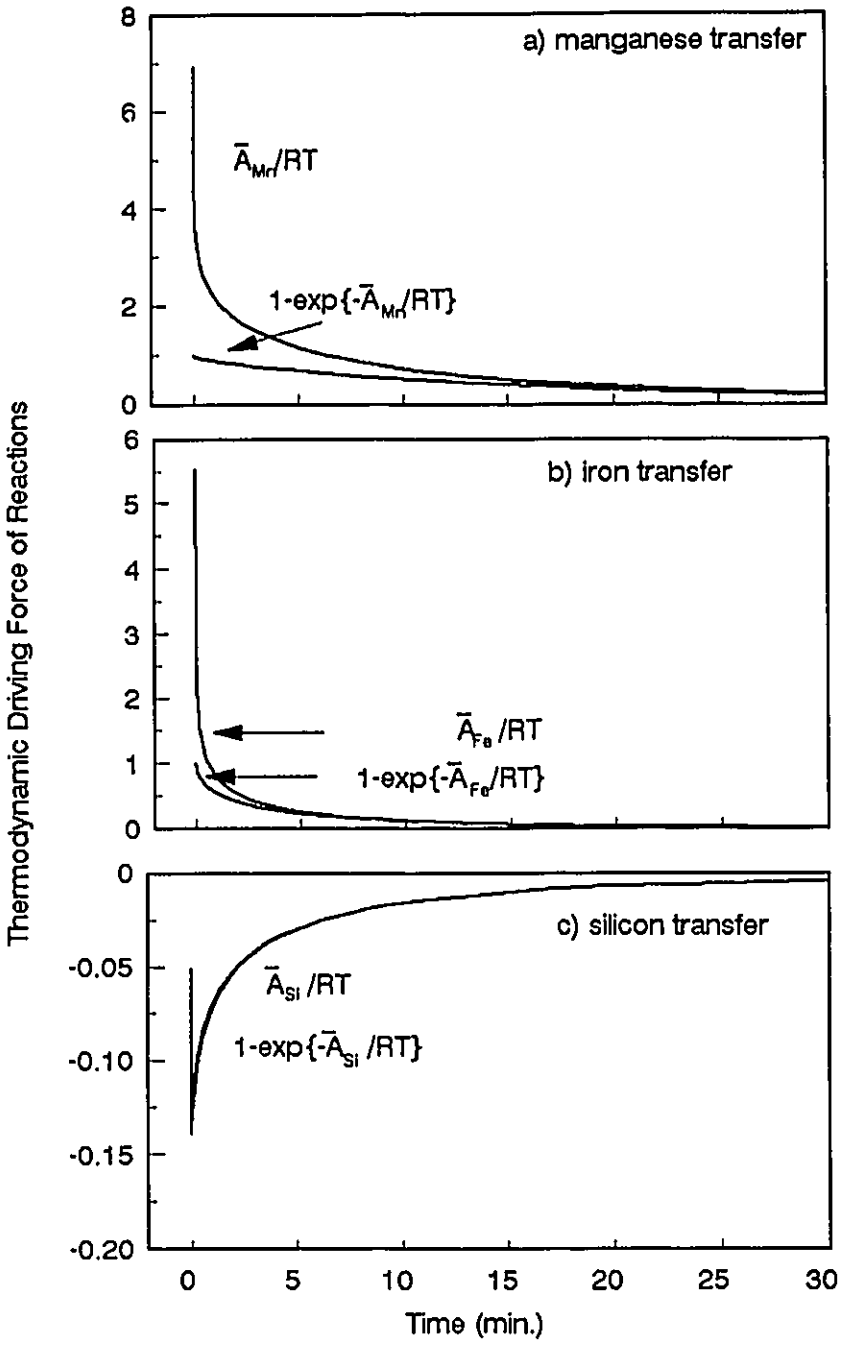

Fig. 7-3: comparison between thermodynamic driving force 1-exp{-$\bar{A}_i/RT$} and its appoximated form $\bar{A}_i/RT$. (computed for reactions with the acid slag)

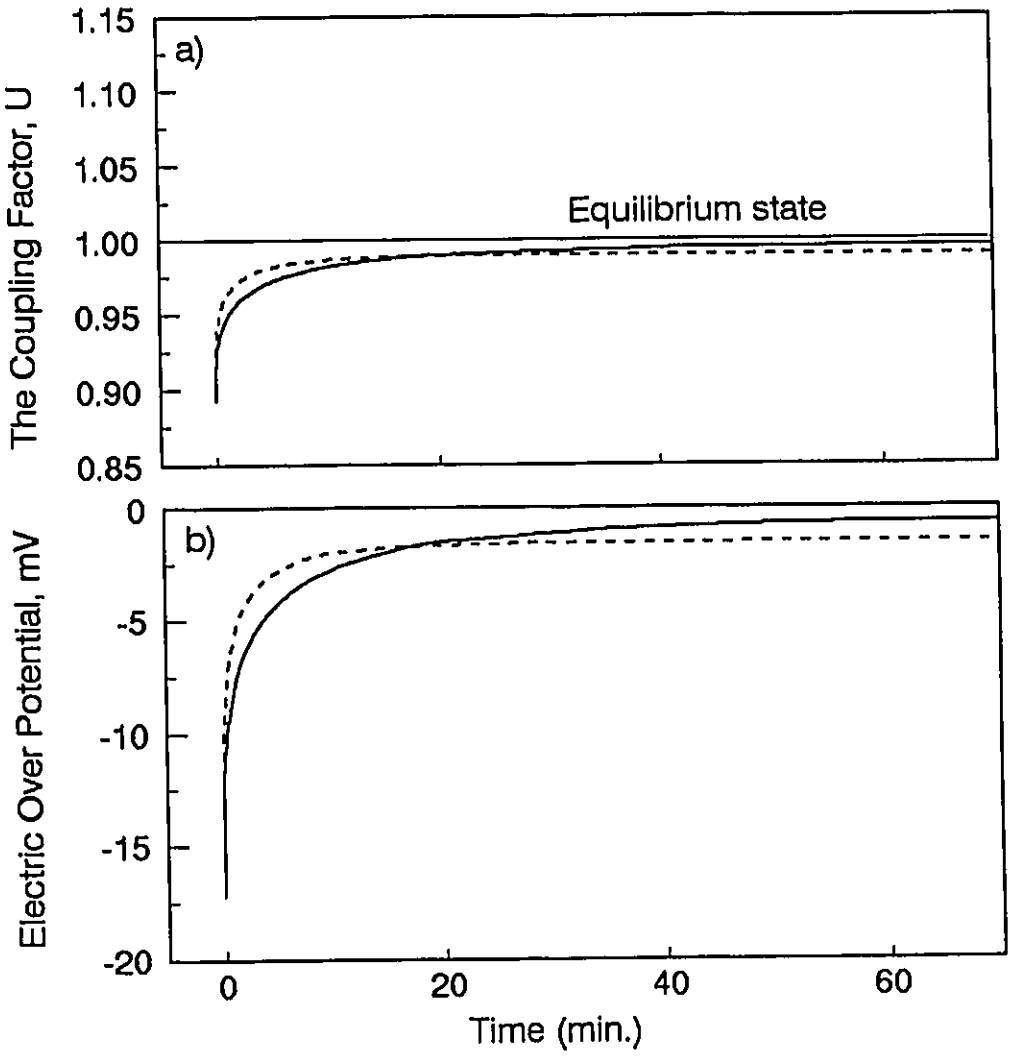

Fig. 7-4: Demonstration of the coupling factor and electric over potential in slag/metal reactions

——— for reactions with the acid slag;
— — — — for reactions with the neutral slag.

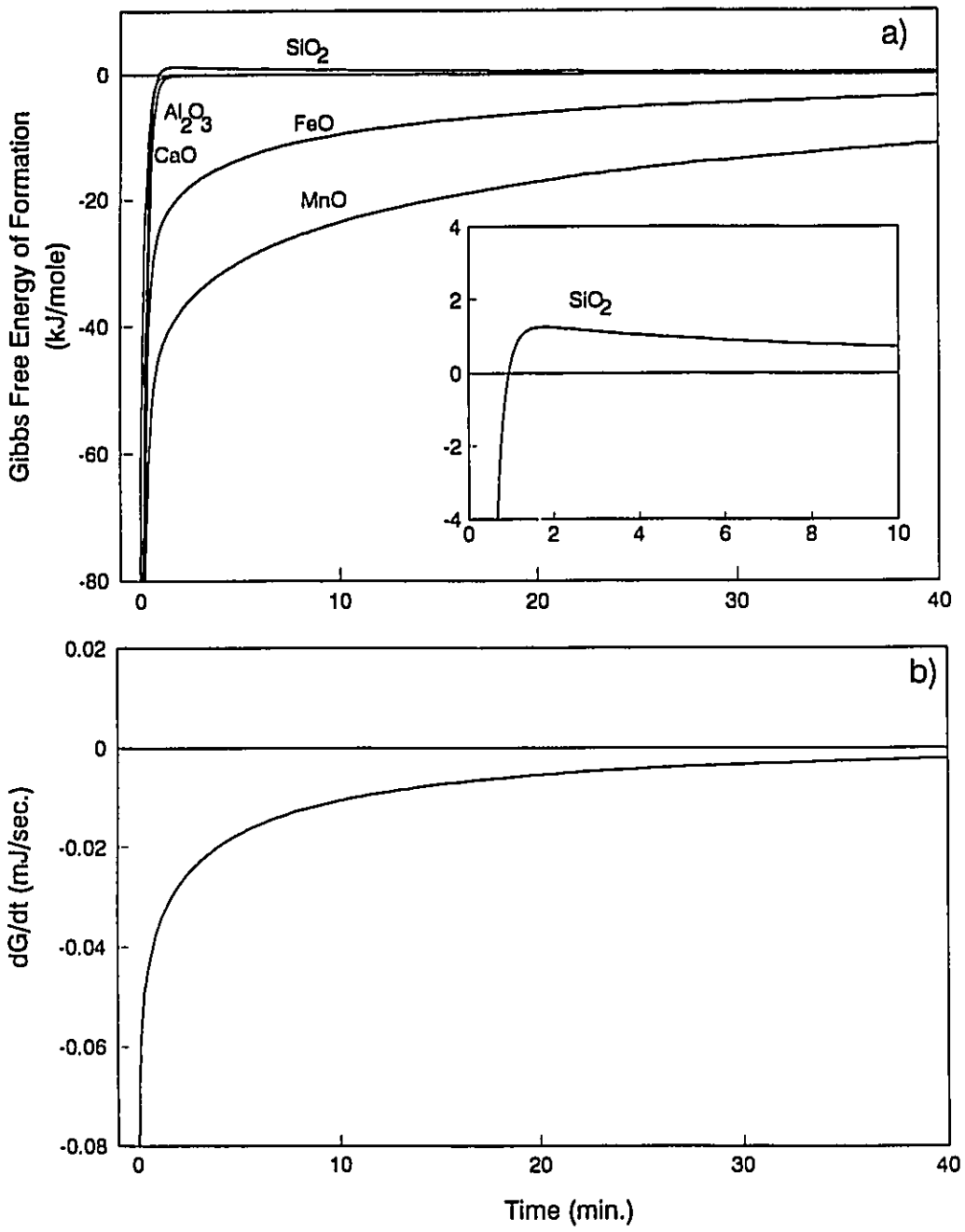

Fig. 7-5: Demonstration of change of Gibbs Free Energy of formation and Gibbs Free Energy of the system (with acid slag).

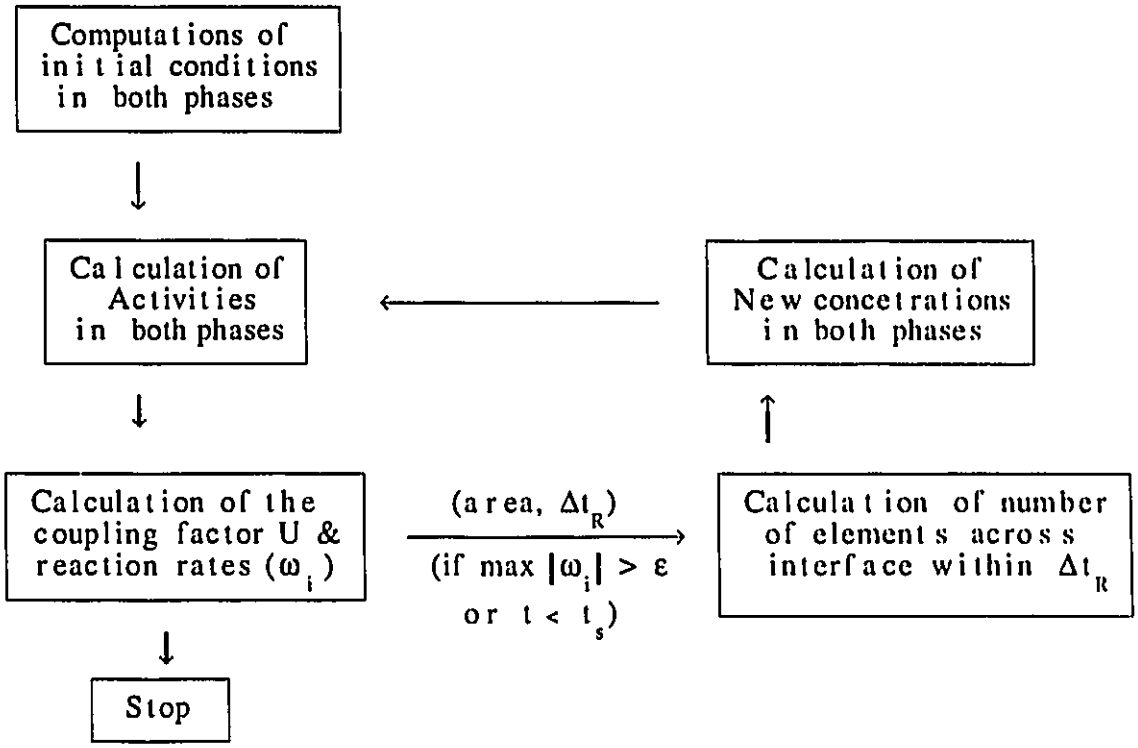

Fig. B1: Flow chart for computations of reaction kinetics in the reaction zone in slag/metal system, where t_s is pre-determined reaction time at which computations stop, e is pre-determined value of reaction rate to stop computations.